

8-2013

Modeling Chemical Reactions in Aqueous Solutions

Osman Uner

University of Arkansas, Fayetteville

Follow this and additional works at: <http://scholarworks.uark.edu/etd>



Part of the [Physical Chemistry Commons](#)

Recommended Citation

Uner, Osman, "Modeling Chemical Reactions in Aqueous Solutions" (2013). *Theses and Dissertations*. 887.
<http://scholarworks.uark.edu/etd/887>

This Thesis is brought to you for free and open access by ScholarWorks@UARK. It has been accepted for inclusion in Theses and Dissertations by an authorized administrator of ScholarWorks@UARK. For more information, please contact scholar@uark.edu, ccmiddle@uark.edu.

MODELING CHEMICAL REACTIONS IN AQUEOUS SOLUTIONS

MODELING CHEMICAL REACTIONS IN AQUEOUS SOLUTIONS

A thesis submitted in partial fulfillment
of the requirements for the degree of
Master of Science in Chemistry

by

Osman Uner
Karadeniz Technical University
Bachelor of Science in Chemistry, 2008

August 2013
University of Arkansas

This thesis is approved for recommendation to the Graduate Council.

Dr. Peter Pulay
Thesis Director

Dr. Jim Hinton
Committee Member

Dr. Ingrid Fritsch
Committee Member

Dr. Colin Heyes
Committee Member

ABSTRACT

The energy barriers for S_N2 ligand exchange reactions between the chloride anion and para-substituted benzyl chlorides were investigated both in water solution and in the gas phase by using quantum chemical simulations at the DFT and Hartree-Fock levels. The question addressed was the effect of the solvent (water) and of the substituent on the barrier height. The para substituent groups included NH_2 , OH , OCH_3 , CH_3 , $C(CH_3)_3$, H , F , Cl , Br , I , CF_3 , CN , NO_2 , and SO_3^- . The calculations in aqueous solution were carried out with the recently developed Ultrafast Monte Carlo method using the TIP3P explicit water model. The PQS program system was used for all calculations. The minimum energy reaction path was determined in the gas phase for each exchange reaction by optimizing all geometry parameters except the reaction coordinate which was defined as the difference of the C-Cl distances for the approaching and leaving chlorine atoms and the reaction center (the central carbon atom). This difference was varied in small steps from $-11.0 a_0$ to $+11.0 a_0$ (about -5 to 5 \AA). These reaction paths were used in Monte Carlo simulations to determine the energy barriers in aqueous solution.

The behavior of S_N2 reactions in the water solution is different from the gas phase, particularly for substituents with high Hammett constants. These substituents make the central carbon atom more positively charged, resulting in shorter C-Cl distances at the transition state, and therefore less efficient screening of the atomic charges by the polar water molecules.

Solvation alone is expected to increase reaction barriers because the solvation shells have to be partially broken up. However, solvation by polar solvents like water (which have high dielectric constants) greatly diminishes the energy required for ion pair separation. If the barrier is dominated by ion pair separation, as in the chloride exchange reaction of para- SO_3^- benzyl chloride, then solvation diminishes the barrier and increases the reaction rate.

ACKNOWLEDGMENTS

I really appreciate my research advisor, Dr. Peter Pulay because of his valuable assistances and instructions. He helped me enhance my knowledge in computer programs because I did not know anything about computational chemistry before I met Dr. Pulay. He was always very nice and supportive to me during the pursuit of my research. Also, I express sincere thanks to Dr. Tomasz Janowski, who advised me about most of my calculations, for his valuable contributions and discussions.

I would like to thank to my M.S. Advisory Committee members, Dr. Jim Hinton, Dr. Ingrid Fritsch, and Dr. Colin Heyes. They gave me valuable suggestions during the pursuit of my research.

Furthermore, I am really grateful to my wife, Oznur Uner for her support and patience during the pursuit of my research. She has always pushed me to study hard, and I am so happy to be in her world. Finally, I really appreciate my teachers who have educated me during my lifetime.

DEDICATION

This thesis of *Modeling Chemical Reactions in Aqueous Solutions* is dedicated to my parents.

TABLE OF CONTENTS

I.	INTRODUCTION	1
II.	BACKGROUND	2
III.	COMPUTATIONAL METHODOLOGY	5
IV.	GEOMETRY OPTIMIZATION	8
V.	MONTE CARLO SIMULATIONS	11
A.	Hartree Fock Results	11
B.	DFT Results	17
VI.	CONCLUSIONS	23
VII.	REFERENCES	27

LIST OF TABLES

Table 1.	The effect of water solvent on the barrier height for the S _N 2 chloride exchange between para-substituted benzyl chloride and the chloride ion at the Hartree-Fock level. The barrier in water minus the barrier in the gas phase is shown. The solute was treated at the Hartree Fock/6-311G(d,p) level. The Monte Carlo simulations use the TIP3P water model and include the polarizability of the solute.	16
Table 2.	The effect of water solvent on the barrier height for the S _N 2 chloride exchange between para-substituted benzyl chloride and the chloride ion at the B3LYP density functional theory level. The barrier in water minus the barrier in the gas phase is shown. The solute was treated at the B3LYP/6-311G(d,p) level. The Monte Carlo simulations use the TIP3P water model and include the polarizability of the solute.	20
Table 3.	The barrier heights for the S _N 2 chloride exchange between para-substituted benzyl chloride and the chloride ion both in the gas phase and in water at the Hartree-Fock level and B3LYP density functional theory level. The Monte Carlo simulations use the TIP3P water model and include the polarizability of the solute.	24

LIST OF FIGURES

Figure A.	Resonance form of the 4-hydroxy-benzyl chloride	14
Figure B.	C-Cl bond lengths at the transition states at the RHF/6-311G(d,p) level	15
Figure C.	C-Cl bond lengths at the transition states at the B3LYP/6-311G(d,p)level	19
Figure D.	The S _N 2 reaction between the para-SO ₃ ⁻ benzyl chloride and the chloride ion	22
Figure 1.	Energies (relative to infinite separation, in kcal/mole) <i>versus</i> the reaction coordinate (c=a-b a ₀) of the S _N 2 reaction between para substituted benzyl chlorides with different para substitutions and the chloride ion in the gas phase at the RHF/6-311G(d,p) level	30
Figure 2.	Energies (kcal/mole) <i>versus</i> the reaction coordinate (c=a-b a ₀) of the S _N 2 reaction between para-substituted benzyl chlorides and the chloride ion in the gas phase with different para-substitutions at the B3LYP/6-311G(d,p)level relative to infinite separation	31
Figure 3.	Barrier heights (relative to the minimum energy, in kcal/mole) <i>versus</i> Hammett constants for the S _N 2 reaction between para substituted benzyl chlorides with different para-substitutions and the chloride ion in the gas phase at the RHF/6-311G(d,p)level	32
Figure 4.	Barrier heights (relative to the minimum energy, in kcal/mole) <i>versus</i> Hammett constants for the S _N 2 reaction between para substituted benzyl chlorides with different para-substitutions and the chloride ion in the gas phase at the B3LYP/6-311G(d,p)level	33
Figure 5.	Barrier heights (relative to the minimum energy, in kcal/mole) <i>versus</i> Hammett constants for the S _N 2 reaction between para substituted benzyl chlorides with different para-substitutions and the chloride ion in the gas phase at the MP2/6-311G(d,p)level	34
Figure 6.	Hartree-Fock energies (kcal/mole) <i>versus</i> the reaction coordinate (a ₀) of the S _N 2 reaction between the para-OCH ₃ benzyl chloride and the chloride ion in water and in the gas phase	35
Figure 7.	Hartree-Fock energies (kcal/mole) <i>versus</i> the reaction coordinate (a ₀) of the reaction between the para-OH benzyl chloride and the chloride ion in water and in the gas phase	36

LIST OF FIGURES, Continued

Figure 8.	Hartree-Fock energies (kcal/mole) <i>versus</i> the reaction coordinate (a_0) of the S_N2 reaction between the para- CH_3 benzyl chloride and the chloride ion in water and in the gas phase	37
Figure 9.	Hartree-Fock energies (kcal/mole) <i>versus</i> the reaction coordinate (a_0) of the S_N2 reaction between the para- NH_2 benzyl chloride and the chloride ion in water and in the gas phase	38
Figure 10.	Hartree-Fock energies (kcal/mole) <i>versus</i> the reaction coordinate (a_0) of the S_N2 reaction between the para- $\text{C}(\text{CH}_3)_3$ benzyl chloride and the chloride ion in water and in the gas phase	39
Figure 11.	Hartree-Fock energies (kcal/mole) <i>versus</i> the reaction coordinate (a_0) of the the S_N2 reaction between the benzyl chloride and the chloride ion in water and in the gas phase	40
Figure 12.	Hartree-Fock energies (kcal/mole) <i>versus</i> the reaction coordinate (a_0) of the S_N2 reaction between the para-F benzyl chloride and the chloride ion in water and in the gas phase	41
Figure 13.	Hartree-Fock energies (kcal/mole) <i>versus</i> the reaction coordinate (a_0) of the S_N2 reaction between the para-Cl benzyl chloride and the chloride ion in water and in the gas phase	42
Figure 14.	Hartree-Fock energies (kcal/mole) <i>versus</i> the reaction coordinate (a_0) of the S_N2 reaction between the para-Br benzyl chloride and the chloride ion in water and in the gas phase	43
Figure 15.	Hartree-Fock energies (kcal/mole) <i>versus</i> the reaction coordinate (a_0) of the S_N2 reaction between the para-I benzyl chloride and the chloride ion in water and in the gas phase	44
Figure 16.	Hartree-Fock energies (in kcal/mole) <i>versus</i> the reaction coordinate (a_0) of the S_N2 reaction between para- CF_3 benzyl chloride and the chloride ion in water and in the gas phase. Because of symmetry, only half of the reaction path is shown	45
Figure 17.	Hartree-Fock energies (kcal/mole) <i>versus</i> the reaction coordinate (a_0) of the S_N2 reaction between the para-CN benzyl chloride and the chloride ion in water and in the gas phase	46
Figure 18.	Hartree-Fock energies (kcal/mole) <i>versus</i> the reaction coordinate (a_0) of the S_N2 reaction between the para- NO_2 benzyl chloride and the chloride ion in water and in the gas phase	47

LIST OF FIGURES, Continued

Figure 19.	B3LYP energies (kcal/mole) <i>versus</i> the reaction coordinate (a_0) of the S_N2 reaction between para-OCH ₃ benzyl chloride and the chloride ion in water and in the gas phase	48
Figure 20.	B3LYP energies (kcal/mole) <i>versus</i> the reaction coordinate (a_0) of the S_N2 reaction between the para-OH benzyl chloride and the chloride ion in water and in the gas phase	49
Figure 21.	B3LYP energies (kcal/mole) <i>versus</i> the reaction coordinate (a_0) of the S_N2 reaction between the para-C(CH ₃) ₃ benzyl chloride and the chloride ion in water and in the gas phase	50
Figure 22.	B3LYP energies (kcal/mole) <i>versus</i> the reaction coordinate (a_0) of the S_N2 reaction between the para-CH ₃ benzyl chloride and the chloride ion in water and in the gas phase	51
Figure 23.	B3LYP energies (kcal/mole) <i>versus</i> the reaction coordinate (a_0) of the S_N2 reaction between the benzyl chloride and the chloride ion in water and in the gas phase	52
Figure 24.	B3LYP energies (kcal/mole) <i>versus</i> the reaction coordinate (a_0) of the S_N2 reaction between the para-NH ₂ benzyl chloride and the chloride ion in water and in the gas phase	53
Figure 25.	B3LYP energies (kcal/mole) <i>versus</i> the reaction coordinate (a_0) of the S_N2 reaction between the para-F benzyl chloride and the chloride ion in water and in the gas phase	54
Figure 26.	B3LYP energies (kcal/mole) <i>versus</i> the reaction coordinate (a_0) of the S_N2 reaction between the para-Cl benzyl chloride and the chloride ion in water and in the gas phase	55
Figure 27.	B3LYP energies (kcal/mole) <i>versus</i> the reaction coordinate (a_0) of the S_N2 reaction between the para-Br benzyl chloride and the chloride ion in water and in the gas phase	56
Figure 28.	B3LYP energies (kcal/mole) <i>versus</i> the reaction coordinate (a_0) of the S_N2 reaction between the para-I benzyl chloride and the chloride ion in water and in the gas phase	57
Figure 29.	B3LYP energies (kcal/mole) <i>versus</i> the reaction coordinate (a_0) of the S_N2 reaction between the para-CF ₃ benzyl chloride and the chloride ion in water and in the gas phase	58

LIST OF FIGURES, Continued

Figure 30.	B3LYP energies (kcal/mole) <i>versus</i> the reaction coordinate (a_0) of the S_N2 reaction between the para-CN benzyl chloride and the chloride ion in water and in the gas phase	59
Figure 31.	B3LYP energies (kcal/mole) <i>versus</i> the reaction coordinate (a_0) of the S_N2 reaction between the para-NO ₂ benzyl chloride and the chloride ion in water and in the gas phase	60
Figure 32.	B3LYP energies (kcal/mole) <i>versus</i> the reaction coordinate (a_0) of the S_N2 reaction between the para-SO ₃ ⁻ benzyl chloride and the chloride ion in water and in the gas phase	61
Figure 33.	Transition state energies (relative to infinite separation, in kcal/mole) <i>versus</i> Hammett constants of the S_N2 reaction between para-substituted benzyl chlorides with different para substitutions and the chloride ion in the gas phase, at the RHF/6-311G(d,p)level	62
Figure 34.	Transition state energies (relative to infinite separation, in kcal/mole) <i>versus</i> Hammett constants of the S_N2 reaction between para-substituted benzyl chlorides with different para substitutions and the chloride ion in the gas phase, at the B3LYP/6-311G(d,p)level	63
Figure 35.	Transition state energies (relative to infinite separation, in kcal/mole) <i>versus</i> Hammett constants of the S_N2 reaction between para-substituted benzyl chlorides with different para substitutions and the chloride ion in the gas phase, at the MP2/6-311G(d,p)level	64
Figure 36.	Energies of the reaction complex (relative to infinite separation, in kcal/mole) <i>versus</i> Hammett constants for the S_N2 reaction between para-substituted benzyl chlorides with different para-substitutions and the chloride ion in the gas phase at the RHF/6-311G(d,p)level	65
Figure 37.	Energies of the reaction complex (relative to infinite separation, in kcal/mole) <i>versus</i> Hammett constants for the S_N2 reaction between para-substituted benzyl chlorides with different para-substitutions and the chloride ion in the gas phase at the B3LYP/6-311G(d,p)level	66
Figure 38.	Energies of the reaction complex (relative to infinite separation, in kcal/mole) <i>versus</i> Hammett constants for the S_N2 reaction between para-substituted benzyl chlorides with different para-substitutions and the chloride ion in the gas phase at the MP2/6-311G(d,p)level	67

I. INTRODUCTION

Water has unique physical properties, such as large heat capacity, unusual density, high surface tension, hydrogen bonds, fluidity, high dielectric constant, higher boiling and freezing temperatures than molecules of similar size and mass. These physical properties affect the life of human-beings on a daily basis. About 60 percent of the human body is comprised of water, and water is the most abundant liquid on Earth.

Chemical reactions using water as a solvent are crucial for life, the environment, and technology. Therefore, researching chemical reactions with computational modeling can give us valuable insight on the reactivity of water. Computational modeling of aqueous reactions has a long history. However, despite our knowledge about modeling of aqueous reactions, water is still one of the most difficult solvents to model because of its highly polar and strongly hydrogen-bonding nature. The high dielectric constant of water has a profound influence on chemical reactions that involve charge separation or polar groups. In this thesis, comparisons will be made between the energy profiles and barriers in S_N2 reactions in a vacuum and in aqueous solution.

Computational chemistry can, in principle, provide information about reactions that are difficult to obtain experimentally. Chemical reactions in water solution behave differently from the chemical reactions in a vacuum because of hydrogen bonds and electrostatic interactions between water molecules and reactants. The barrier energies of chemical reactions in a water solution can show changes compared to those in a vacuum. According to the study of $CCl_4 + OH^-$ which used combined quantum mechanical/molecular mechanics (QM/MM), the reaction barrier for the aqueous solution was 10.5 kcal/mol higher than the barrier in the gas phase (Chen, Yin, Wang, Valiev, 2012).

When reactants favorably interact with water molecules, they dissolve in water. Dissolving reactants in water molecules affects the chemical reactions energetically, so considering the dissolving process during the reaction pathway will give more information about potential energy surfaces of reactions. If the simple S_N2 reaction between Cl^- and CH_3Br is considered in water, it can be seen that energy changes depend on the free energy change of the reactants in water. As an example, the rate constant of the $Cl^- + CH_3Br$ reaction in water is 15 orders of magnitude smaller than in the gas phase (Chen, Yin, Wang, Valiev, 2012), and the reaction rate for the S_N2 reaction of $Cl^- + CH_3Cl \rightarrow ClCH_3 + Cl^-$ in the gas phase is 20 orders of magnitude higher than that in the aqueous solution (Mineva, Russo, Scilia, 1998). When two reactants come into direct contact in solution, the solvation shells have to be partially broken up. Thus, we can expect that solvated molecules react more slowly than in vacuum. However, other reactions are sped up in water. For instance, barriers of charge separation are greatly reduced in high dielectric constant solvents, and such reactions are faster in water.

Computational chemistry has become an advantageous way to work on materials which are too expensive and too difficult to find before doing real experiments. This gives additional information that helps scientists better plan their experiments. That is, computational chemistry will help us save time and money. However, the calculations via computational chemistry must be fast and reliable, the latter meaning close to physical reality.

II. BACKGROUND

The S_N2 reaction profile of $Cl^- + CH_3Cl$ in the aqueous solution was first published with simulations explicitly including 250 water molecules and thermal averaging by Jorgensen and his coworkers. They used ab initio 6-31G* calculations first to obtain the energy profile of this

reaction in the gas phase. This was followed by the calculation of the potential of the mean force in aqueous solution in the NPT ensemble at 1 atm and 25 °C (Chandrasekhar, Smith, Jorgensen, 1984). The approaches for modeling the solvent effect have been further developed for the last 30 years. These can be separated into two parts which are explicit models and implicit models. Explicit models are more accurate than implicit models.

Explicit solvent models consider a large number (typically hundreds or thousands) of solvent molecules, such as water, placed around the simulated solute to resemble the physical reality. They have been the methods used for carrying out simulations in solvent when more accurate results have been desired. However, calculations with explicit models are expensive because of the large number of particles involved. Treating hundreds or thousands of solvent molecules at a high quantum mechanical level is nearly impossible even with the most powerful supercomputers. The usual strategy is to treat only the solute at the quantum mechanical (QM) level, and model the solvent with much less expensive Molecular Mechanics (MM) methods. This is permissible if the solvent is a small, rigid molecule which does not participate directly in the reaction. Essentially all accurate solution modelings are performed using such QM/MM methods. Even if inexpensive MM methods are used for the solvent, QM/MM calculations need orders of magnitude more CPU time than gas phase calculations on the same molecule, mainly because of the need to average over a large number of solvent configurations. The solvation shell around a molecule is very flexible, and is continuously rearranging even at room temperature. The observable data correspond to a Boltzmann average of the solvent configurations.

Implicit models use the solvent as a continuous medium surrounding the solute outside of its van der Waals surface, with the average properties of the real solvent. A variety of continuum models have been described, such as the Surface Area (SA), and generalized Born (GB) models

(Zhou, 2003). However, implicit model does not completely reflect the physical reality, so calculations with implicit models may be less accurate or even misleading.

From the paper “Solvent Effect on S_N2 Reaction between Substituted Benzyl Chloride and Chloride Ion” by Ebrahimi and his coworker in 2012, the free energies of some S_N2 reactions, not all of which my study covers, were calculated by DFT and ab initio methods. However, they used the polarizable continuum model, which is an implicit water model. The focus of the study of Ebrahimi was the effects of solvent on S_N2 reaction using the polarizable continuum model, so they did not deeply investigate the behaviors of the S_N2 reactions in water. Therefore, researching S_N2 reactions and their behaviors can give more detailed information by using explicit water models to enlighten scientists concerning its nature. Also, in the study “Water Assisted Reaction Mechanism of OH^- with CCl_4 in Aqueous Solution”, an approximate (averaged) polarization, which is a procedure similar to charge fitting, was used (Chen, Yin, Wang, Valiev, 2013). Overall, most previous work neglects the polarization. However, calculations with polarizabilities in solute will give more reliable results because molecules, in reality, have polarizations during the reaction time. One of the goals of this study is to assess the importance of the polarization of the quantum (QM) system for the barrier.

To obtain good statistics for the free energy, explicit models require a large number of calculations ($\sim 10^6$) for each point on the reaction path. In these calculations, the solvent configurations are different, and are averaged to obtain thermodynamic variables like free energy. The main problem is that the quantum calculations have to be repeated many times, since the surroundings, mainly the electrostatic potential around the solute, are different for each solvent configuration. Even if a single quantum (QM) calculation takes only a few minutes, millions of them would take years or centuries. Therefore, in this study, the S_N2 reactions have been

simulated in water using an ultrafast QM/MM model. Ultrafast QM/MM (Janowski, Wolinski, Pulay, 2012) can calculate energies and other properties of quantum systems in solutions much faster (by about four orders of magnitude or more) than traditional QM/MM. In this method, a single energy evaluation takes only ~ 0.01 seconds, while it preserves the full accuracy of QM/MM. This is achieved by pre-calculating the response of the system to the electrostatic field of the solvent molecules. It uses the fact that the principal effect of the polar solvent on the solute is electrostatic, and the response of the system to electrostatic field of the solvent can be evaluated from its response properties in advance, by determining its generalized polarizability (GP) components. Once the Generalized Polarizabilities are available, no quantum calculations are necessary to perform simulations with an arbitrary number of solvent configurations.

III. COMPUTATIONAL METHODOLOGY

The main methods used in this thesis are the Restricted Hartree-Fock (RHF, that is closed shell Hartree-Fock), and the Density Functional Theory (DFT) techniques. The results also depend on the atomic orbital basis sets chosen to describe the molecular orbitals. However, this effect saturates for larger basis sets, and for the relatively large basis sets used here is expected to be small. DFT also depends on the exchange-correlation functional used. However, most functionals give results which are similar. We employed the most widely used variant, the 3-component Becke-Lee-Yang-Parr hybrid functional (B3LYP). For the vacuum calculations, we also used a higher level correlation method, second order Møller-Plesset perturbation theory. However, the programs to use MP2 in the solvation simulations are not yet available.

Hartree Fock (HF) and Density Functional theories (DFT) are different methods to perform computational chemistry. HF theory is a wavefunction approach depending on the mean field approximation. In the Hartree-Fock theory, the energy has this form,

$$\text{Energy (HF)} = h + J - K + V_{\text{nuc}}$$

where h represents the one-electron (potential+kinetic) energy, J represents the classical Coulomb repulsion of electrons, K represents the exchange energy which arises from the quantum (fermion) nature of electrons, and V_{nuc} represents the nuclear repulsion energy.

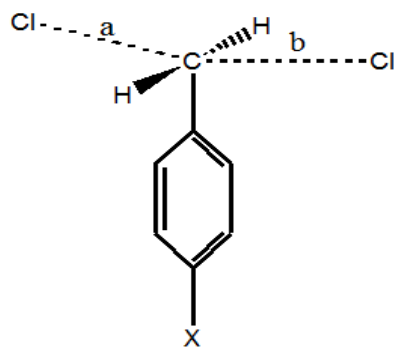
The DFT method obtains the energies from the electron density rather than the more complicated wavefunctions. In the density functional theory, the exchange-correlation functional is used instead of the Hartree Fock exchange for a single determinant. This exchange-correlation functional can have terms giving exchange energy and the electron correlation as well. However, this electron correlation is omitted from the Hartree Fock method. In the DFT theory, the energy simply has this form below which is stated as a functional of the molecular electron density (ρ).

$$\text{Energy (DFT)} = T[\rho] + V_{\text{ne}}[\rho] + J[\rho] + E_{\text{x}}[\rho] + E_{\text{c}}[\rho] + V_{\text{nuc}}$$

where $T[\rho]$ represents the kinetic energy, $V_{\text{ne}}[\rho]$ represents the nuclei-electron interaction, $E_{\text{x}}[\rho]$ and $E_{\text{c}}[\rho]$ represent the exchange and correlation energy functionals respectively.

Using both DFT and Hartree-Fock theory allows us to estimate the errors in the calculations, as these methods often bracket the correct results. DFT is generally more reliable for molecular geometries, and it was used to obtain the molecular geometries for the Monte Carlo simulations (MC).

In this study, S_N2 halogen exchange reactions were studied between para-substituted benzyl chlorides and the chloride ion. The substituents were $-NH_2$, $-OH$, $-Cl$, $-F$, $-Br$, $-I$, $-OCH_3$, $-NO_2$, $-CF_3$, $-CN$, $-CH_3$, $-C(CH_3)_3$, and the parent compound, benzyl chloride. The gas phase reactions are fairly straightforward on modern computers, and several different methods (Restricted Hartree-Fock = RHF), density functional theory with the B3LYP exchange-correlation functional, and second-order Møller-Plesset perturbation theory (MP2) and basis sets, such as the 6-311G(d,p) and aug-cc-pVDZ were employed to explore the sensitivity of the results to electron correlation effects and basis set choices. All calculations were performed by the PQS program. However, with the exception of the Generalized Polarizabilities, a number of quantum chemistry packages have the capability of performing these calculations. The reaction coordinates have been scanned from $-11.0 a_0$ to $+11.0 a_0$ (Bohr radius or atomic unit of distance; $1 a_0 \approx 0.529177 \text{ \AA}$) of the value (a-b). The latter is the difference of the two C-Cl distances, from the central carbon (the reaction center) to the two chlorines. Then, the molecular configurations along the reaction path have been determined by optimizing the geometry under constraint of a fixed value of the reaction coordinate. These coordinates have been used in Monte Carlo simulations to obtain solvation energies. In principle, solvation may change the reaction path but in practice this effect is expected to be minor in our case.



Step size is $0.05 a_0$ for a-b,
e.g 0.0, 0.05, 0.10, 0.15, 0.20, 0.25, 0.30, 0.35,
0.40, 0.45, 0.50, so on

X = NH_2 , OH , OCH_3 , CH_3 , $C(CH_3)_3$, H , F , Cl , Br ,
 I , CF_3 , CN , NO_2 , etc.

The figure above helps visualize these quantities. The quantity **a** is the distance between the central carbon and the leaving Cl atom on the left above the figure. **b** is the distance between the approaching Cl atom and the C atom at the reaction center. The difference of the two, **c**, characterizes the progress of the reaction.

The gas phase reaction paths were used to obtain the energies and free energies of the S_N2 reactions in water by QM/MM Monte Carlo simulations.

IV. GEOMETRY OPTIMIZATION

Geometry optimization is a tool to obtain minimum energy structures and minima on the potential energy surface. Another name for geometry optimization is energy minimization of molecules. During geometry optimization, the coordinates of the atoms are modified to decrease its energy until it hits a local minimum which corresponds to the desired chemical species.

Geometry optimizations was performed by the PQS program for 440 values of the reaction coordinate **c=a-b** -11.0 a₀ to +11.0 a₀, in steps of 0.05 a₀. As this is an exchange of identical atoms, the reaction paths are symmetrical to the origin, and **c** and **-c** should give the same energies. We decided to map the whole reaction path to check whether it is symmetrical, and identify possible problems or inaccuracies. The coordinates corresponding to **c** values between 0.0 a₀ and 7.0 a₀, were used in the Monte Carlo simulations.

Figures 1 and 2 show that all systems show a deep potential well in the gas phase at about **c**=2.8 a₀ (about 1.5 Å), bound by 7-14 kcal/mol relative to infinite separation. This is common for both the Hartree-Fock and the DFT levels, and corresponds to a reactive complex of a substituted benzyl chloride with a chloride anion, held together by electrostatic forces. However, as I will show later, (Figures 12 to 37), the reaction complex is much less strongly bound in

aqueous solution. This is expected, as water strongly screens the electrostatic interaction between the molecule and the chloride ion at larger distances. The barrier to chloride exchange relative to the reaction complex increases with the electronegativity of the substituent but is in the 15 kcal/mol range at the Hartree-Fock (RHF) level, in the 5-6 kcal/mol level at the B3LYP level, and the 10-11 kcal/mol level at the MP2 level in the gas phase. The last result should be the most reliable because Hartree-Fock theory generally overestimates reaction barriers, and DFT underestimates them. Note that in the presence of water as a solvent, the differences in the barriers diminish, and Hartree-Fock is only 3-5 kcal/mol higher (in the 15-23 kcal/mol range) than DFT with the B3LYP functional (12-19 kcal/mol); see table 3. The accurate value is probably between these two.

Changing the $-x$ axis as Hammett constant and the $-y$ axis as free energies (kcal/mole), figures 3 through 5 were obtained for the barrier heights of S_N2 reactions in the gas phase in order to compare the energy changes at RHF, B3LYP, and MP2 levels. Hammett constants are scaled from -1 to +1 because this scale gives more insights to comment on reactions. The scale of -1 through 0 roughly shows that substituted groups behave as electron-donating, while the scale of 0 through +1 roughly shows that substituted groups behave as electron-withdrawing. Calculating reaction rates should not be logical because Cl exchanges with Cl. Also, to obtain more insights for the S_N2 ligand exchange reactions between the chloride anion and para-substituted benzyl chlorides in the gas phase, figures 33 through 38 were created.

From the figures 3 through 5 and 33 through 38, $-NH_2$ and $-OH$ substituent groups deviate from the correlations that the other substituent groups make, because C-C-N-H torsional bond was restricted to 120° and C-C-O-H torsional bond was restricted to 0° for the S_N2

reactions with -NH_2 and -OH substituent groups respectively in order to obtain symmetric reaction coordinates during the $\text{S}_{\text{N}}2$ reaction.

In fact, geometry coordinates from the MP2 results were not obtained in this study. The reason to obtain a correlation from the MP2 calculations in this study is to verify the accuracies of the calculations for the $\text{S}_{\text{N}}2$ reactions in the gas phase using the Hartree Fock theory and the DFT theory.

In the gas phase, nucleophiles, such as Cl^- , which will make bonds with the central carbon with stronger electrostatic character cause lower energetic barriers because of decreased electron repulsion at the transition state (Uggerud, 2006). That is, the energy barriers of $\text{S}_{\text{N}}2$ reactions in this study decrease as the central carbon is made more electrostatic by the substituent groups. However, the interactions between substituent groups and Cl^- anion should be considered as well.

In addition, these substituent groups affect the reaction rate. To illustrate, because of the CN group, which is an electron-attractor, the charge on the reactive carbon atom of $\text{Cl}(\text{CH}_2)_n\text{CN}$ is decreased as the chain molecule gets shorter. This causes a higher reaction rate (Pagliai, Raugei, Cardini, & Schettino, 2003).

The reactions in this study were calculated in a vacuum by using the RHF method with the 6-311G(d,p) basis, the DFT method with the 6-311G(d,p) basis and the MP2 method with aug-cc-pvdz basis set. However, MP2 method was not used for Monte Carlo simulations. Actually, MP2 results were obtained for verifying the results with Hartree Fock and DFT methods, because calculating energy with the MP2 method at the Monte Carlo simulations in water would take too long, approximately up to 20 days for a calculation. It is known that DFT

calculations are a compromise between time and accuracy for calculations. Therefore, DFT and HF methods were used for all calculations in this work.

V. MONTE CARLO SIMULATIONS

The Monte Carlo (MC) method is a stochastic technique, which means that it is based on the random numbers and probability statistics to examine problems. The Monte Carlo method is very important for physical chemistry, computational sciences, and related applied fields, such as weather forecasting where ensemble models are used (Weickmann, Whitaker, Roubicek & Smith, 2001).

In this study, the energy behaviors of S_N2 reactions between the chloride ion and the benzyl chloride with some para-substitutions have been examined by using a QM/MM model and Monte Carlo simulations. Two different calculations have been done for each S_N2 reaction. While one calculation is with polarizability in solute system, the other is without polarizability. Both calculations have been achieved by applying the Hartree Fock (HF) theory and the density functional theory (DFT).

A. Hartree Fock Results

As seen in figure 6 through figure 18, the calculations have been obtained using the Restricted Hartree Fock method at the 6-311G(d,p) basis set and Monte Carlo simulation with explicit water model (TIP3P) with respect to infinite separations. In figure 6 through figure 18, X axis represents the difference (a_0) between a value and b value, and Y axis represents the energies (kcal/mole) with respect to infinite separations. The calculations have been done from 0.00 a_0 to 7.00 a_0 of the a-b values by taking 0.05 a_0 of the step size. That is, 141 different calculations

have been done for each S_N2 reaction using the Monte Carlo method with geometry coordinates obtained from the PQS program in the gas phase.

The figures from 6 to 18 show the half reaction coordinates for the S_N2 reaction between the para-substituted benzyl chloride and the chloride ion in the gas phase and in water because all the reaction coordinates for S_N2 reactions are symmetric. Also, two different calculations for these reactions have been done in water, which are with polarizability and without polarizability in solute in order to see the importance of the use of polarizabilities in solute in terms of energy changing.

The reactions in water, without polarizability in solute, do not show smooth reaction paths energetically because they are still decreasing until $7.00 a_0$ of the a-b values; see figure 6 to 18. To obtain the minimum energy values of the calculations in order to compare the energies in the gas phase, with polarizability in solute in water, and without polarizability in solute in water, the points beyond $7.00 a_0$ were calculated for the reaction between the chloride ion and the benzyl chloride with para-OH substitution in water; see the blue line in figure 7. However, the minimum energy is obtained around $9.0 a_0$, which is a long distance for atoms in water. After the point of $9.00 a_0$, the energy of the system for the reaction with para-OH substitution increases, where it is possible to see long range errors. Therefore, the elaborate comparison of these energies without polarizability in solute is difficult because the minimum energy point cannot be fixed to zero (kcal/mole). However, it can be easily seen that the reaction barriers for these reactions without polarizability in solute in water are dramatically higher than the reaction barriers for the reactions with polarizability in solute in water, and also in the gas phase; see figures 6 to 18. Consequently, it can be said that including polarizability in solute for Hartree Fock theory is necessary for calculations in water.

The minima of the other two lines, representing the reactions with polarizability in solute in water and in the gas phase (see figures 6 to 18), were fixed to zero energetically in order to compare the energy changes between these reactions. Many reaction barriers in water in this study are higher than the reaction barriers in the gas phase because the solvation shells have to be partially broken for two reactants to come into direct contact in solution. Also, this can be explained, making an activated complex in aqueous solution is prevented by the solvation cluster around the para-substituted benzyl chloride and the chloride ion. To support this idea, it is difficult to form an activated complex of OH^- and CH_3Cl in aqueous solution because this is prevented by the solvation cluster around the OH^- . This is caused by the increase in the HOMO volume of the excess charge during the approach of the OH^- to CH_3Cl (Hori, Takahashi, Nitta, 2002). On the other hand, the interaction between the chloride ion and para-substituent for each reaction in this study should be taken into account because some substituents facilitate the making of an activated complex, such as para- NH_3^+ group attracting the chloride ion towards the benzyl chloride molecule, while the others obstruct the making of an activated complex, such as para- SO_3^- repulsing the chloride ion; seen in DFT calculations.

To obtain better insight in the para-substituent effect, it is useful to examine resonance forms of molecules. For instance, the OH group is an electron donating group; see figure A.

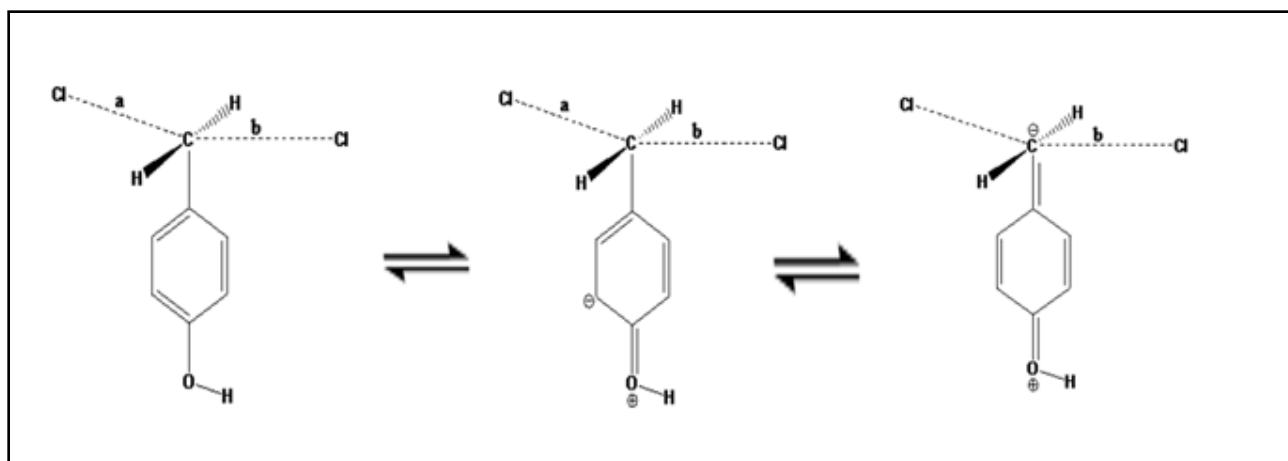


Figure A. Resonance form of the 4-hydroxy-benzyl chloride at the transition state

From the resonance form of the molecule above, it is easy to see that the -OH group makes the central carbon atom partially negatively charged at the transition state. This causes the bond distance between the central carbon atom and the chloride ion to be longer during the transition state because of the repulsion between the central carbon atom (δ^-) and the negatively charged chloride ion. This repulsion makes the bond lengths of each reaction in this study for the chloride ion and the central carbon atom longer during the transition states; see figure B on the next page. Overall, this affects the energy barriers in the gas phase and in water at the energetically different amounts. For example, two reactants will need more energy to get rid of the solvation cluster around the chloride anion and the central carbon until the bond length comes to a sufficient distance in order to form a new C-Cl bond during the transition state. That is, energy barriers increase in water, while the Hammett constants go up for the para-substituents.

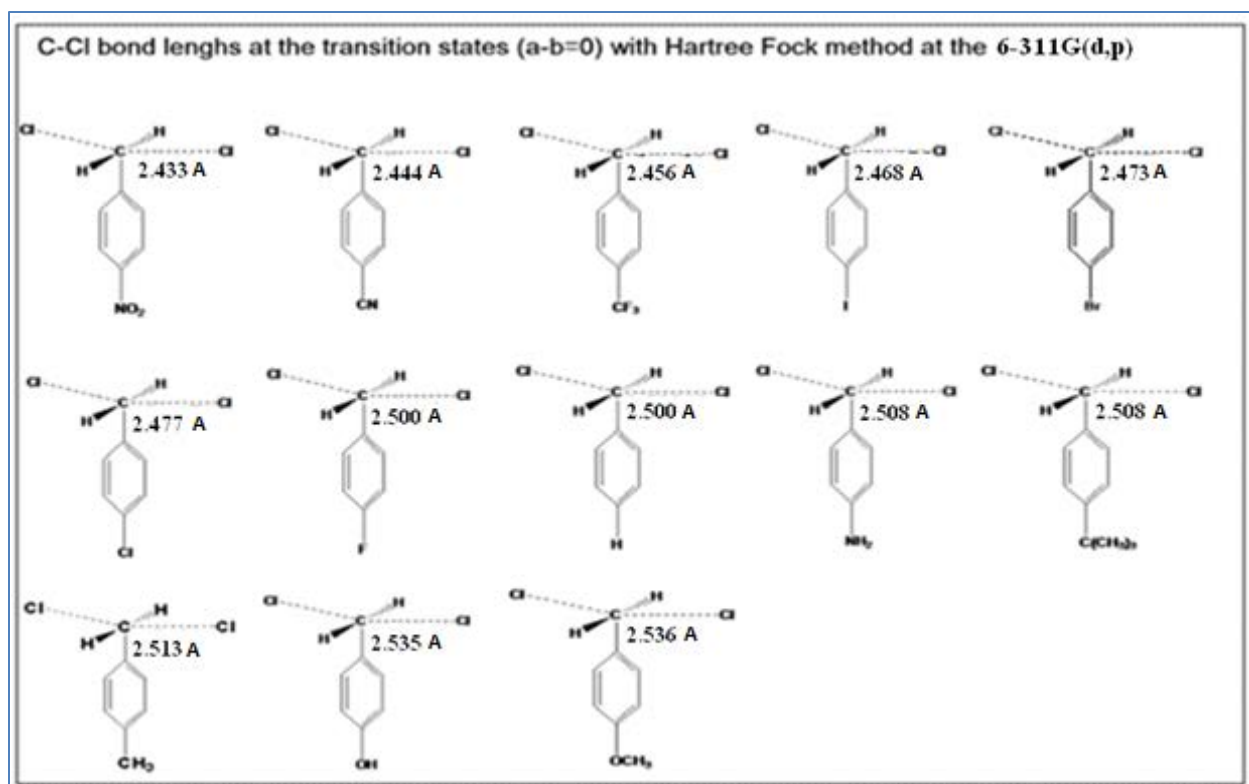


Figure B. C-Cl bond lengths at the transition states at the RHF/ 6-311G(d,p) level. Hammett constants increase from right to left.

For a comparison of energy differences between the reactions in the gas phase and the reactions with polarizability in solute in water at the transition states, a table has been created representing energy differences versus Hammett constants; see table 1 on the next page. It is easy to see that energy differences between the reactions in the gas phase and the reactions with polarizability in solute in water generally increase, as does the Hammett constants.

However, some deviations can be seen from electron donating groups in table 1. For instance, para-NH₂ with the hammett constant of -0.660 shows a higher energy difference at the transition state than para-OH with the Hammett constant of -0.370; see table 1. Actually, the reaction with para-NH₂ was anticipated to show a lower energy difference between in the gas phase and in water with polarizabilities in solute, compared to the reaction with para-OH. This is probably caused by the making of H bonds in water for para-OH and para-NH₂. To clarify, an

OH group exhibits stronger bonding than a NH₂ group when comparing amines to alcohols because oxygen is more electronegative than nitrogen. Therefore, the barrier height of the S_N2 reaction with para-OH in water is lower than that with para-NH₂ because the stronger making of H bonds for para-OH in water stabilizes the reaction more compared to para-NH₂.

	Substituents	Hammett Constants	Energy differences approximately between in gas phase and in water with polarizabilities
<i>Electron donating groups</i>	para-OCH ₃	-0.268	0.7 kcal/mol
	para-OH	-0.370	1.0 kcal/mol
	para-CH ₃	-0.170	1.4 kcal/mol
	para-NH ₂	-0.660	2.0 kcal/mol
	para-C(CH ₃) ₃	-0.197	2.1 kcal/mol
<i>No-substitution</i>	para-H	0.000	2.4 kcal/mol
<i>Electron accepting groups</i>	para-F	0.062	3.4 kcal/mol
	para-Cl	0.227	4.2 kcal/mol
	para-Br	0.232	4.6 kcal/mol
	para-I	0.276	5.2 kcal/mol
	para-CF ₃	0.540	5.6 kcal/mol
	para-CN	0.660	6.8 kcal/mol
	para-NO ₂	0.778	6.9 kcal/mol

Table 1. The effect of water solvent on the barrier height for the S_N2 chloride exchange between para-substituted benzyl chloride and the chloride ion at the Hartree-Fock level. The barrier in water minus the barrier in the gas phase is shown. The solute was treated at the Hartree Fock/6-311G(d,p) level. The Monte Carlo simulations use the TIP3P water model and include the polarizability of the solute.

Moreover, the electron donating degrees to the central carbon, where S_N2 reactions occur, change when para-substituents make H bonds with water molecules. This, also, affects the barrier heights of reactions. Furthermore, torsional angles may cause this unexpected results for

the S_N2 reaction with para-OH and para-NH₂ because we restricted these torsional angles to obtain symmetric paths. On the other side, steric effects of para-substitutional groups should be taken into account to compare reactions energetically because this, also, can affect the barrier height, such as para-CH₃ and para-C(CH₃)₃ for HF method.

B. DFT Results

As seen in figure 19 through figure 32, the calculations were obtained from the Density Functional Theory (DFT) at the 6-311G(d,p) basis set and from Monte Carlo simulation with explicit water model (TIP3P) with respect to infinite separations. In figure 19 through figure 32, X axis represents the difference (a_0) between a value and b value, while Y axis represents the energies (kcal/mole) with respect to infinite separations. The calculations were done from 0.00 a_0 to 7.00 a_0 of the a-b values by taking 0.05 a_0 of the step size. This means that 141 different calculations for each point, at the same number as HF calculations, were done for each S_N2 reaction using the Monte Carlo method with geometry coordinates obtained from PQS program in the gas phase.

The figures from 19 to 32 display the half reaction coordinates for the S_N2 reaction between the para-substituted benzyl chloride and the chloride ion in the gas phase and in water since all the reaction coordinates for S_N2 reactions are symmetric. Similar to HF calculations, two different DFT calculations for these reactions were done in water, which are with polarizability and without polarizability in solute in order to see the importance of the use of polarizabilities in solute in terms of energy changing.

Similar to HF calculations, DFT calculations need polarizability in solute in water because the S_N2 reactions without polarizability in solute in water do not show smooth reaction

paths energetically, which are still decreasing until 7.00 a_0 of the a-b values; see figure 19 to figure 32. Therefore, polarizability in solute is essential for both DFT and HF calculations.

The minimum points of the two lines, representing the half S_N2 reaction paths with polarizability in solute in water and in the gas phase (see figures 19 to 31), were fixed to zero energetically in order to compare the energy changes between these reactions in terms of energy barriers. These energy barriers of the reactions with polarizability in solute in water are higher than the energy barriers of the reactions in the gas phase, which is similar to Hartree Fock calculations. The reason for the reaction barriers in water being higher than those in the gas phase is caused by the solvation shells which are able to be partially broken for two reactants to come into direct contact in water.

While two reactants are coming into direct contact in water, each S_N2 reaction with different para-substituents in this study needs different bond lengths at their transition states, which depend on para-substituent groups; see figure C. If para-substituent groups make the central carbon partially negatively charged, a repulsion between Cl anions and the central carbon occurs; see the resonance form of the 4-hydroxy-benzyl chloride at the transition state in figure A. At the transition state, this repulsion makes the bond lengths between the central carbon and Cl anions longer. Moreover, an attraction between Cl anions and the central carbon can happen by making partially positively charged on the central carbon at the transition state when the electron accepting groups are used for the para-substituent group of benzyl chloride. Unlike the repulsion between Cl anions and the central carbon, the attraction between Cl anions and the central carbon makes the bond lengths between the central carbon and Cl anions smaller at the transition state. Therefore, it can be concluded that electron donating groups at the para position of benzyl chloride cause the bond lengths between Cl anions and the central carbon longer than

those for benzyl chloride without any substitution group, while electron accepting groups at the para position of benzyl chloride cause the bond lengths between Cl anions and the central carbon shorter than those for benzyl chloride without any substitution group; see figure C below.

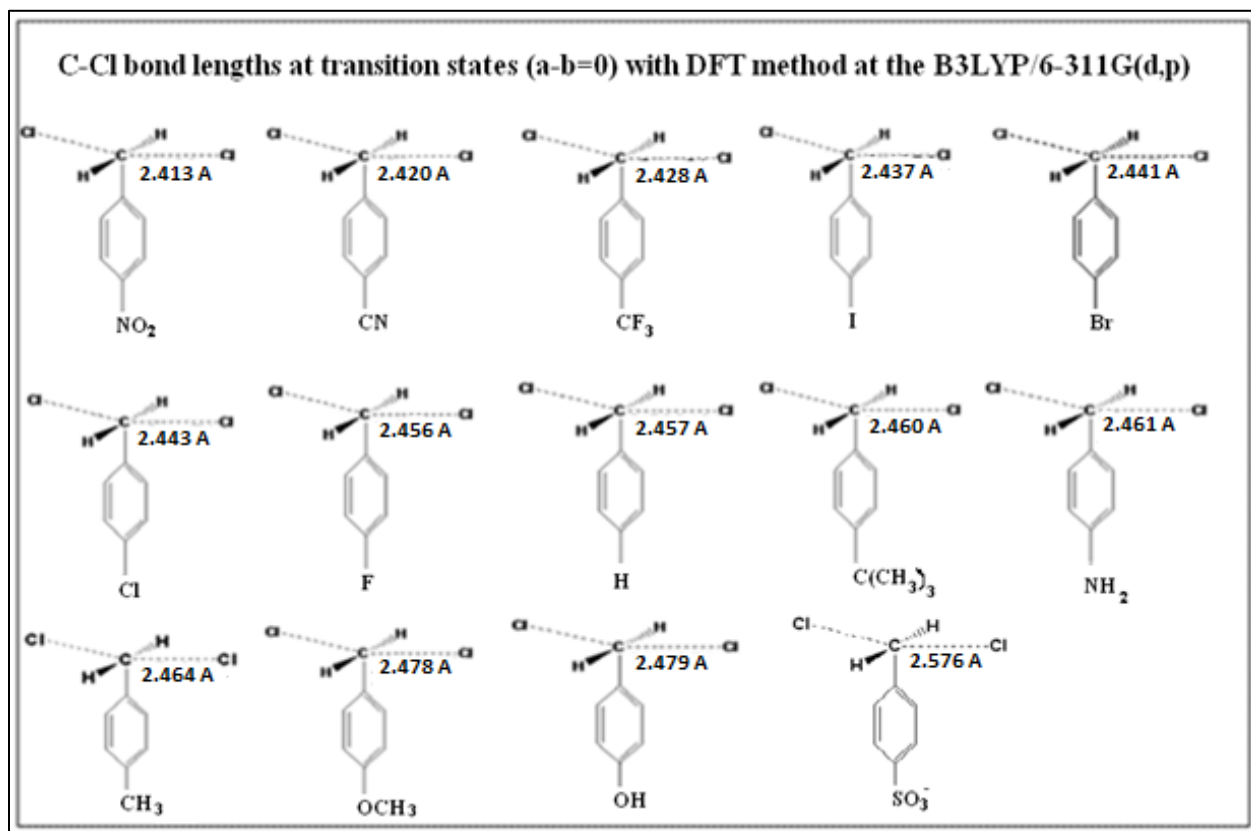


Figure C: C-Cl bond lengths at the transition states at the RHF/ 6-311G(d,p) level. Hammett constants increase from right to left except for the para-SO₃⁻ with Hammett constant of 0.09.

The energy barriers of these S_N2 reactions in water are affected with a large amount of energy (the range of 6.40 kcal/mole because of the substituent groups changing the distances of the bond lengths between Cl anions and the central carbon at the transition states, while the energy barriers of these S_N2 reactions in the gas phase are affected with a small amount of energy; such as the highest energy change is 0.80 kcal/mole; see table 3. That is, two reactants in water need more energy, compared to two reactants in the gas phase, to get rid of the solvation

cluster around the Cl^- anion and the central carbon until the bond length comes to a sufficient distance in order to form a new C-Cl bond during the transition state.

To obtain better insight, table 2 was created which shows the energy behaviors of the $\text{S}_{\text{N}}2$ reactions in this study by comparing their Hammett constants to the energy differences at the transition states between the reactions in water, which has polarizability in solute and the reactions in the gas phase. From table 2 calculations using the DFT method, it is easy to see that energy differences between the reactions in the gas phase and the reactions with polarizability in solute in water generally increase, as does the Hammett constants.

	Substituents	Hammett Constants	Energy differences approximately between in the gas phase and in water with polarizabilities
Electron donating groups	para- OCH_3	-0.268	6.2 kcal/mol
	para-OH	-0.370	6.8 kcal/mol
	para- $\text{C}(\text{CH}_3)_3$	-0.197	7.6 kcal/mol
	para- CH_3	-0.170	7.9 kcal/mol
No-substitution	para-H	0.000	8.0 kcal/mol
Electron donating group	para- NH_2	-0.660	8.3 kcal/mol
Electron accepting groups	para-F	0.062	8.9 kcal/mol
	para-Cl	0.227	9.6 kcal/mol
	para-Br	0.232	9.7 kcal/mol
	para-I	0.276	9.8 kcal/mol
	para- CF_3	0.540	10.6 kcal/mol
	para-CN	0.660	12.0 kcal/mol
	para- NO_2	0.778	13.2 kcal/mol

Table 2. The effect of water solvent on the barrier height for the $\text{S}_{\text{N}}2$ chloride exchange between para-substituted benzyl chloride and the chloride ion at the B3LYP density functional theory level. The barrier in water minus the barrier in the gas phase is shown. The solute was treated at the B3LYP/6-311G(d,p) level. The Monte Carlo simulations use the TIP3P water model and include the polarizability of the solute.

Table 2 and figure C show similar results in that electron donating groups decrease the energy barriers of these S_N2 reactions compared to hydrogen, while electron accepting groups increase the energy barriers in water. This is caused by the resonance form of the para-substituted benzyl chloride; see figure A. To clarify, electron donating groups make the central carbon partially negatively charged. This causes the bond lengths between the central carbon and Cl anions for the S_N2 reactions with an electron donating group at the para position to be longer than the bond lengths between the central carbon and Cl anions for the S_N2 reactions without any groups at the para position; see figure C. That is, S_N2 reactions with electron donating groups at the para position in water have lower energy barriers than those without any substituent groups in order to come into sufficient bond lengths between the central carbon and Cl anions at the transition states by breaking the solvation shells. In contrast, the S_N2 reactions with electron accepting groups at the para position in water have higher energy barriers compared to those without a group at the para position.

Generally, the energy differences between the reactions in water, which has polarizability in solute, and the reactions in the gas phase increase for the S_N2 reaction between the para-substituted benzyl chloride and the chloride ion at the transition states when Hammett constants of para-substituents go up. However, there are some deviations caused by electron donating groups. These deviations probably come from the making of hydrogen bonds between water molecules and para-substituents; such as $-OH$ and $-NH_2$. Another possibility of these deviations could be torsional restrictions. To obtain symmetrical reaction coordinates, the torsional angles of para- OH benzyl chloride and para- NH_2 benzyl chloride were restricted to 120° for C-C-N-H torsional bond and 0° for C-C-O-H torsional bond.

So far, all of the reactions in water show higher barrier heights than those in the gas phase, but some S_N2 reactions for the para-substituted benzyl chloride and the chloride ion behave differently when the para-substituent group change with charged substituent group; such as $-\text{SO}_3^-$ and $-\text{NH}_3^+$.

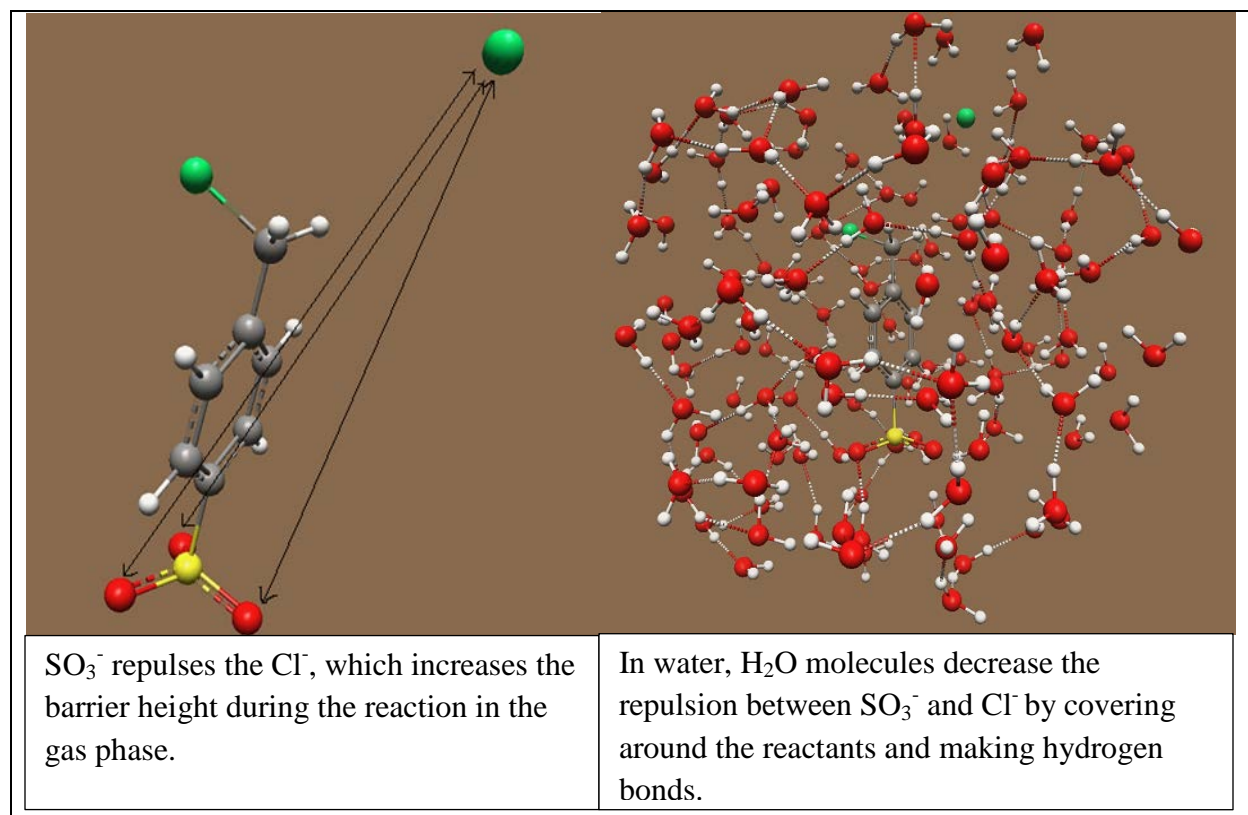


Figure D. The S_N2 reaction between the para- SO_3^- benzyl chloride and the chloride ion.

As seen in figure D, SO_3^- repulses the Cl^- anion during the reaction, which makes the energy barrier for this S_N2 reaction in the gas phase dramatically higher than the energy barrier for this S_N2 reaction in water; see figure 32. Water molecules stabilize this repulsion by covering SO_3^- and the chloride anion. Therefore, the energy barrier for this S_N2 reaction in water is lower than the barrier for this S_N2 reaction in the gas phase. Also, we can conclude that the percentage of this reaction occurring in the gas phase is low, while the percentage of this reaction occurring in water is considerably high when considering their energy barriers.

Unlike $-\text{SO}_3^-$ substituent group, $-\text{NH}_3^+$ attracts the Cl^- anion during the $\text{S}_{\text{N}}2$ reaction between the para- NH_3^+ benzyl chloride and the chloride ion in the gas phase, and this reaction ends up with para- NH_2 benzyl chloride and HCl . That is, $\text{S}_{\text{N}}2$ reaction occurring for this reaction in the gas phase is almost impossible, while a $\text{S}_{\text{N}}2$ reaction occurring for this reaction in water is noticeably possible.

VI. CONCLUSIONS

In the gas phase and in water solution, I calculated the $\text{S}_{\text{N}}2$ reactions of the chloride ion and the benzyl chloride with different groups at the para position using an ultrafast QM/MM model for PQS program and MC simulations, and these calculations took a much shorter time than traditional calculations. With this ultrafast QM/MM model (Janowski, Wollinski, Pulay, 2012), a single energy evaluation takes only ~ 0.01 seconds, while it preserves the full accuracy of QM/MM.

This study proves that the $\text{S}_{\text{N}}2$ reactions in water solution behave differently from those in the gas phase because of electrostatic interactions and hydrogen bonds between water molecules and reactants. In the gas phase, nucleophiles, such as Cl^- , which will make bonds with the central carbon with stronger electrostatic character cause lower energetic barriers because of decreased electron repulsion at the transition state, while, in water solution, nucleophiles which will make bonds with the central carbon with stronger electrostatic character cause higher energetic barriers because the solvation shells have to be partially broken up for two reactants to come into direct contact in water.

The calculations using both Hartree Fock theory and Density Functional theory show that energy barriers for the $\text{S}_{\text{N}}2$ reactions of the para-substituted benzyl chloride and the chloride anion in water increase, as do the Hammett constants of para-substituent groups; see table 3. The

DFT calculations for the reactions in this study are generally consistent with the HF calculations, although DFT and HF are different methods. Also, these calculations demonstrate that adding polarizability in solute in water to the calculations is necessary in order to obtain reliable results from Monte Carlo simulation because molecules, in reality, have polarizations during the reaction time.

Para Substituents	Barrier heights (kcal/mole)			
	RHF/6-311G(d,p) in the gas phase	B3LYP/6-311G(d,p) in the gas phase	RHF/6-311G(d,p) with polarizability in solute in water	B3LYP/6-311G(d,p) with polarizability in solute in water
OCH ₃	14.09	5.75	14.80	11.95
OH	14.02	5.72	15.04	12.52
CH ₃	14.75	5.90	16.20	13.80
NH ₂	14.95	5.88	16.95	14.18
C(CH ₃) ₃	14.91	5.87	17.04	13.47
H	15.12	5.97	17.52	14.00
F	14.63	5.73	18.03	14.63
Cl	15.05	5.58	19.25	15.18
Br	15.17	5.57	19.77	15.27
I	15.24	5.54	20.44	15.34
CF ₃	15.42	5.45	20.82	16.05
CN	15.31	5.18	22.11	17.18
NO ₂	15.40	5.16	22.30	18.36

Table 3. The barrier heights for the S_N2 chloride exchange between para-substituted benzyl chloride and the chloride ion both in the gas phase and in water at the Hartree-Fock level and B3LYP density functional theory level. The Monte Carlo simulations use the TIP3P water model and include the polarizability of the solute.

While electron donating groups make the central carbon partially negatively charged, electron accepting groups make the central carbon partially positively charged. This affects the bond lengths of the central carbon and Cl anions at the transition states. For two reactants to

come into direct contact in water, the solvation shells have to be partially broken up. However, electron accepting groups at the para position for the S_N2 reaction in this study raise the barrier heights because the chloride anion has to approach the central carbon to initiate the reaction until the direct contact in water; see table 3. Thus, solvated molecules react more slowly than in vacuum. However, other reactions are sped up. For example, barriers of charge separation are much reduced in high dielectric constant solvents, and such reactions are faster in water; such as SO_3^- .

The significant inference from this study is to speed up the S_N2 reactions in water using different para-substituent groups with low Hammett constants because these substituent groups make the central carbon more negatively charged during the transition states. More negatively charged central carbon decreases the energy barrier of the S_N2 reaction in water by causing the bond between the central carbon and the chloride anion to be longer during the transition state. Therefore, the reaction rate of the S_N2 reactions in water can be increased by making the central carbon negatively charged because the tunneling probability across the barrier increases with decreasing barrier height.

On the other side, the repulsions emerged from the interaction between other groups (such as SO_3^-) and nucleophiles (such as Cl^-) during the S_N2 reaction do not have to be ignored because these interactions increase the barrier heights in the gas phase dramatically, while their barrier heights are decreased by water molecules covering the charged groups to stabilize in water. Moreover, some S_N2 reactions in the gas phase are almost impossible, while the chance of these reactions occurring is highly possible in water. For instance, NH_3^+ attracts the chloride ion during the S_N2 reaction between the para- NH_3^+ benzyl chloride and the chloride ion in the gas phase, and this reaction ends up with para- NH_2 benzyl chloride and HCl. However, the S_N2

reaction between the para-NH₃⁺ benzyl chloride and the chloride ion in water is more possible in water compared to in the gas phase.

In the future, for many S_N2 reactions in water, different ways could be used to make the central carbon partially more negatively charged, which will cause the barrier height of the reaction to be lower. By decreasing barrier heights of the reactions, a high percentage of major products can be obtained in a shorter time than usual. This will provide extra time and prevent wasting money for all manufacturing companies and related places.

VII. REFERENCES

- Bizzarri, AR and Cannistraro, S. (2002). Molecular dynamics of water at the protein-solvent interface. *J. Phys. Chem. B*, **106**, 6617-6633
- Bogdanov, B., & McMahon, T. (2006). Gas phase S(N)2 reactions of halide ions with trifluoromethyl halides: Front- and back-side attack vs. complex formation. *Journal of Physical Chemistry a*, *110*(4), 1350-1363. doi: 10.1021/jp0541011
- Chandrasekhar, J., Smith, S. F., & Jorgensen, W. L. (1983). *American Chemical Society*, 106, 3049-3050.
- Chandrasekhar, J., Smith, S., & Jorgensen, W. (1984). Sn2 reaction profiles in the gas-phase and aqueous-solution. *Journal of the American Chemical Society*, *106*(10), 3049-3050. doi: 10.1021/ja00322a059
- Chen, J., Yin, H., Wang, D., & Valiev, M. (2013). Water assisted reaction mechanism of OH₂ with CCl₄ in aqueous solution – Hybrid quantum mechanical and molecular mechanics investigation. *Chem. Phys. Lett*, <http://dx.doi.org/10.1016/j.cplett.2012.12.058>
- Dill, K. A., Truskett, T. M., Vlachy, V., & Hribar-Lee, B. (2005). Modelling water, the hydrophobic effect and ion solvation. *Annu. Rev. Biophys. Biomol. Struct.* 173-179. Doi: 10.1146/annurev.biophys.34.040204.144517
- Ebrahimi, A., Khorassan, M. H., & Doosti, M. (2011). Solvent Effects on SN2 Reactions between Substituted Benzyl Chloride and Chloride Ion. *International Journal of Quantum Chemistry*, Vol 112 873-881 doi: 10.1002/qua.23083
- Ebrahimi, A., Habibi-Khorassani, S. M., & Doosti, M. (2011). Substituent effects on S(N)2 reaction between substituted benzyl chloride and chloride ion in gas phase. *International Journal of Quantum Chemistry*, *111*(5), 1013-1024. doi: 10.1002/qua.22474
- Ebrahimi, A., Habibi, M., & Amirmijani, A. (2007). The study of counterion effect on the reactivity of nucleophiles in some S(N)2 reactions in gas phase and solvent media. *Journal of Molecular Structure-Theochem*, *809*(1-3), 115-124. doi: 10.1016/j.theochem.2007.01.037
- Frediani, L., Cammi, R., Corni, S., & Tomasi, J. (2004). A polarizable continuum model for molecules at diffuse interfaces. *Journal of Chemical Physics*, *120*(8), 3893-3907. doi: 10.1063/1.1643727
- Hori, T., Takahashi, H., & Nitta, T. (2003). Hybrid QM/MM molecular dynamics simulations for an ionic S(N)2 reaction in the supercritical water: OH⁻+CH₃Cl → CH₃OH+Cl⁻. *Journal of Computational Chemistry*, *24*(2), 209-221. doi: 10.1002/jcc.10134

- Janowski, T., Wolinski, K., & Pulay, P. (2012). Ultrafast Quantum Mechanics/Molecular Mechanics Monte Carlo simulations using generalized multipole polarizabilities. *Chemical Physics Letters*, 530, 1–9. doi:10.1016/j.cplett.2012.01.008
- Jorgensen, W. L., Chandrasekhar, J., Madura, J. D., Impey, R. W., & Klein, M. L. (1983). Comparison of simple potential functions for simulating liquid water. *Journal of Chemical Physics*, 79(2), 926-935. doi: 10.1063/1.445869
- Mineva, T., Russo, N., & Sicilia, E. (1998). Solvation effects on reaction profiles by the polarizable continuum model coupled with the gaussian density functional method. *Journal of Computational Chemistry*, 19(3), 290-299. doi: 10.1002/(SICI)1096-987X(199802)19:3<290::AID-JCC3>3.0.CO;2-O
- Mohamed, A., & Jensen, F. (2001). Steric effects in S(N)2 reactions. the influence of microsolvation. *Journal of Physical Chemistry a*, 105(13), 3259-3268. doi: 10.1021/jp002802
- Nelson, K. V., & Benjamin, I. (2011). Effect of a phase transfer catalyst on the dynamics of an S(N)2 reaction. A molecular dynamics study. *Journal of Physical Chemistry C*, 115(5), 2290-2296. doi: 10.1021/jp110796n
- Nelson, K. V., & Benjamin, I. (2011). A model S(N)2 reaction 'on water' does not show rate enhancement. *Chemical Physics Letters*, 508(1-3), 59-62. doi: 10.1016/j.cplett.2011.04.038
- Pagliai, M., Raugei, S., Cardini, G., & Schettino, V. (2003). Intramolecular solvation effects in the S(N)2 reaction $\text{Cl}^- + \text{Cl}(\text{CH}_2)_n\text{CN}$. *Journal of Chemical Physics*, 119(17), 9063-9072. doi: 10.1063/1.1613940
- Poater, J., Sola, M., Duran, M., & Fradera, X. (2001). Effects of solvation on the pairing of electrons in a series of simple molecules and in the menshutkin reaction. *Journal of Physical Chemistry a*, 105(25), 6249-6257. doi: 10.1021/jp0108364
- Raugei, S., Cardini, G., & Schettino, V. (2001). Microsolvation effect on chemical reactivity: The case of the $\text{Cl}^- + \text{CH}_3\text{BrS(N)2}$ reaction. *Journal of Chemical Physics*, 114(9), 4089-4098. doi: 10.1063/1.1348023
- Re, M., & Laria, D. (1996). Solvation effects on a model S(N)2 reaction in water clusters. *Journal of Chemical Physics*, 105(11), 4584-4596. doi: 10.1063/1.472539
- Truong, T., & Stefanovich, E. (1995). Hydration effects on reaction profiles - an ab-initio dielectric continuum study of the S(n)2 $\text{Cl}^- + \text{CH}_3\text{Cl}$ reaction. *Journal of Physical Chemistry*, 99(40), 14700-14706. doi: 10.1021/j100040a018
- Uggerud, E. (2006). Nucleophilicity-periodic trends and connection to basicity. *Chemistry-a European Journal*, 12(4), 1127-1136. doi: 10.1002/chem.200500639

- Weickmann, K., Whitaker, J., Roubicek, A., & Smith, C. (2001). The Use of Ensemble Forecasts to Produce Improved Medium Range (3-15 days) Weather Forecasts. *Physical Sciences Division*, <http://www.esrl.noaa.gov/psd/spotlight/12012001/index.html>.
- Xin, C., Regan, C. K., Craig, S. L., Krenske, E. H., Houk, K. N., Jorgensen, W. L., & Brauman, J. I. (2009). Steric and Solvation Effects in Ionic SN2 Reactions. *Journal Of The American Chemical Society*, 131(44), 16162-16170.
- Zhou, R. (2003). Free energy landscape of protein folding in water: explicit vs. implicit solvent. *Proteins: Structure, Function, and Bioinformatics*, 55(2), 148-161.
doi:10.1002/prot.10483

FIGURES

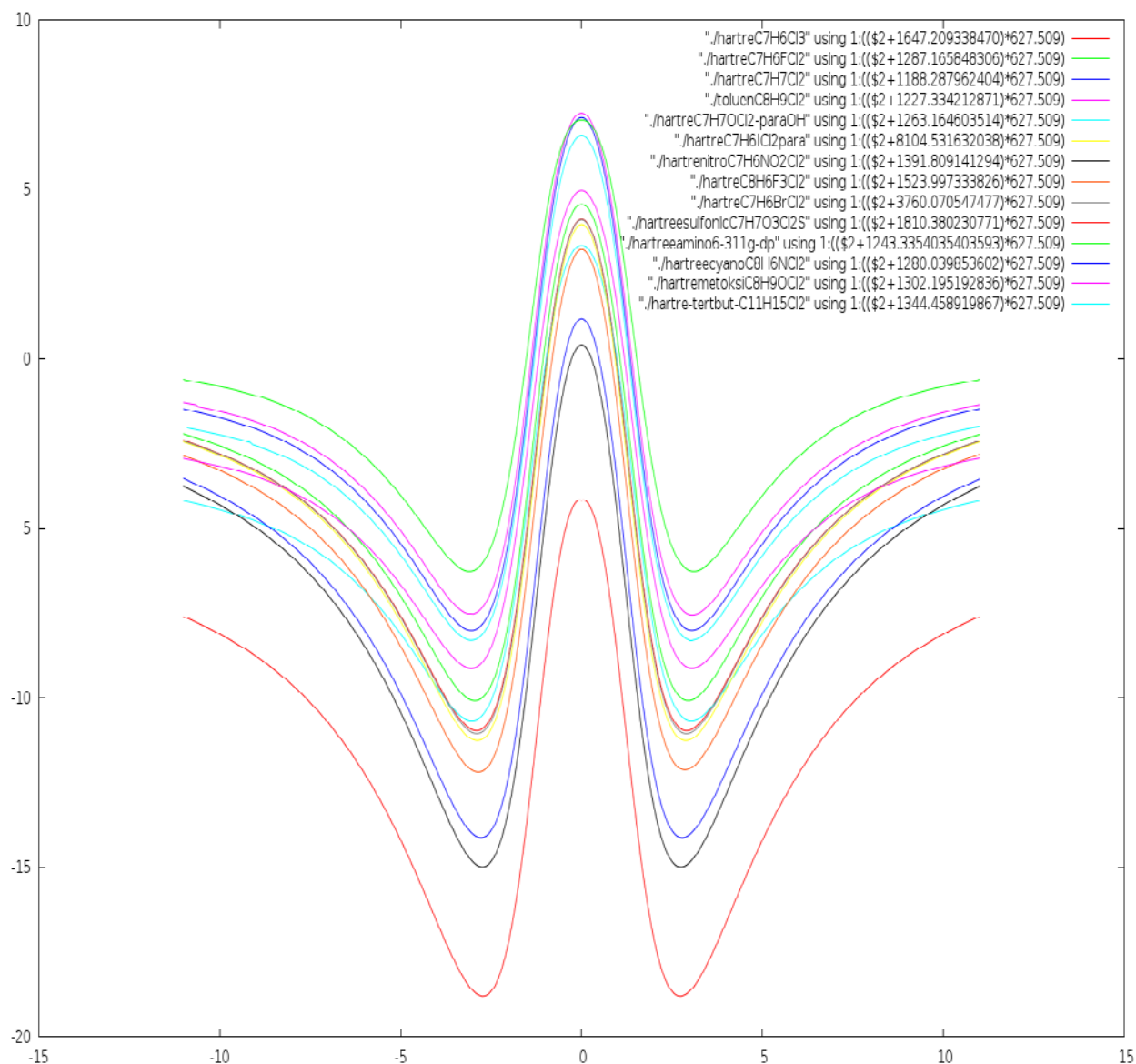


Figure 1. Energies (relative to infinite separation, in kcal/mole) *versus* the reaction coordinate ($c=a-b a_0$) of the S_N2 reaction between para substituted benzyl chlorides with different para substitutions and the chloride ion in the gas phase at the RHF/6-311G(d,p) level

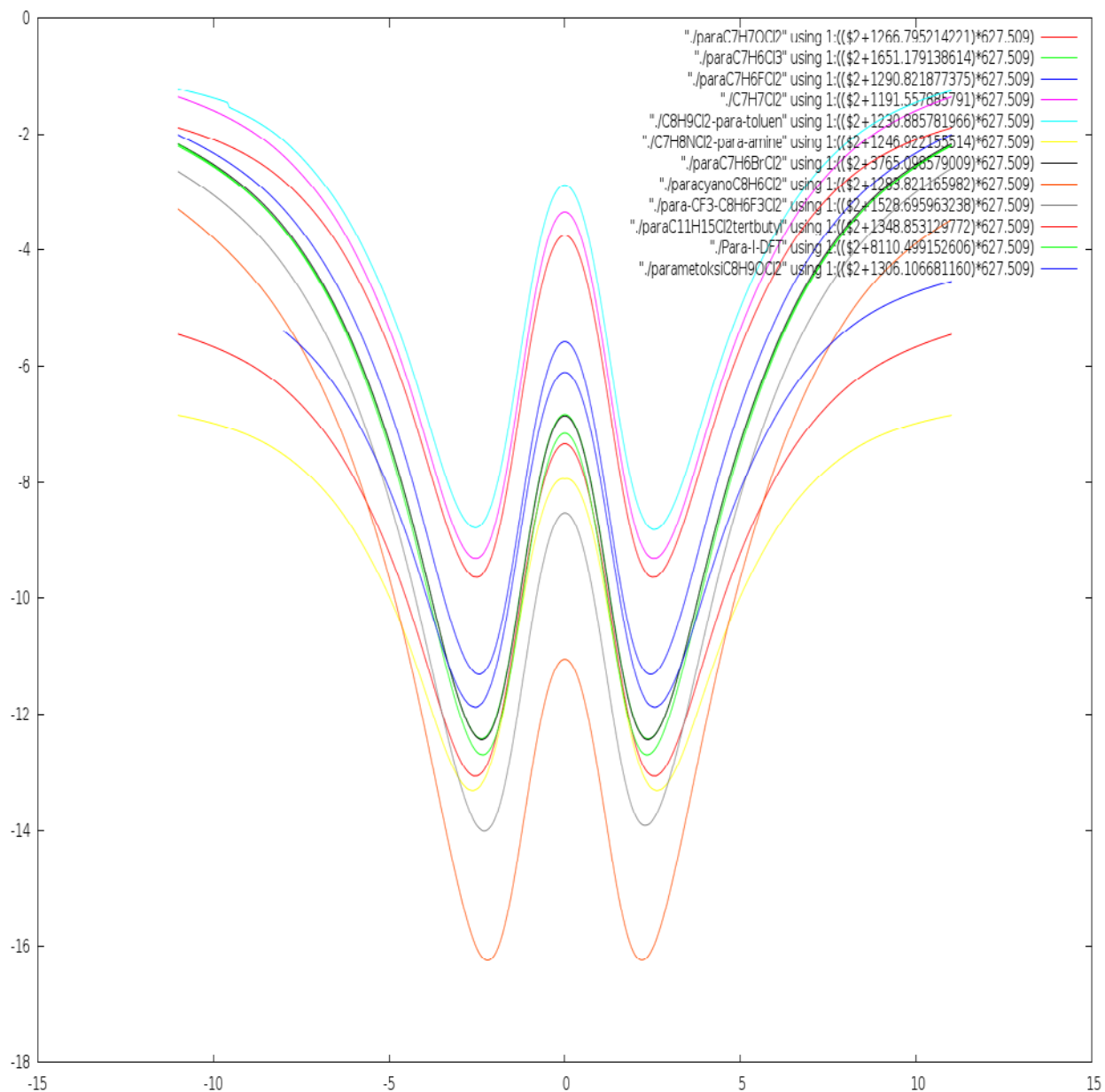


Figure 2. Energies (kcal/mole) *versus* the reaction coordinate ($c=a-b$ a_0) of the S_N2 reaction between para-substituted benzyl chlorides and the chloride ion in the gas phase with different para-substitutions at the B3LYP/6-311G(d,p) level relative to infinite separation

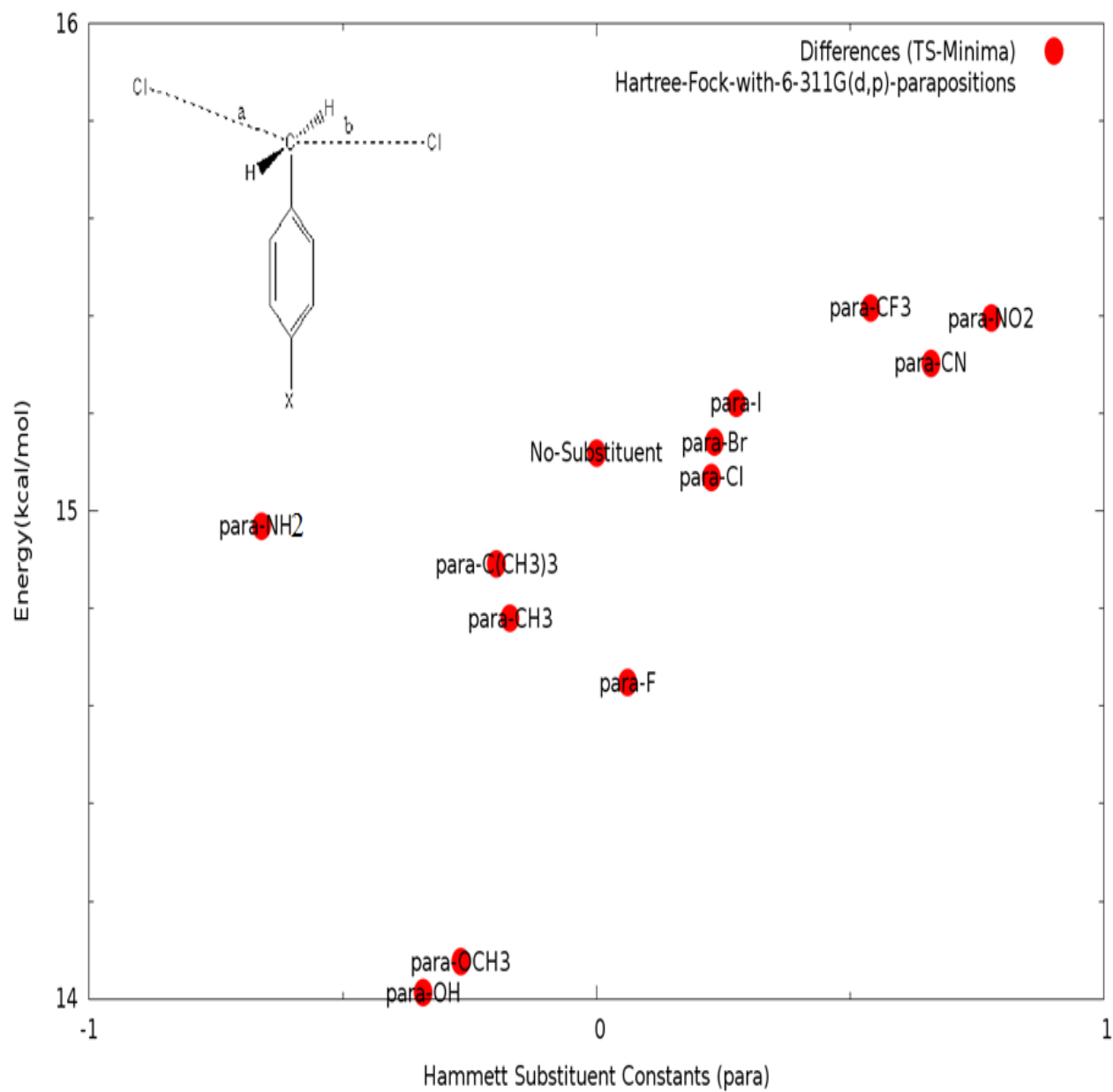


Figure 3. Barrier heights (relative to the minimum energy, in kcal/mole) *versus* Hammett constants for the S_N2 reaction between para substituted benzyl chlorides with different para-substitutions and the chloride ion in the gas phase at the RHF/6-311G(d,p)level.

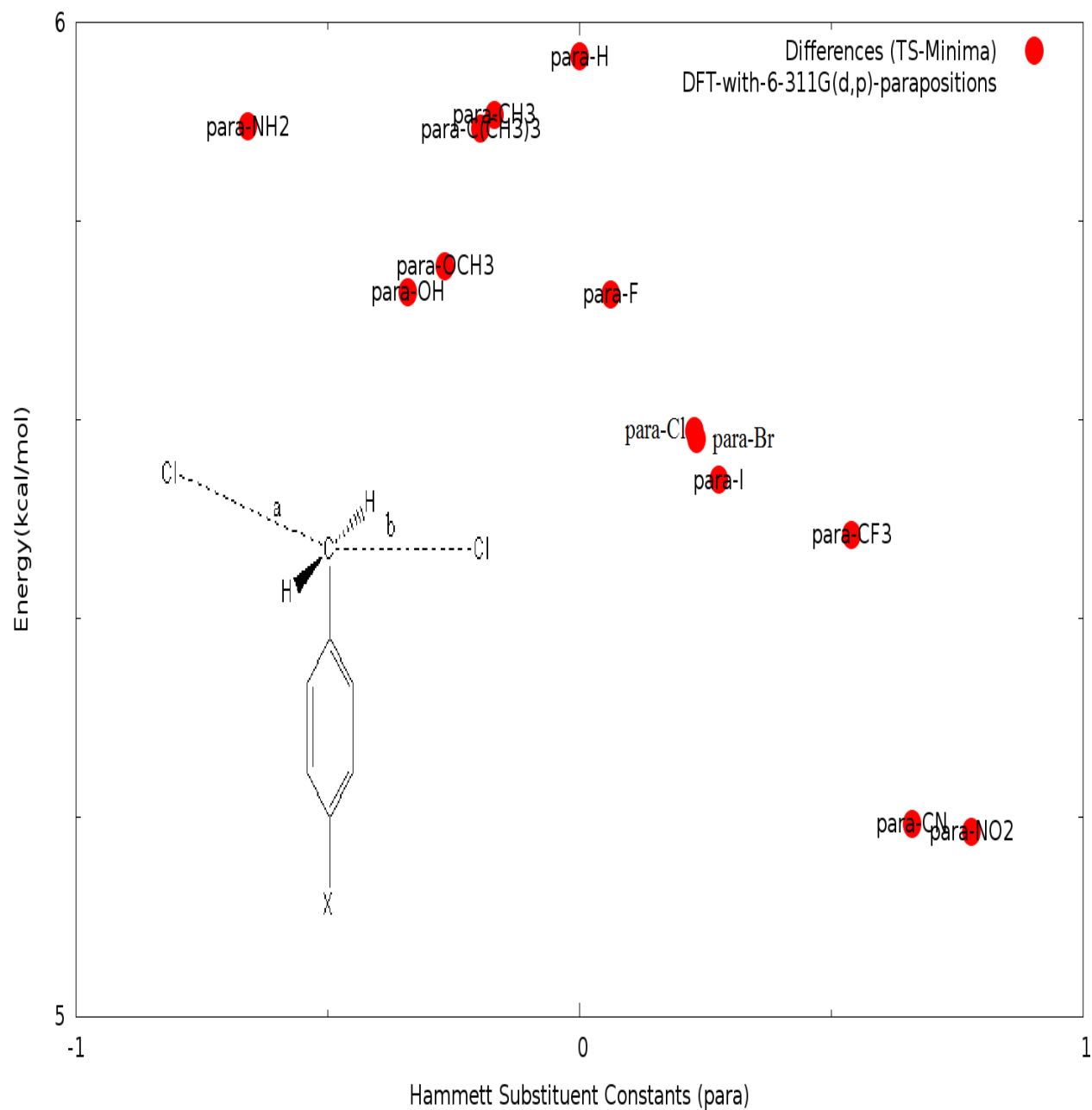


Figure 4. Barrier heights (relative to the minimum energy, in kcal/mole) *versus* Hammett constants for the S_N2 reaction between para substituted benzyl chlorides with different para-substitutions and the chloride ion in the gas phase at the B3LYP/6-311G(d,p)level.

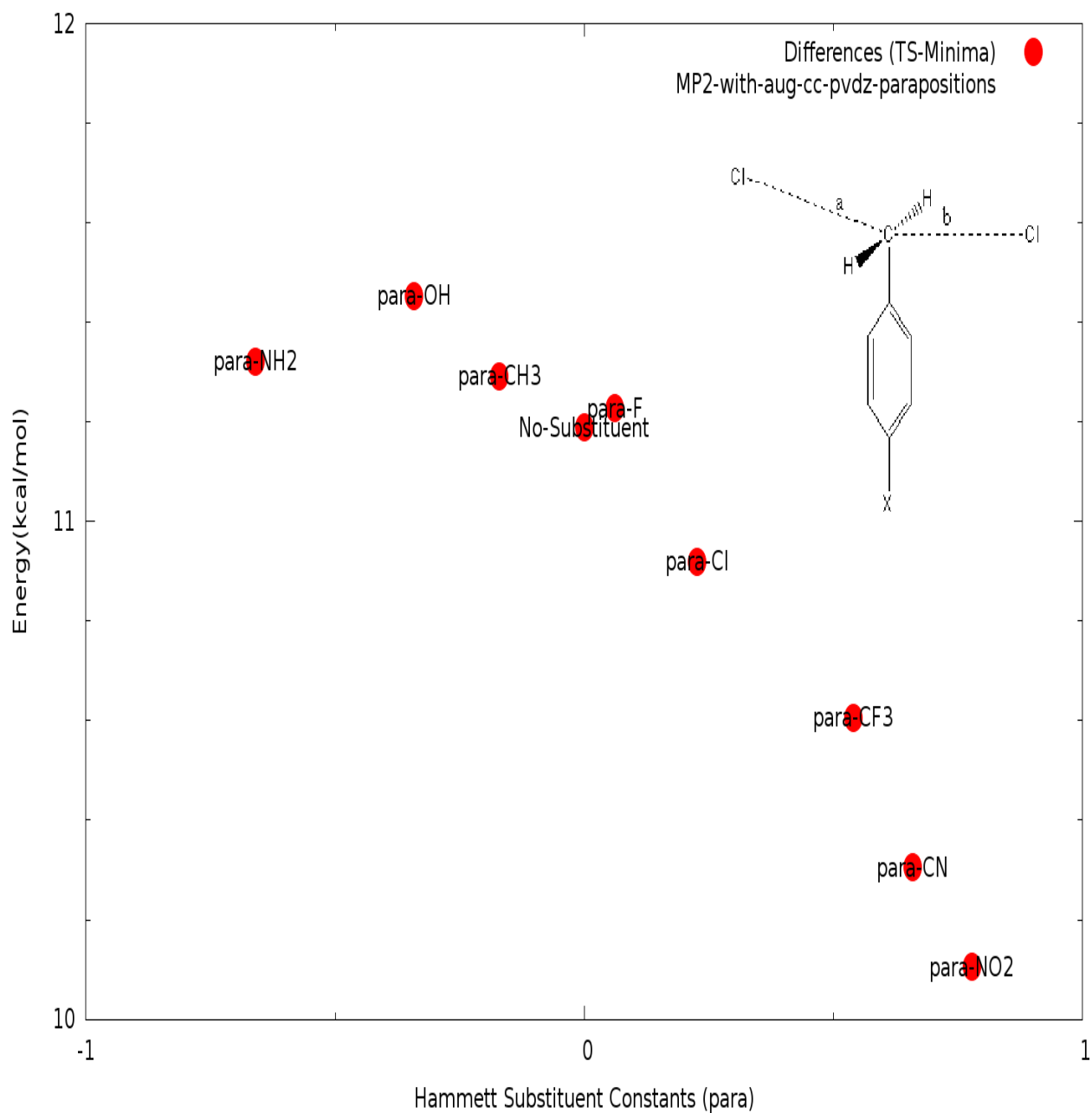


Figure 5. Barrier heights (relative to the minimum energy, in kcal/mole) *versus* Hammett constants for the S_N2 reaction between para substituted benzyl chlorides with different para-substitutions and the chloride ion in the gas phase at the MP2/6-311G(d,p) level.

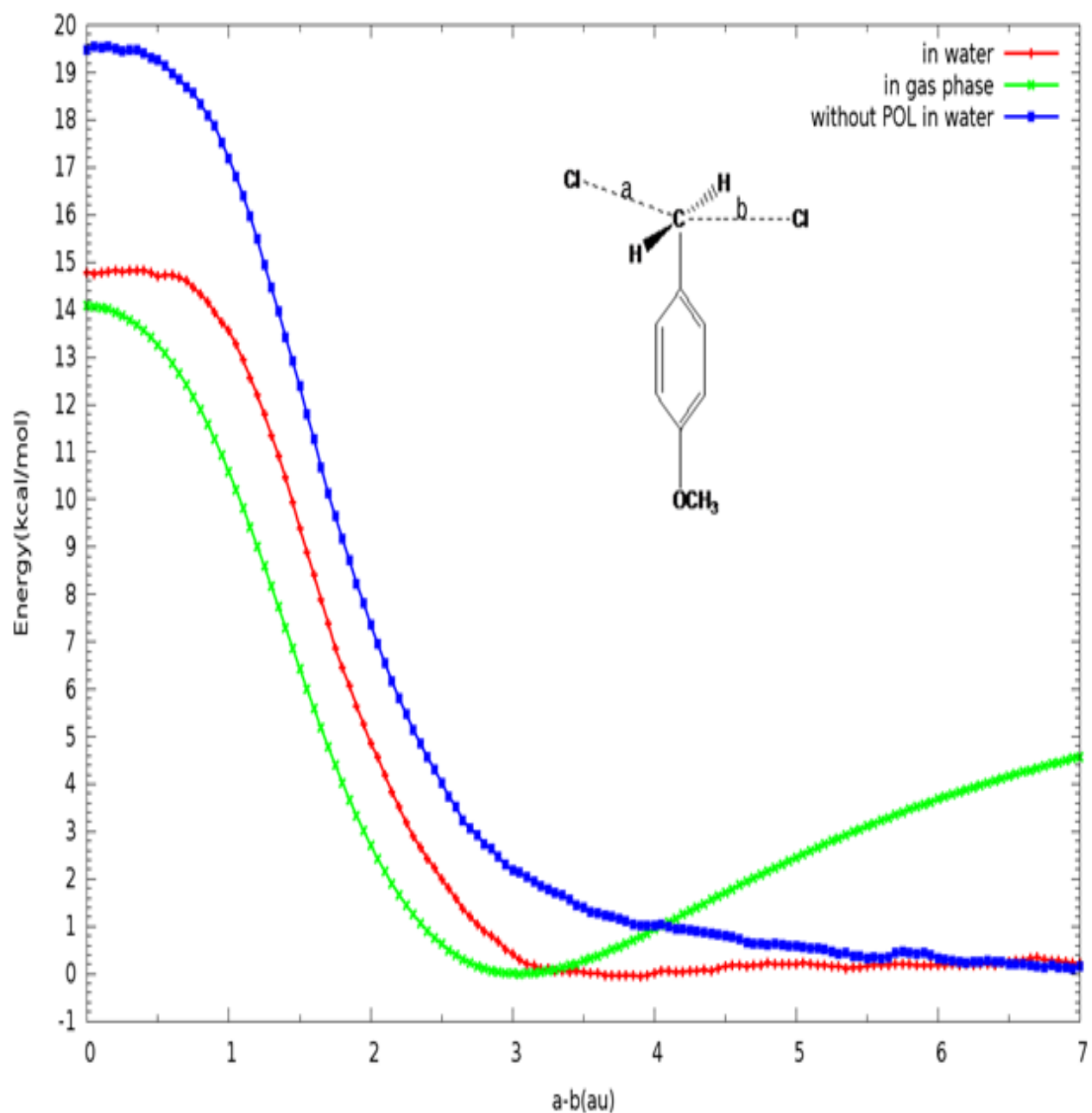


Figure 6. Hartree-Fock energies (kcal/mole) *versus* the reaction coordinate (a_0) of the S_N2 reaction between the para- OCH_3 benzyl chloride and the chloride ion in water and in the gas phase. The red line corresponds to the reaction in water, which has polarizability in solute, while the blue line corresponds to the reaction in water, which does not have polarizability in solute. The green line represents the reaction in the gas phase.

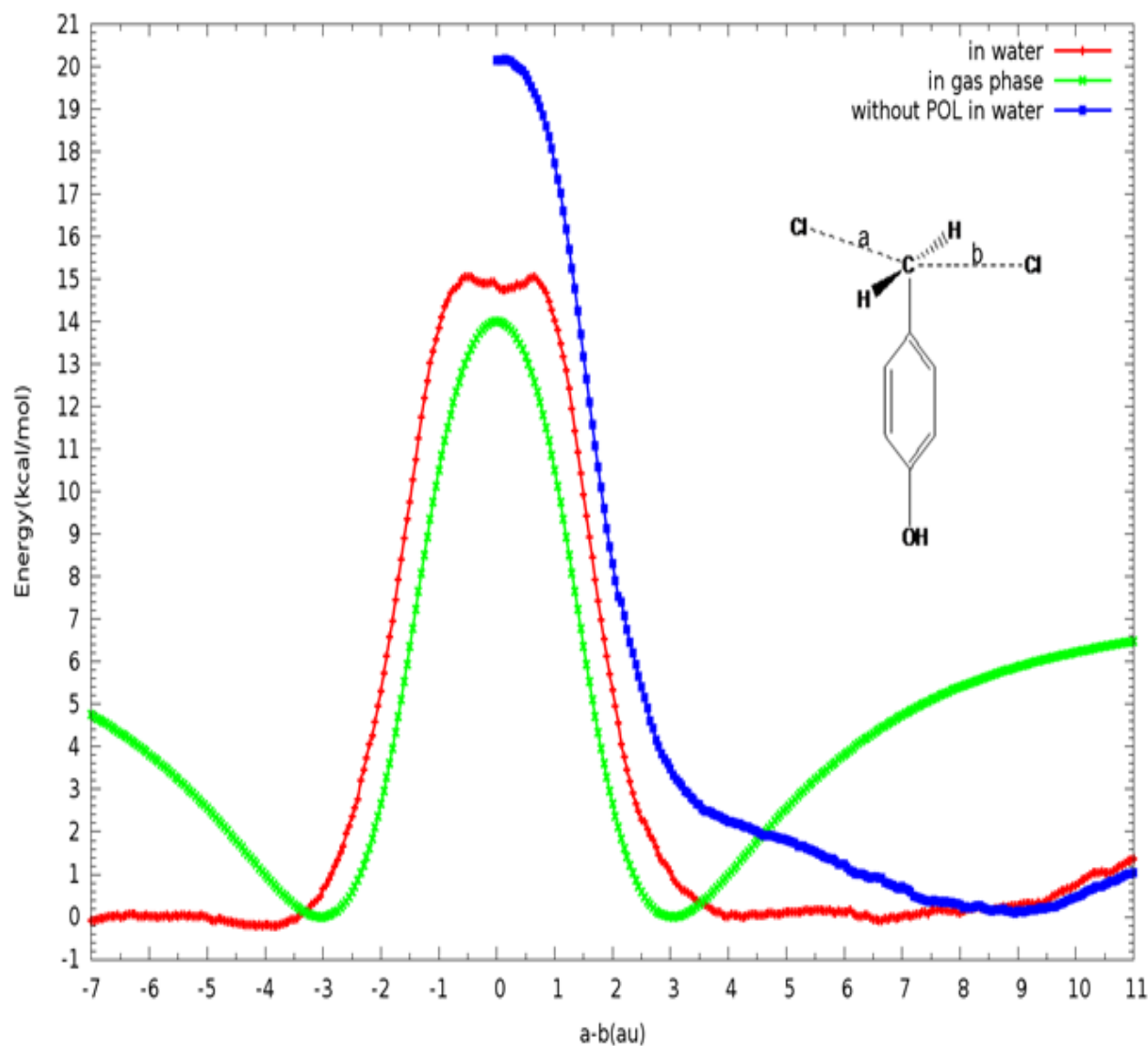


Figure 7. Hartree-Fock energies (kcal/mole) *versus* the reaction coordinate (a_0) of the reaction between the para-OH benzyl chloride and the chloride ion in water and in the gas phase. The red line corresponds to the reaction in water, which has polarizability in solute, while the blue line corresponds to the reaction in water, which does not have polarizability in solute. The green line represents the reaction in the gas phase.

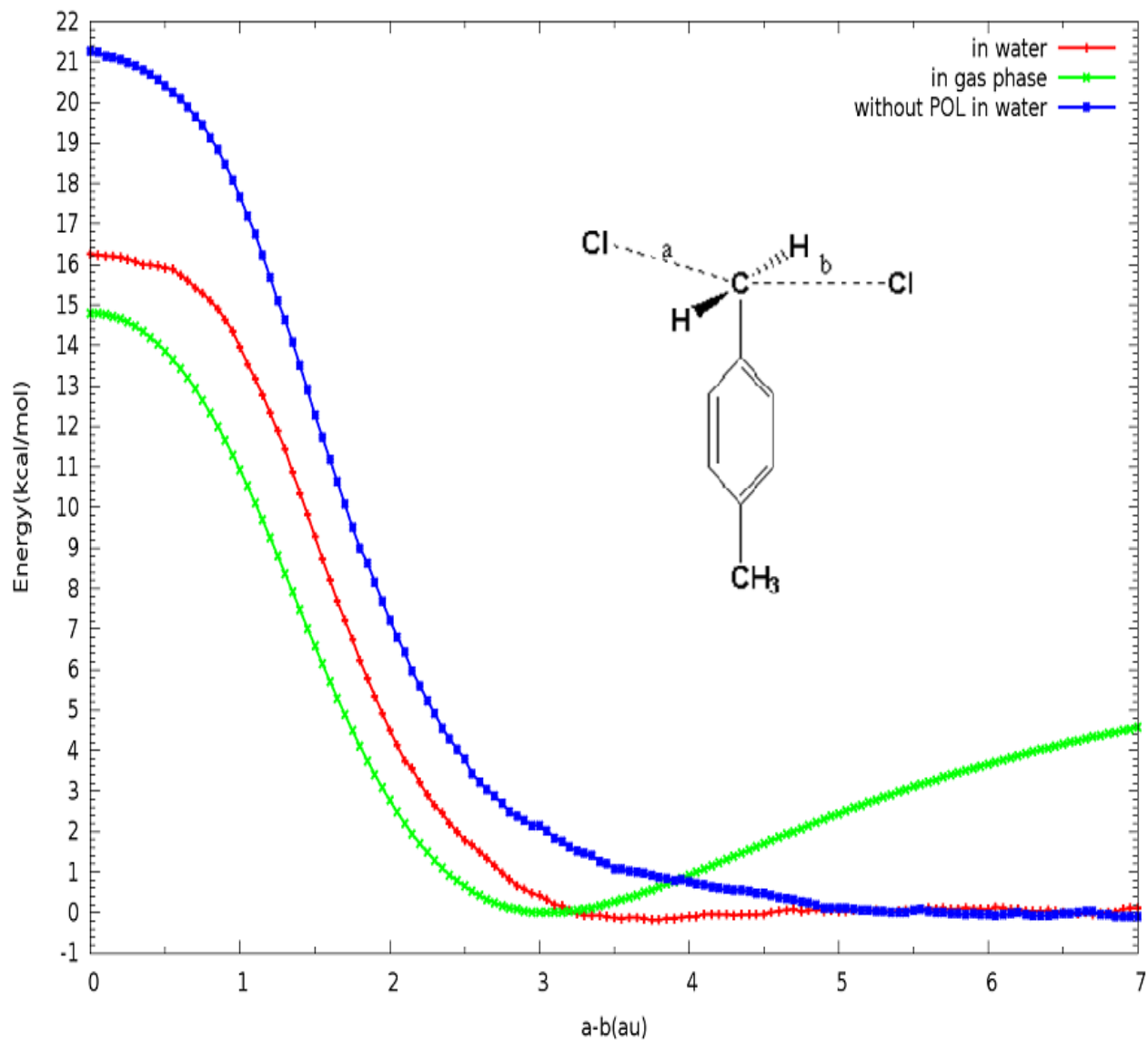


Figure 8. Hartree-Fock energies (kcal/mole) *versus* the reaction coordinate (a_0) of the S_N2 reaction between the para-CH₃ benzyl chloride and the chloride ion in water and in the gas phase. The red line corresponds to the reaction in water, which has polarizability in solute, while the blue line corresponds to the reaction in water, which does not have polarizability in solute. The green line represents the reaction in the gas phase.

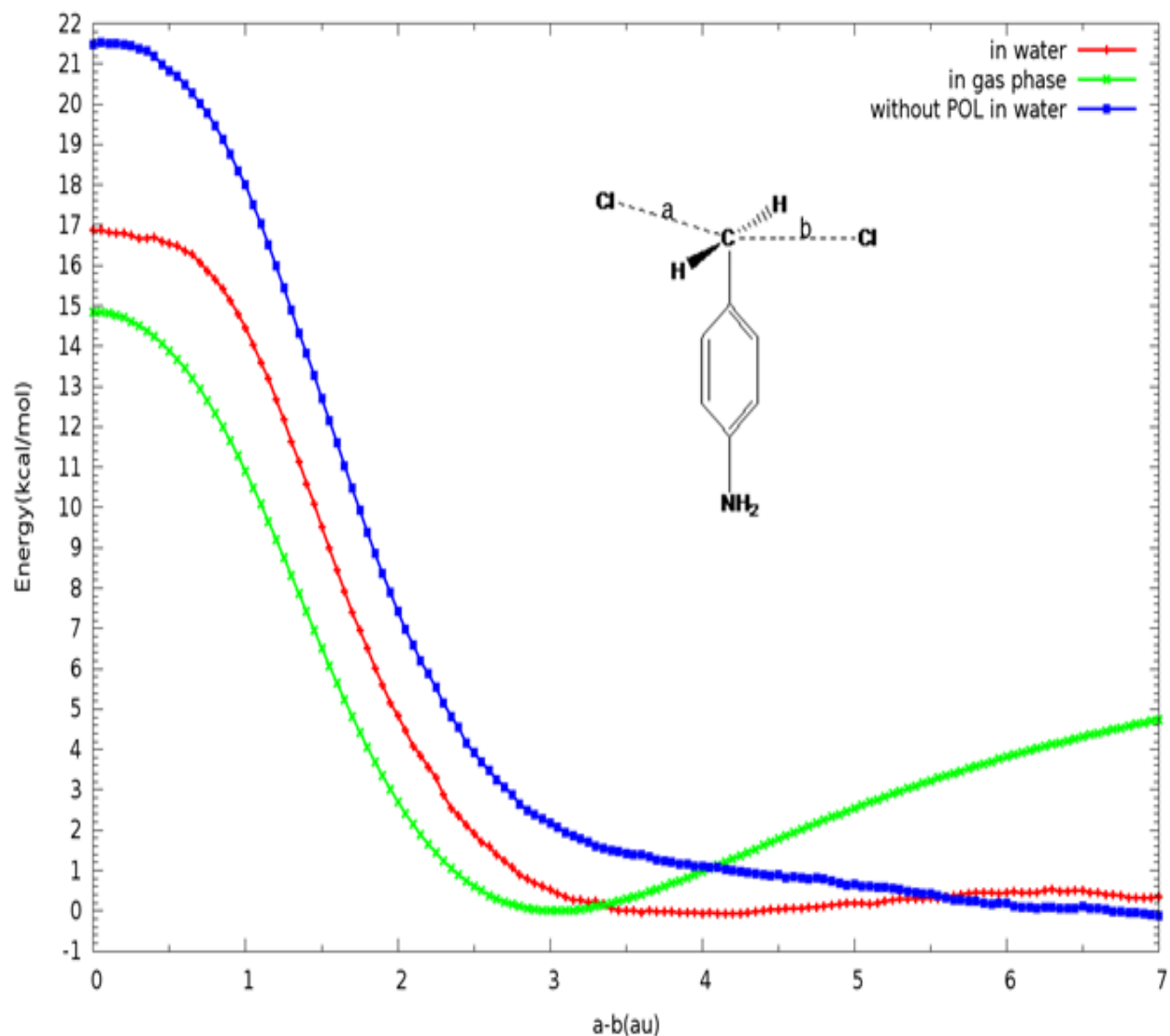


Figure 9. Hartree-Fock energies (kcal/mole) *versus* the reaction coordinate (a_0) of the S_N2 reaction between the para-NH₂ benzyl chloride and the chloride ion in water and in the gas phase. The red line corresponds to the reaction in water, which has polarizability in solute, while the blue line corresponds to the reaction in water, which does not have polarizability in solute. The green line represents the reaction in the gas phase.

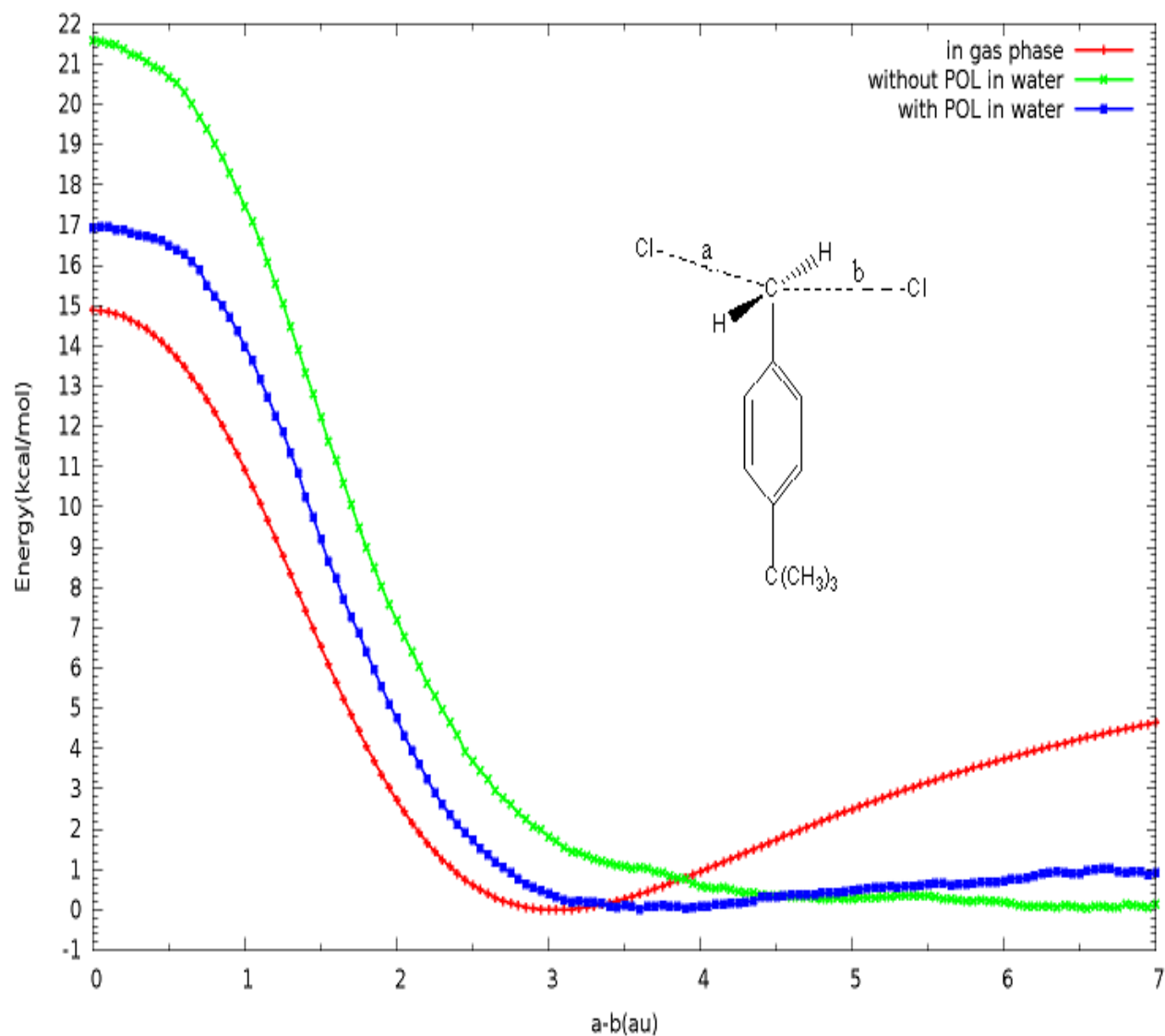


Figure 10. Hartree-Fock energies (kcal/mole) *versus* the reaction coordinate (a_0) of the S_N2 reaction between the para- $C(CH_3)_3$ benzyl chloride and the chloride ion in water and in the gas phase. The blue line corresponds to the reaction in water, which has polarizability in solute, while the green line corresponds to the reaction in water, which does not have polarizability in solute. The red line represents the reaction in the gas phase.

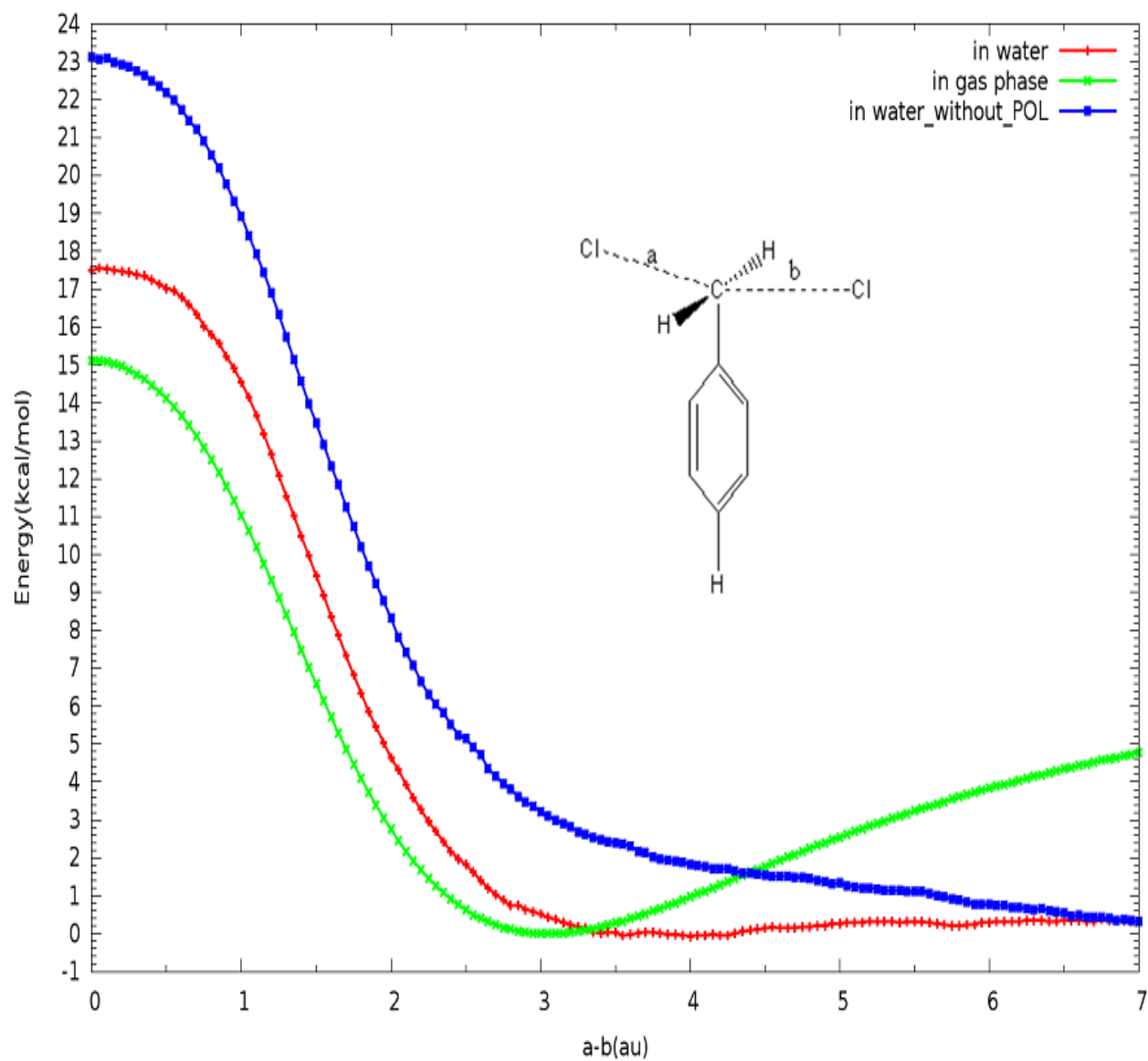


Figure 11. Hartree-Fock energies (kcal/mole) *versus* the reaction coordinate (a_0) of the the S_N2 reaction between the benzyl chloride and the chloride ion in water and in the gas phase The red line corresponds to the reaction in water, which has polarizability in solute, while the blue line corresponds to the reaction in water, which does not have polarizability in solute. The green line represents the reaction in the gas phase.

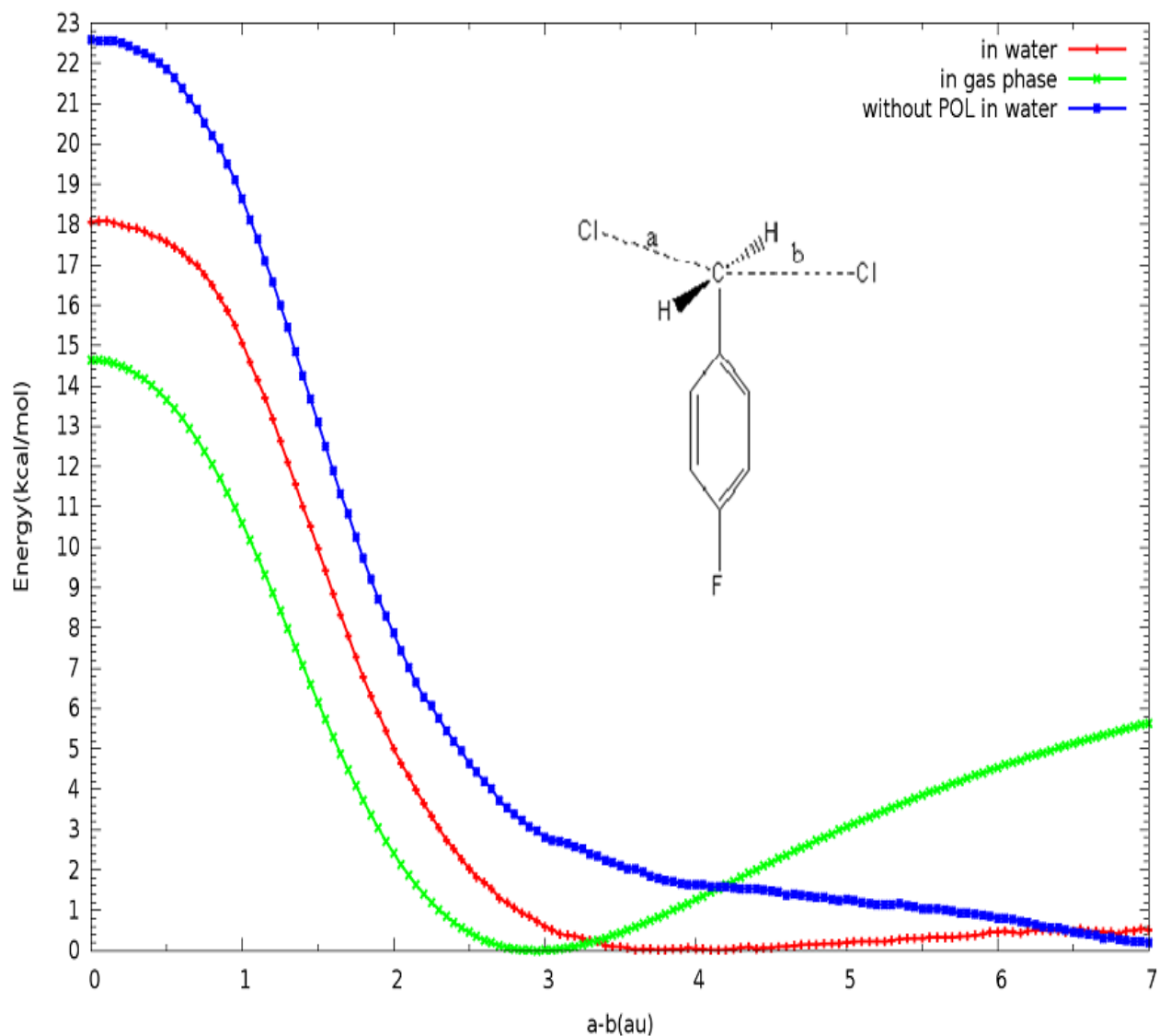


Figure 12. Hartree-Fock energies (kcal/mole) *versus* the reaction coordinate (a_0) of the S_N2 reaction between the para-F benzyl chloride and the chloride ion in water and in the gas phase. The red line corresponds to the reaction in water, which has polarizability in solute, while the blue line corresponds to the reaction in water, which does not have polarizability in solute. The green line represents the reaction in the gas phase.

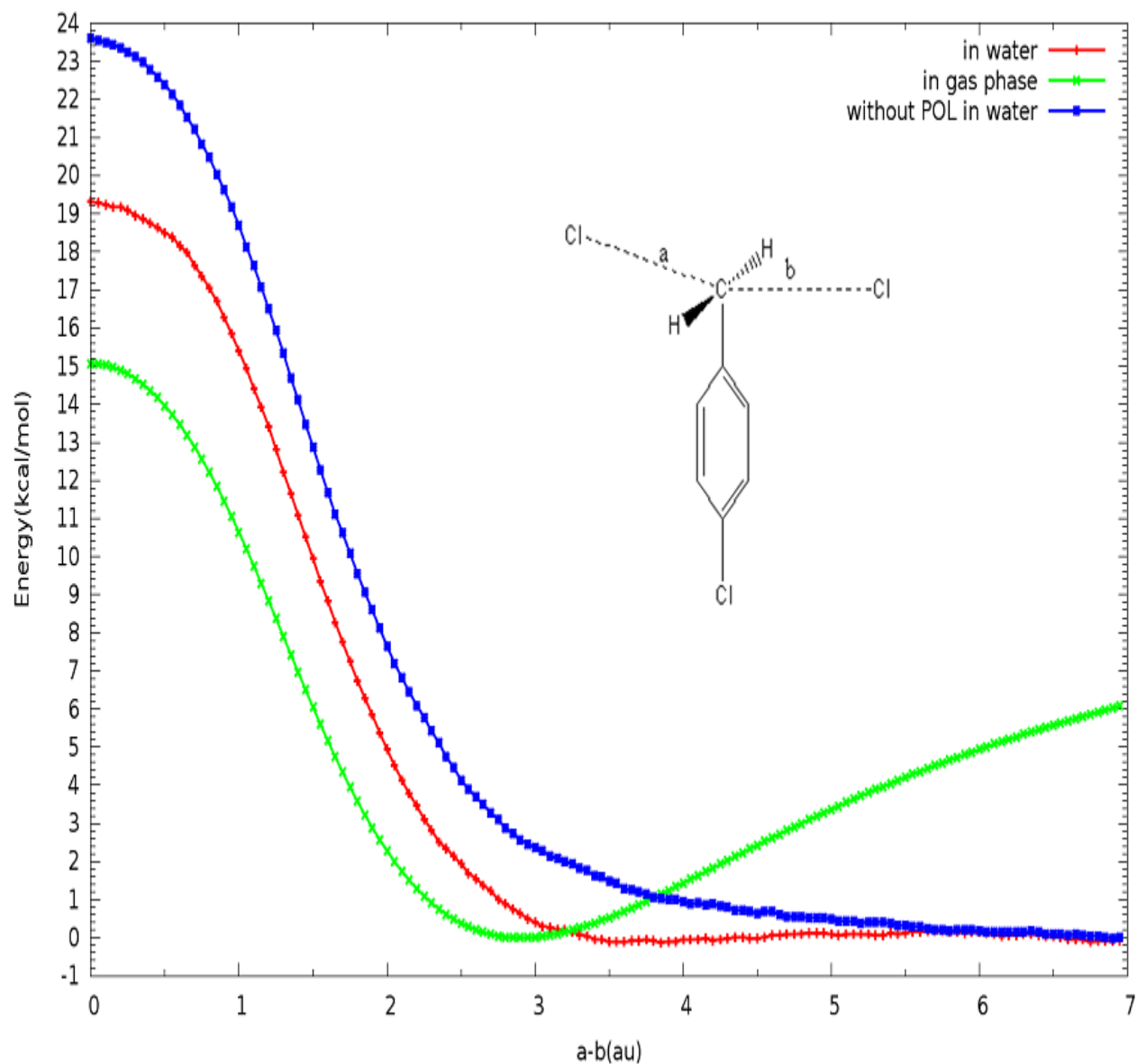


Figure 13. Hartree-Fock energies (kcal/mole) *versus* the reaction coordinate (a_0) of the S_N2 reaction between the para-Cl benzyl chloride and the chloride ion in water and in the gas phase. The red line corresponds to the reaction in water, which has polarizability in solute, while the blue line corresponds to the reaction in water, which does not have polarizability in solute. The green line represents the reaction in the gas phase.

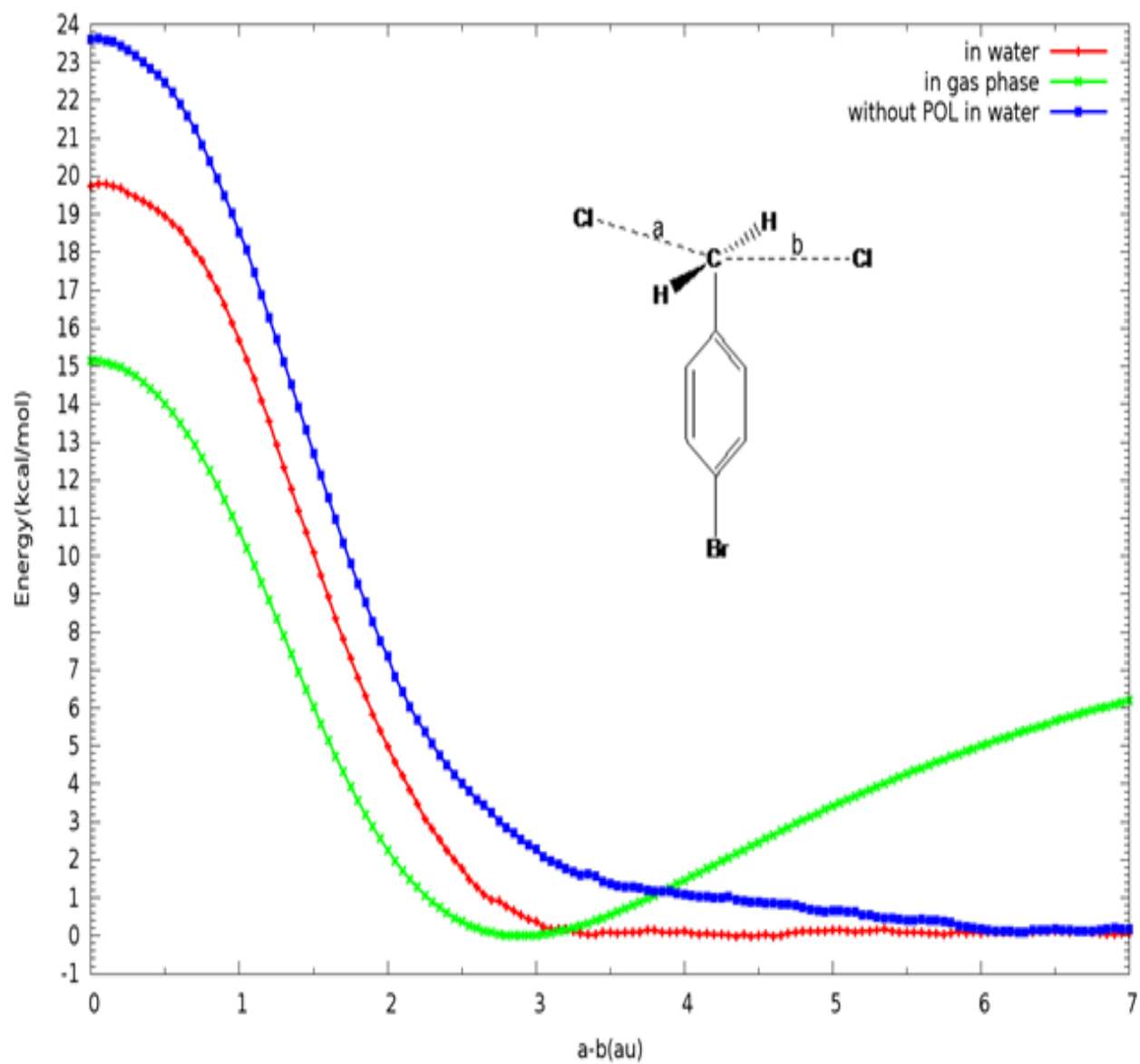


Figure 14. Hartree-Fock energies (kcal/mole) *versus* the reaction coordinate (a_0) of the S_N2 reaction between the para-Br benzyl chloride and the chloride ion in water and in the gas phase. The red line corresponds to the reaction in water, which has polarizability in solute, while the blue line corresponds to the reaction in water, which does not have polarizability in solute. The green line represents the reaction in the gas phase.

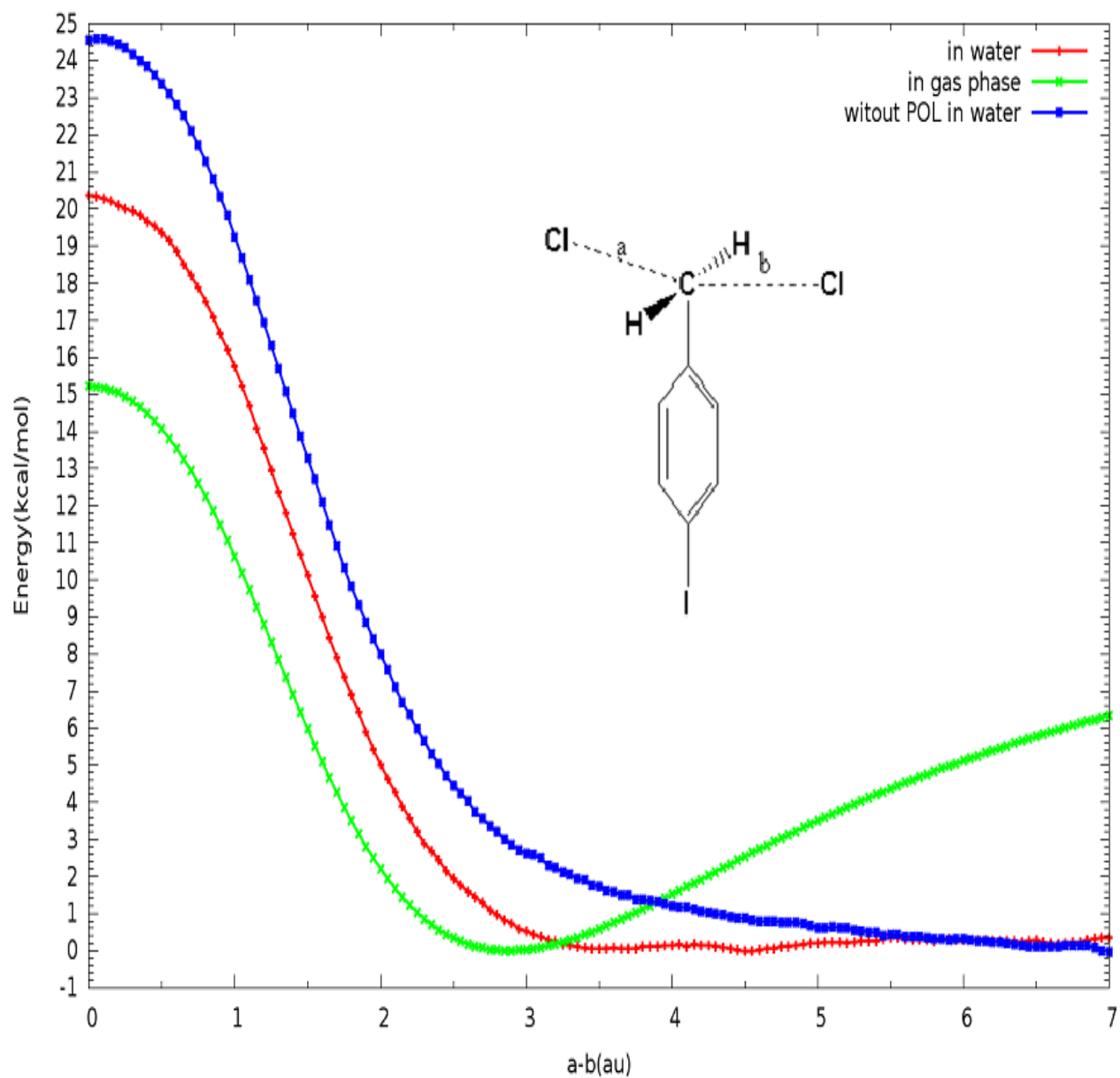


Figure 15. Hartree-Fock energies (kcal/mole) *versus* the reaction coordinate (a_0) of the S_N2 reaction between the para-I benzyl chloride and the chloride ion in water and in the gas phase. The red line corresponds to the reaction in water, which has polarizability in solute, while the blue line corresponds to the reaction in water, which does not have polarizability in solute. The green line represents the reaction in the gas phase.

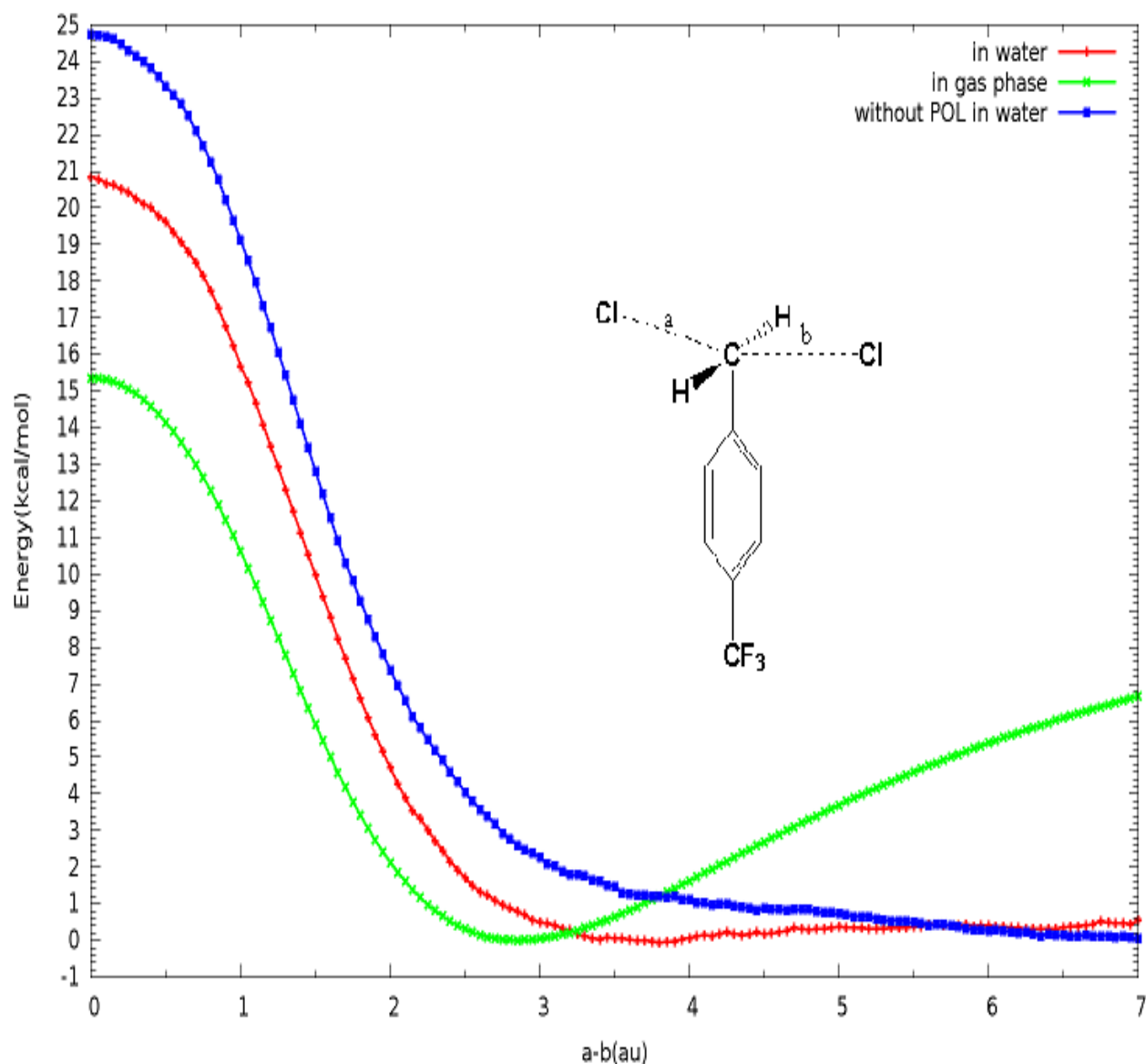


Figure 16. Hartree-Fock energies (in kcal/mole) *versus* the reaction coordinate (a_0) of the S_N2 reaction between para- CF_3 benzyl chloride and the chloride ion in water and in the gas phase. Because of symmetry, only half of the reaction path is shown. The red line corresponds to the reaction in water, which has polarizability in solute, while the blue line corresponds to the reaction in water, which does not have polarizability in solute. The green line represents the reaction in the gas phase.

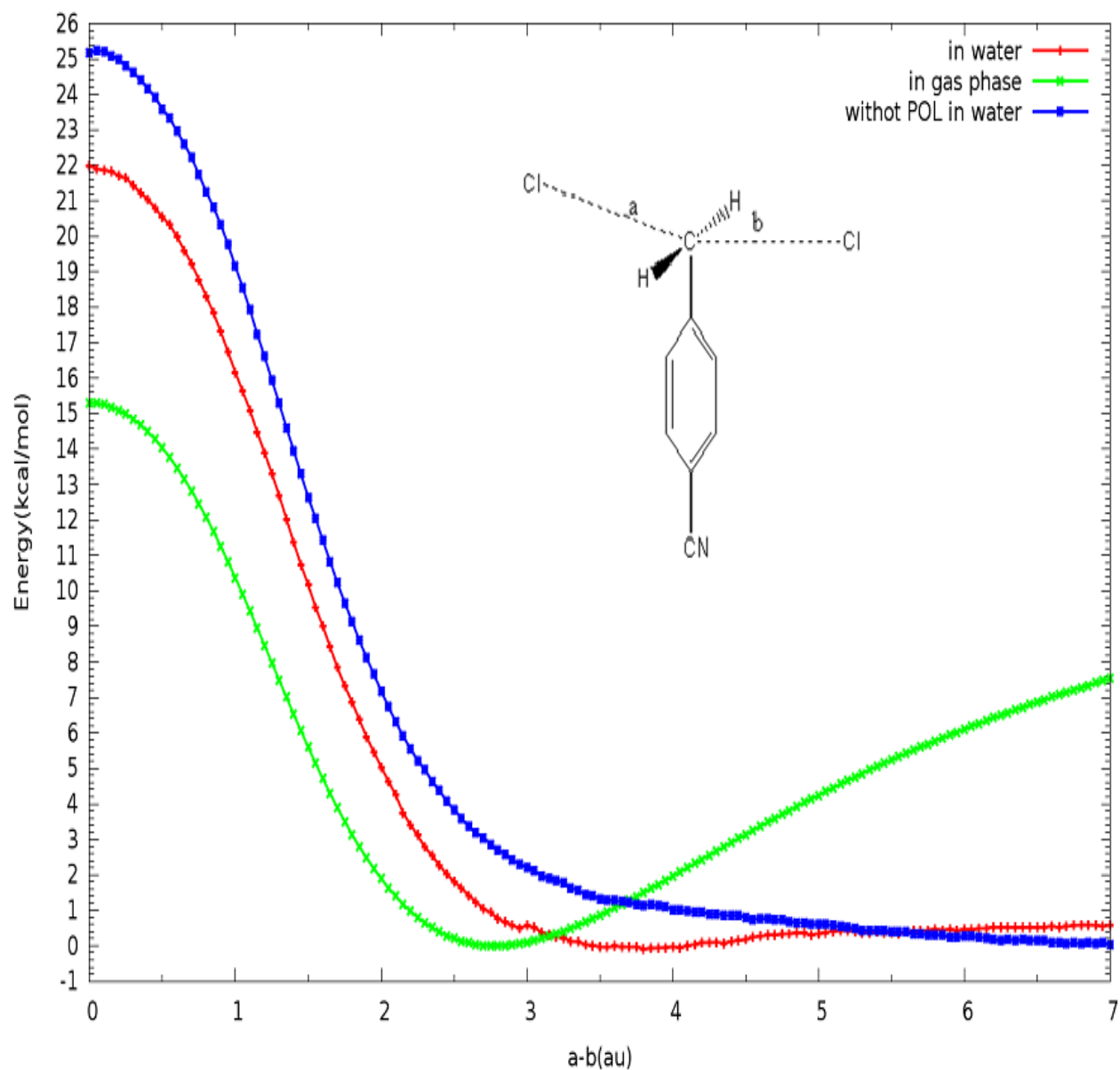


Figure 17. Hartree-Fock energies (kcal/mole) *versus* the reaction coordinate (a_0) of the S_N2 reaction between the para-CN benzyl chloride and the chloride ion in water and in the gas phase. The red line corresponds to the reaction in water, which has polarizability in solute, while the blue line corresponds to the reaction in water, which does not have polarizability in solute. The green line represents the reaction in the gas phase.

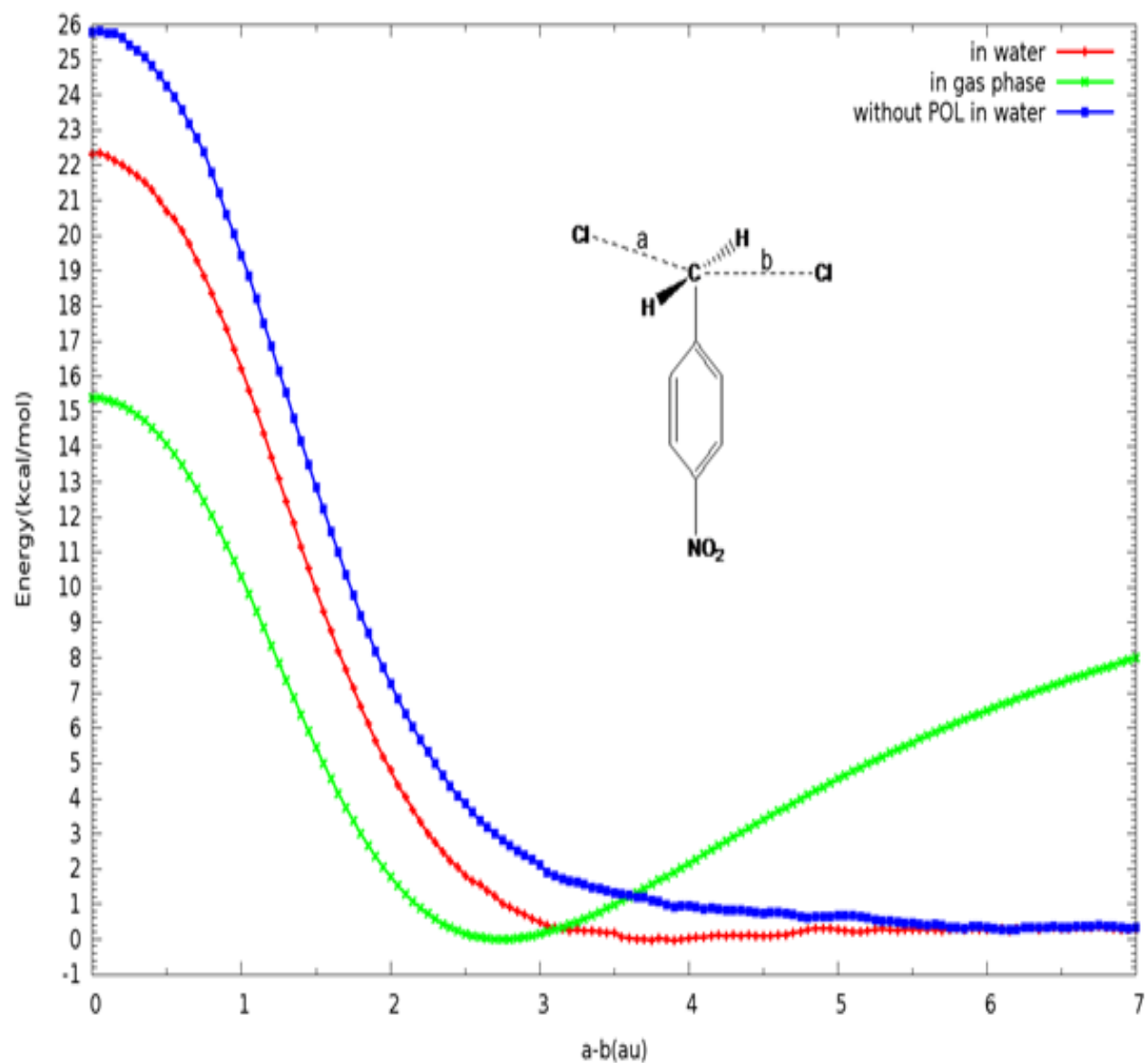


Figure 18. Hartree-Fock energies (kcal/mole) *versus* the reaction coordinate (a_0) of the S_N2 reaction between the para- NO_2 benzyl chloride and the chloride ion in water and in the gas phase. The red line corresponds to the reaction in water, which has polarizability in solute, while the blue line corresponds to the reaction in water, which does not have polarizability in solute. The green line represents the reaction in the gas phase.

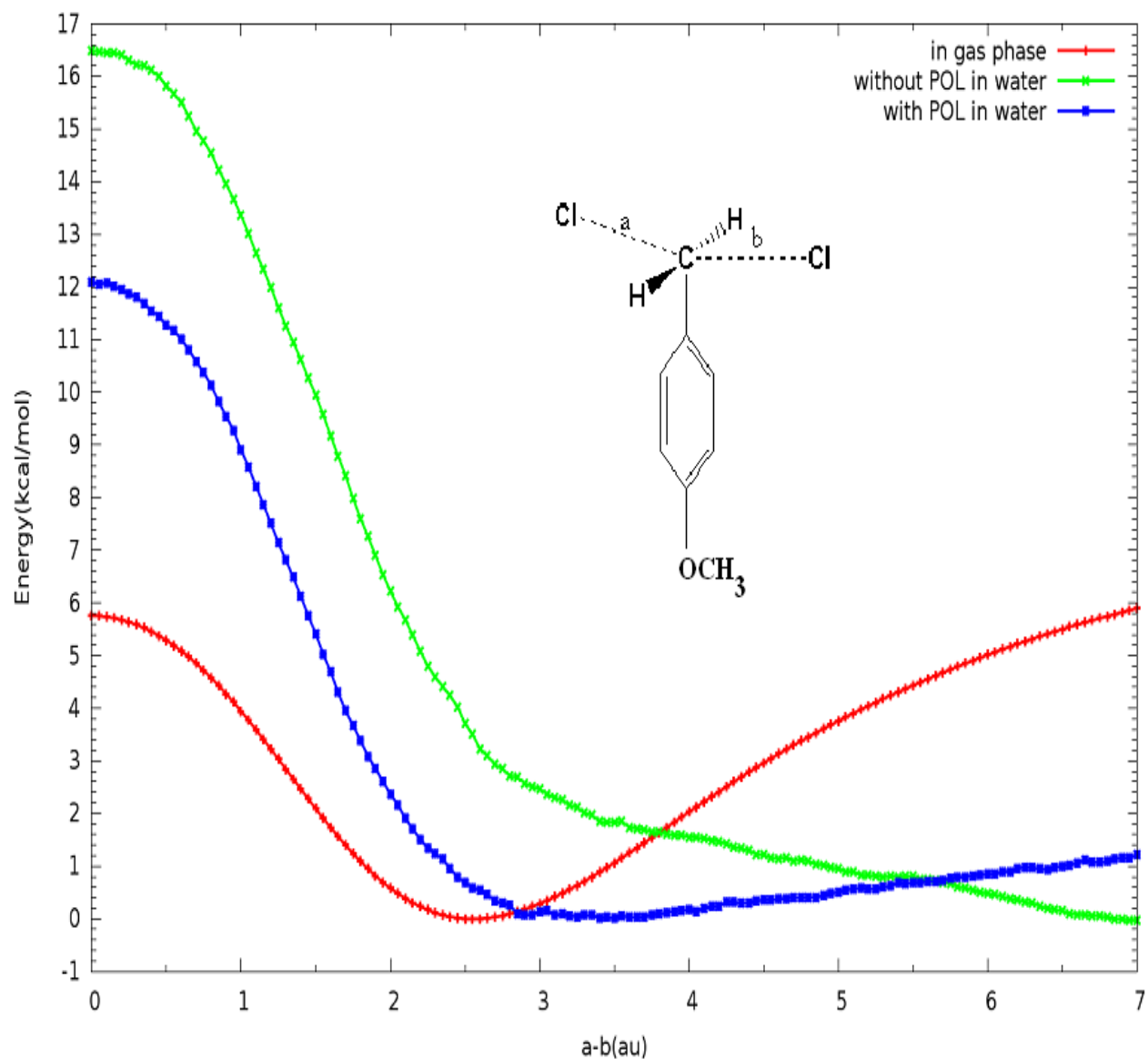


Figure 19. B3LYP energies (kcal/mole)) *versus* the reaction coordinate (a_0) of the S_N2 reaction between para- OCH_3 benzyl chloride and the chloride ion in water and in the gas phase. The blue line corresponds to the reaction in water, which has polarizability in solute, while the green line corresponds to the reaction in water, which does not have polarizability in solute. The red line represents the reaction in the gas phase.

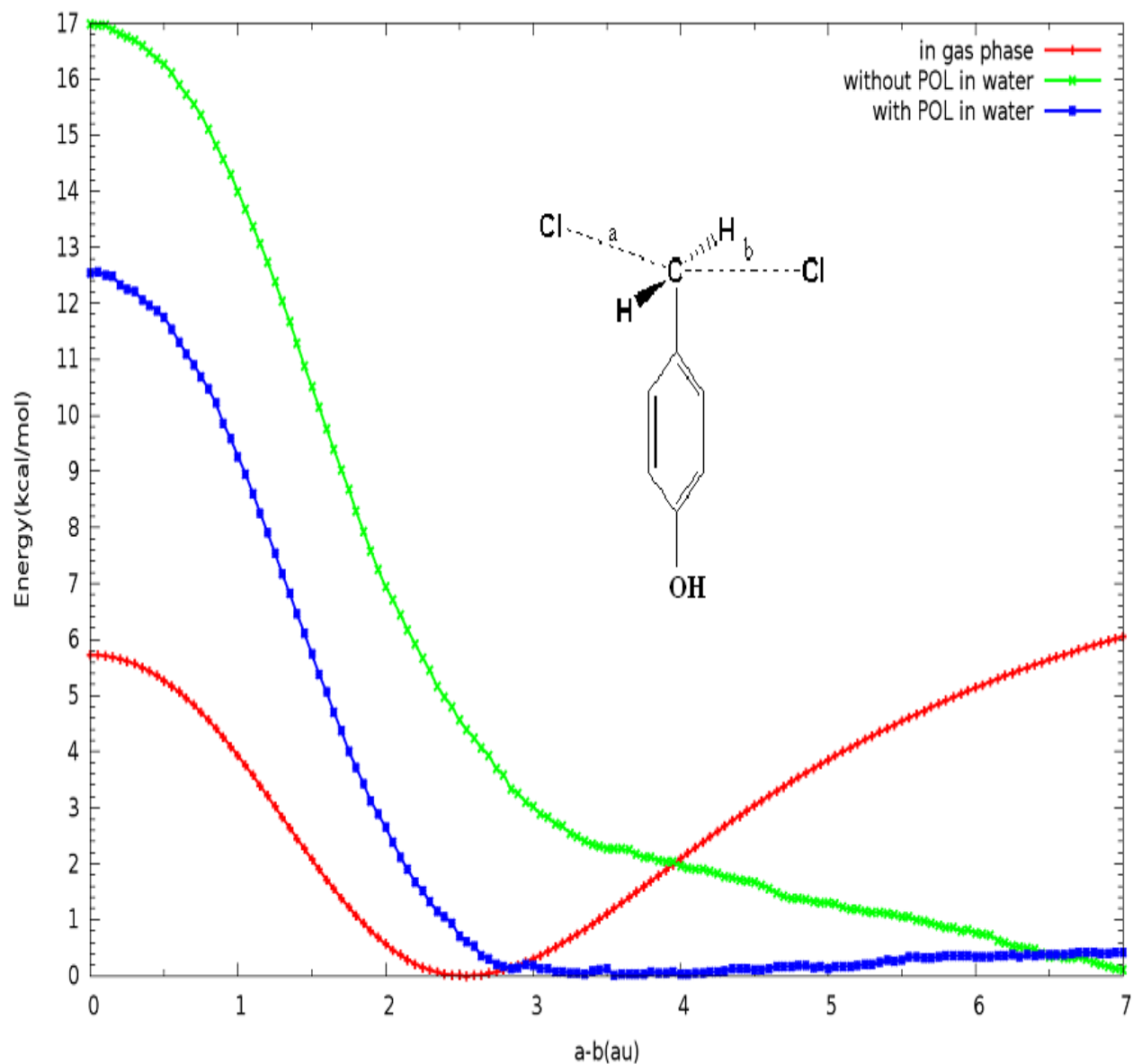


Figure 20. B3LYP energies (kcal/mole) versus the reaction coordinate (a_0) of the S_N2 reaction between the para-OH benzyl chloride and the chloride ion in water and in the gas phase. The blue line corresponds to the reaction in water, which has polarizability in solute, while the green line corresponds to the reaction in water, which does not have polarizability in solute. The red line represents the reaction in the gas phase.

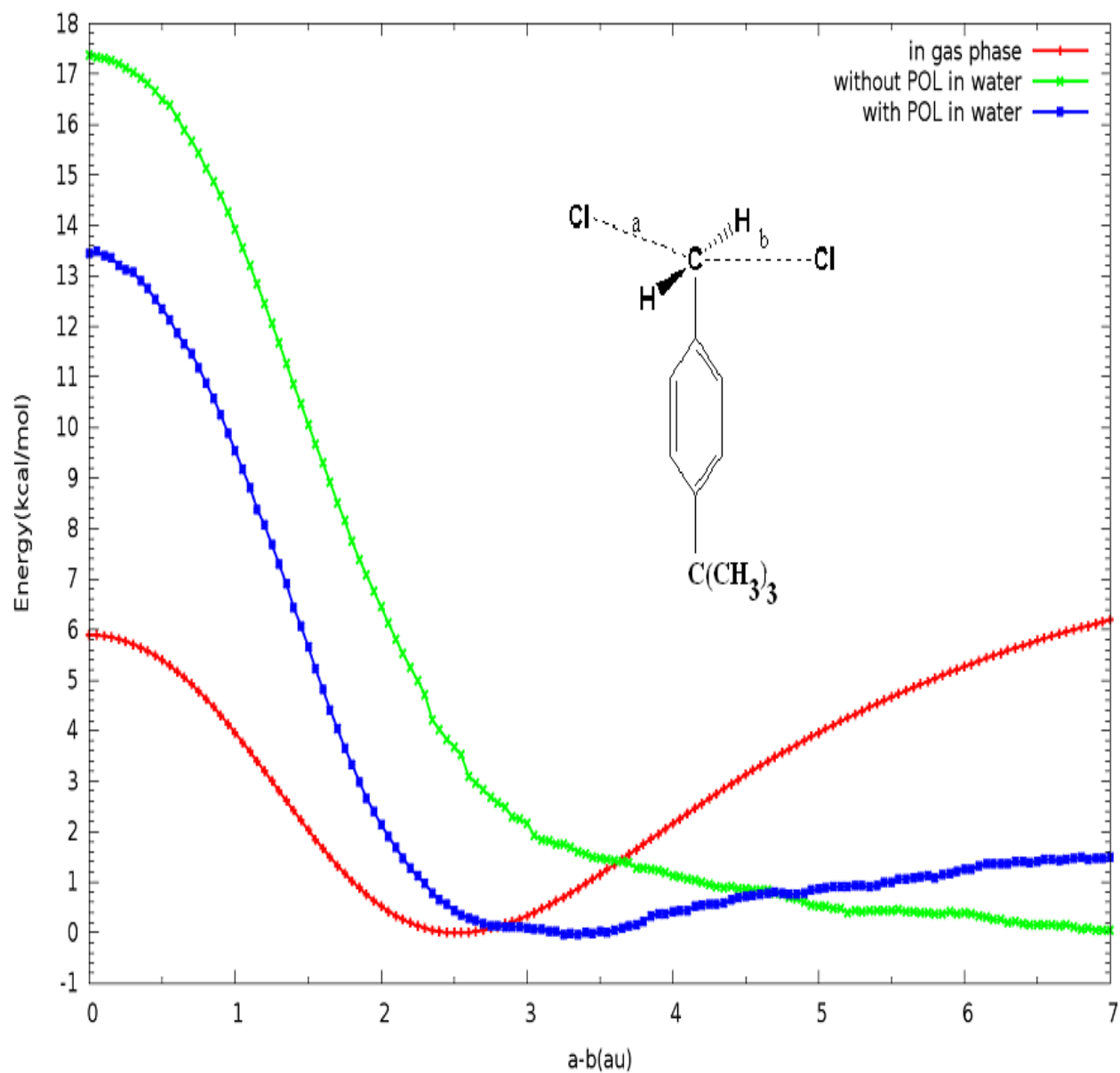


Figure 21. B3LYP energies (kcal/mole) *versus* the reaction coordinate (a_0) of the S_N2 reaction between the para- $C(CH_3)_3$ benzyl chloride and the chloride ion in water and in the gas phase. The blue line corresponds to the reaction in water, which has polarizability in solute, while the green line corresponds to the reaction in water, which does not have polarizability in solute. The red line represents the reaction in the gas phase.

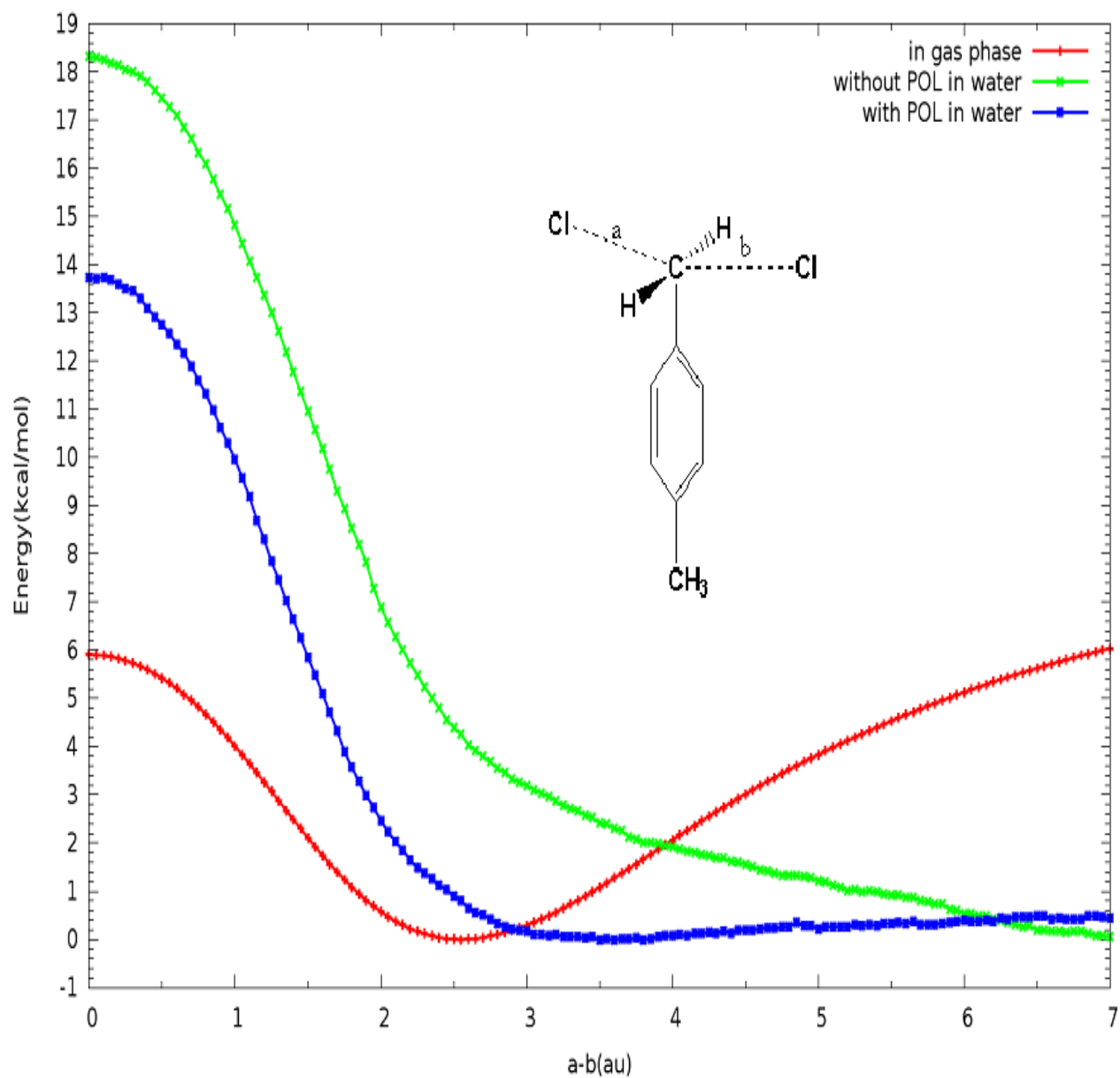


Figure 22. B3LYP energies (kcal/mole) *versus* the reaction coordinate (a_0) of the S_N2 reaction between the para-CH₃ benzyl chloride and the chloride ion in water and in the gas phase. The blue line corresponds to the reaction in water, which has polarizability in solute, while the green line corresponds to the reaction in water, which does not have polarizability in solute. The red line represents the reaction in the gas phase.

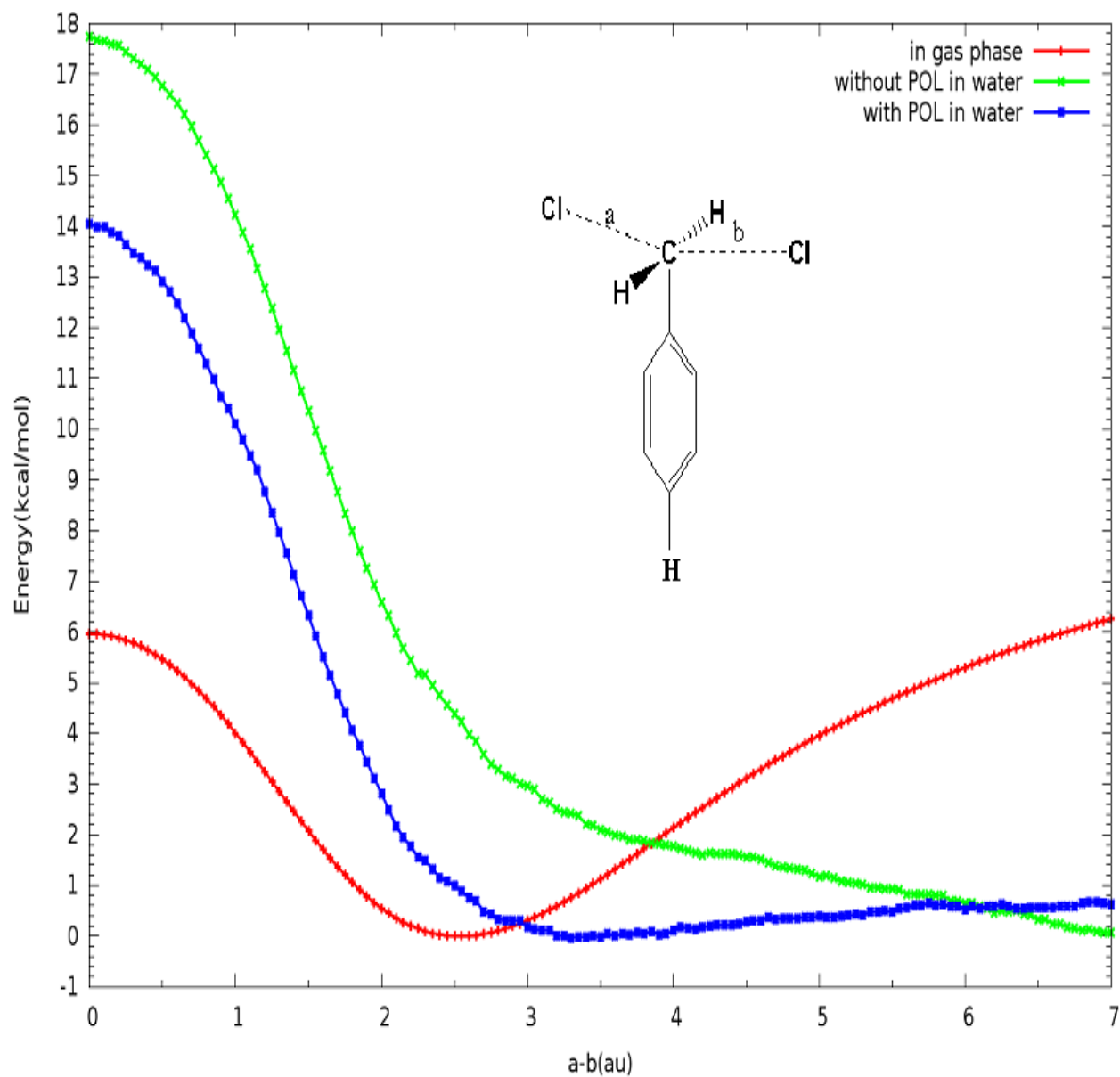


Figure 23. B3LYP energies (kcal/mole) *versus* the reaction coordinate (a_0) of the S_N2 reaction between the benzyl chloride and the chloride ion in water and in the gas phase. The blue line corresponds to the reaction in water, which has polarizability in solute, while the green line corresponds to the reaction in water, which does not have polarizability in solute. The red line represents the reaction in the gas phase.

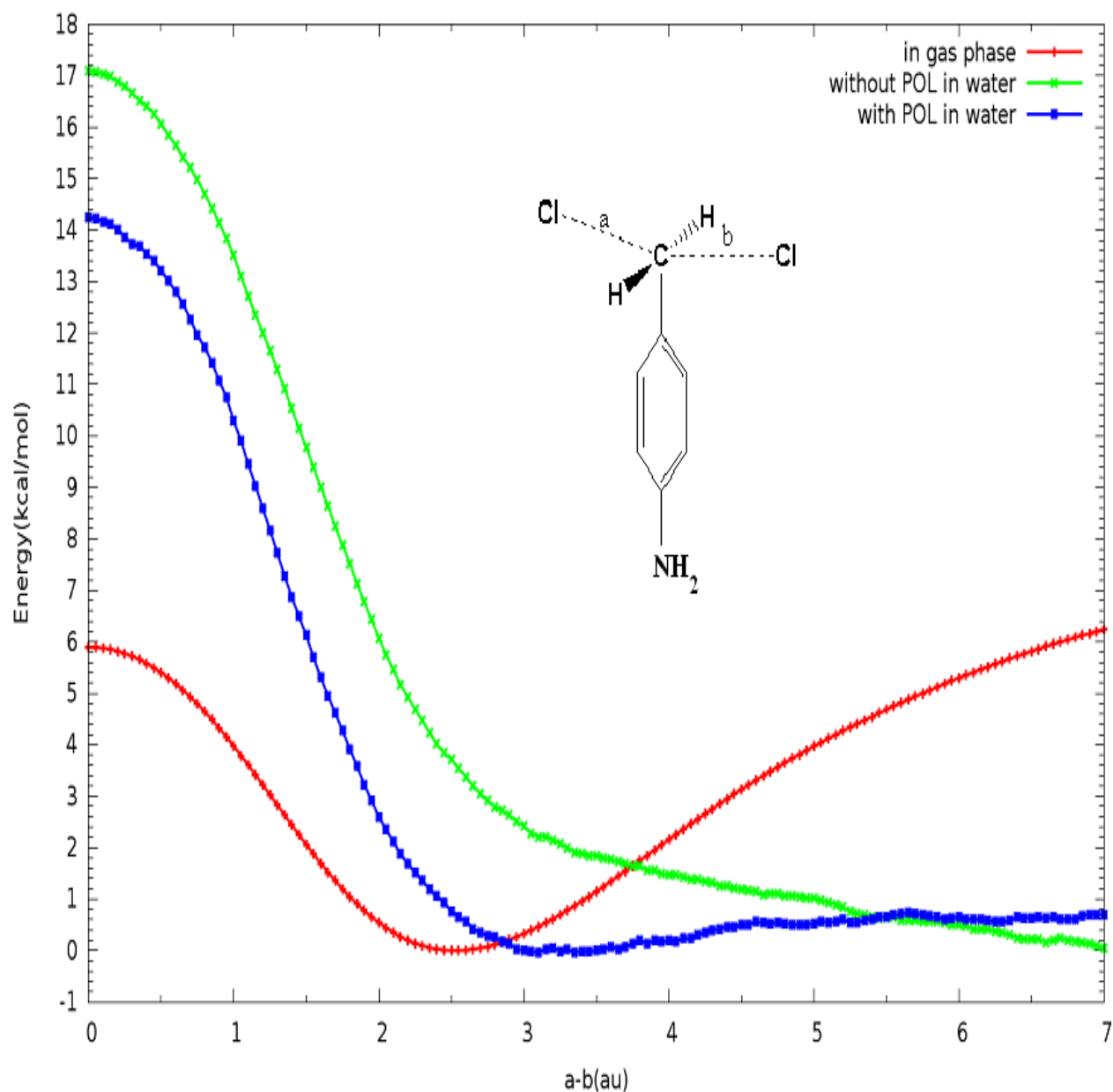


Figure 24. B3LYP energies (kcal/mole) *versus* the reaction coordinate (a_0) of the S_N2 reaction between the para-NH₂ benzyl chloride and the chloride ion in water and in the gas phase. The blue line corresponds to the reaction in water, which has polarizability in solute, while the green line corresponds to the reaction in water, which does not have polarizability in solute. The red line represents the reaction in the gas phase.

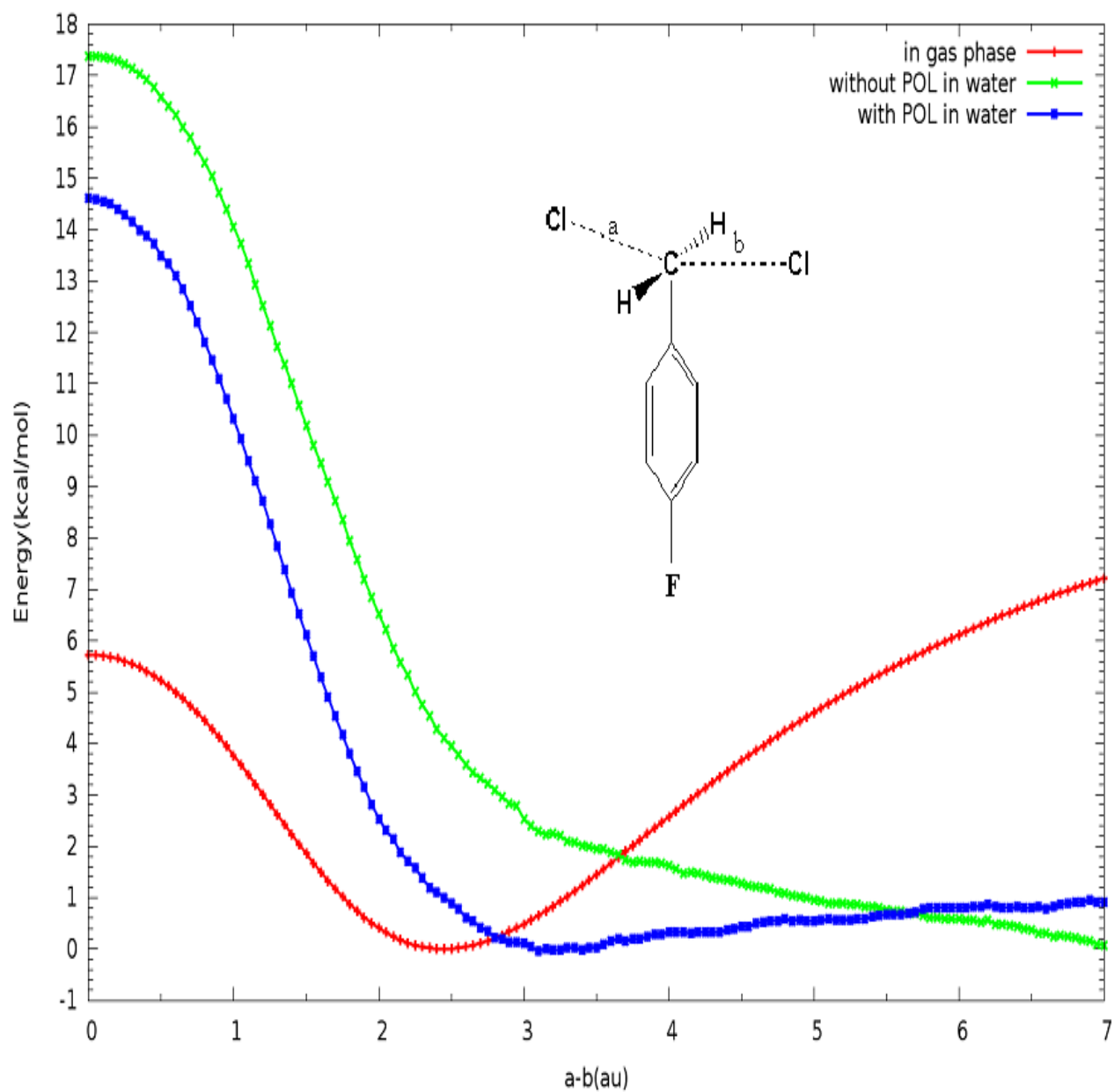


Figure 25. B3LYP energies (kcal/mole) *versus* the reaction coordinate (a_0) of the S_N2 reaction between the para-F benzyl chloride and the chloride ion in water and in the gas phase. The blue line corresponds to the reaction in water, which has polarizability in solute, while the green line corresponds to the reaction in water, which does not have polarizability in solute. The red line represents the reaction in the gas phase.

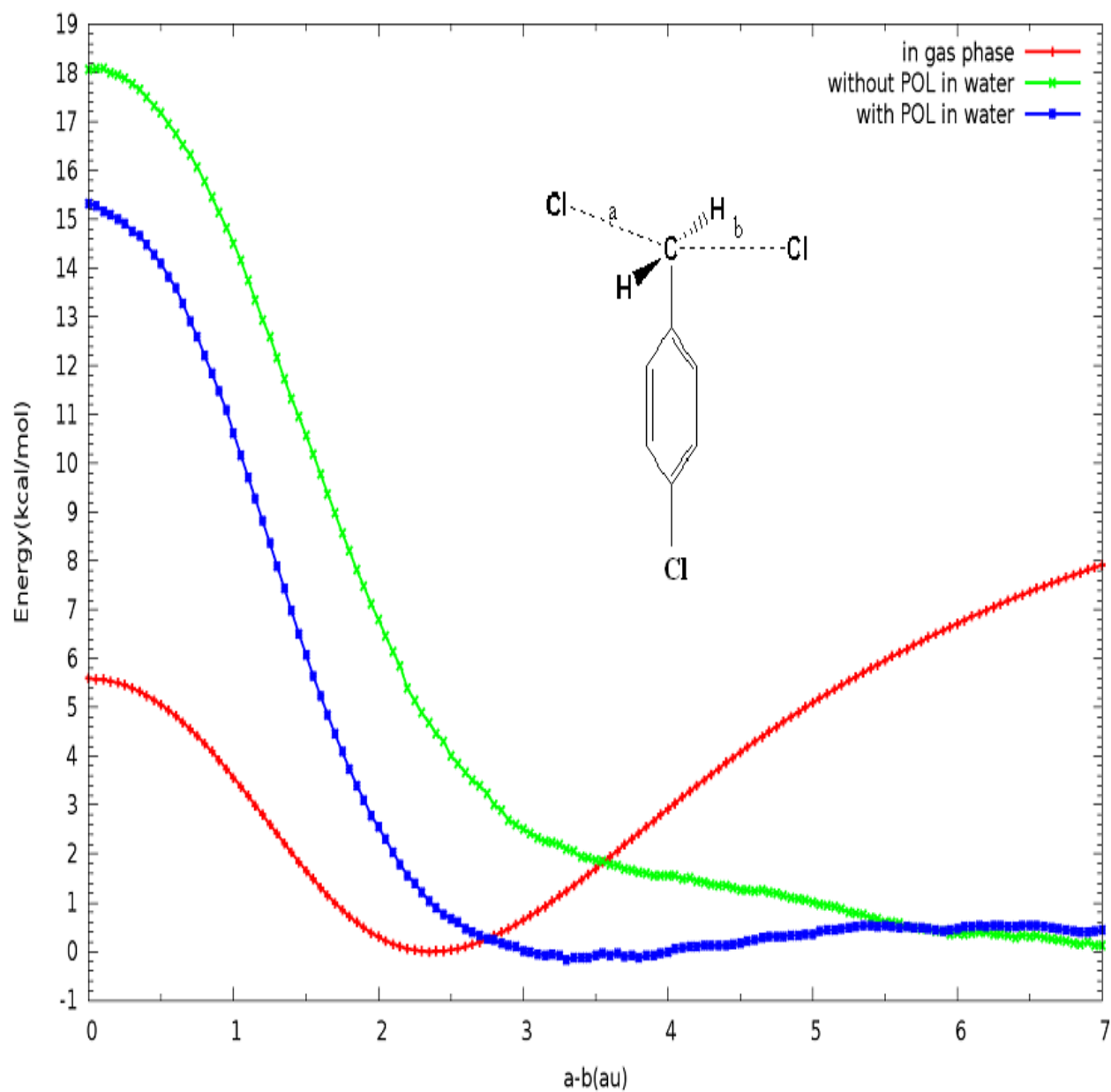


Figure 26. B3LYP energies (kcal/mole) *versus* the reaction coordinate (a_0) of the S_N2 reaction between the para-Cl benzyl chloride and the chloride ion in water and in the gas phase. The blue line corresponds to the reaction in water, which has polarizability in solute, while the green line corresponds to the reaction in water, which does not have polarizability in solute. The red line represents the reaction in the gas phase.

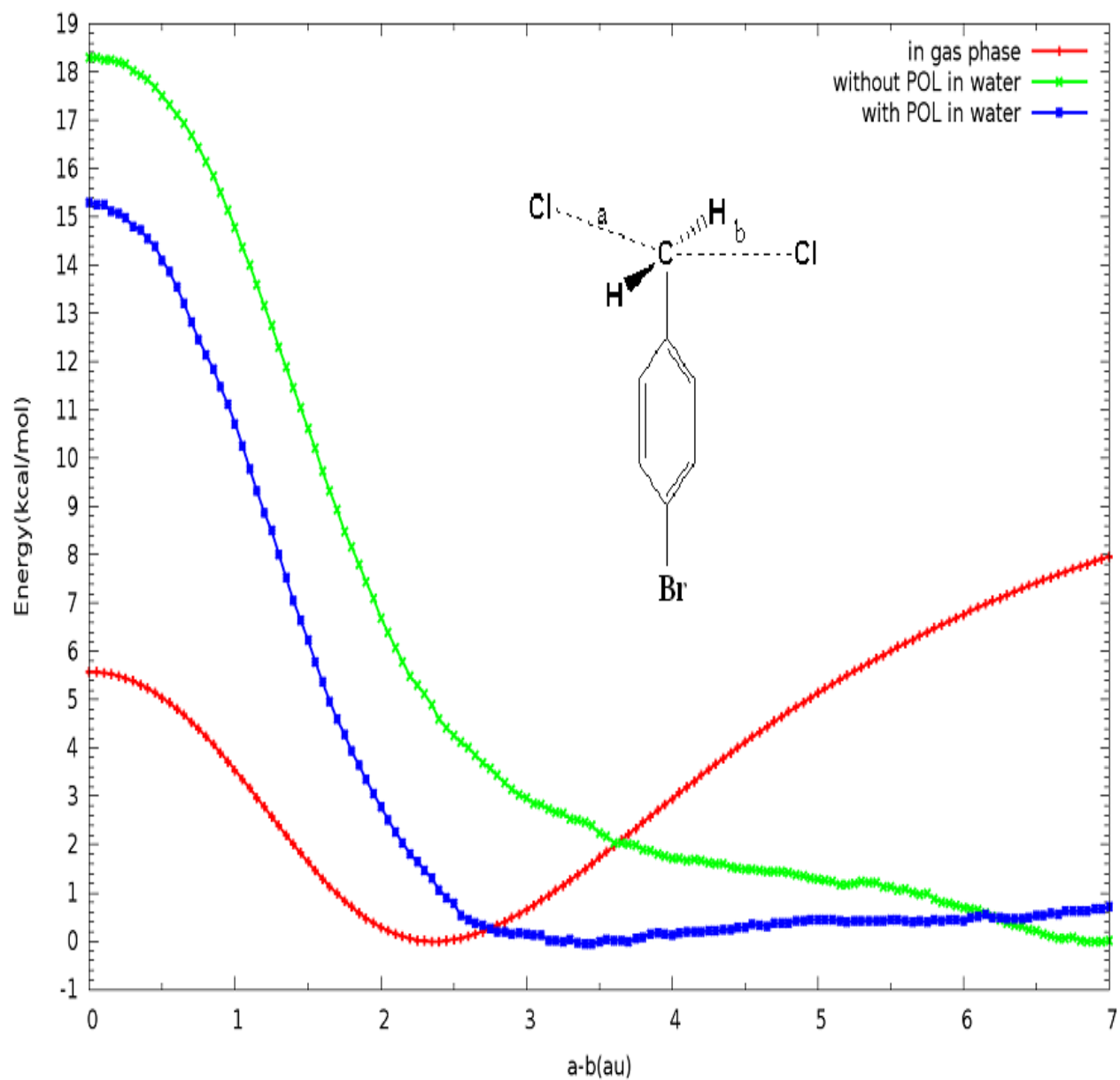


Figure 27. B3LYP energies (kcal/mole) *versus* the reaction coordinate (a_0) of the S_N2 reaction between the para-Br benzyl chloride and the chloride ion in water and in the gas phase. The blue line corresponds to the reaction in water, which has polarizability in solute, while the green line corresponds to the reaction in water, which does not have polarizability in solute. The red line represents the reaction in the gas phase.

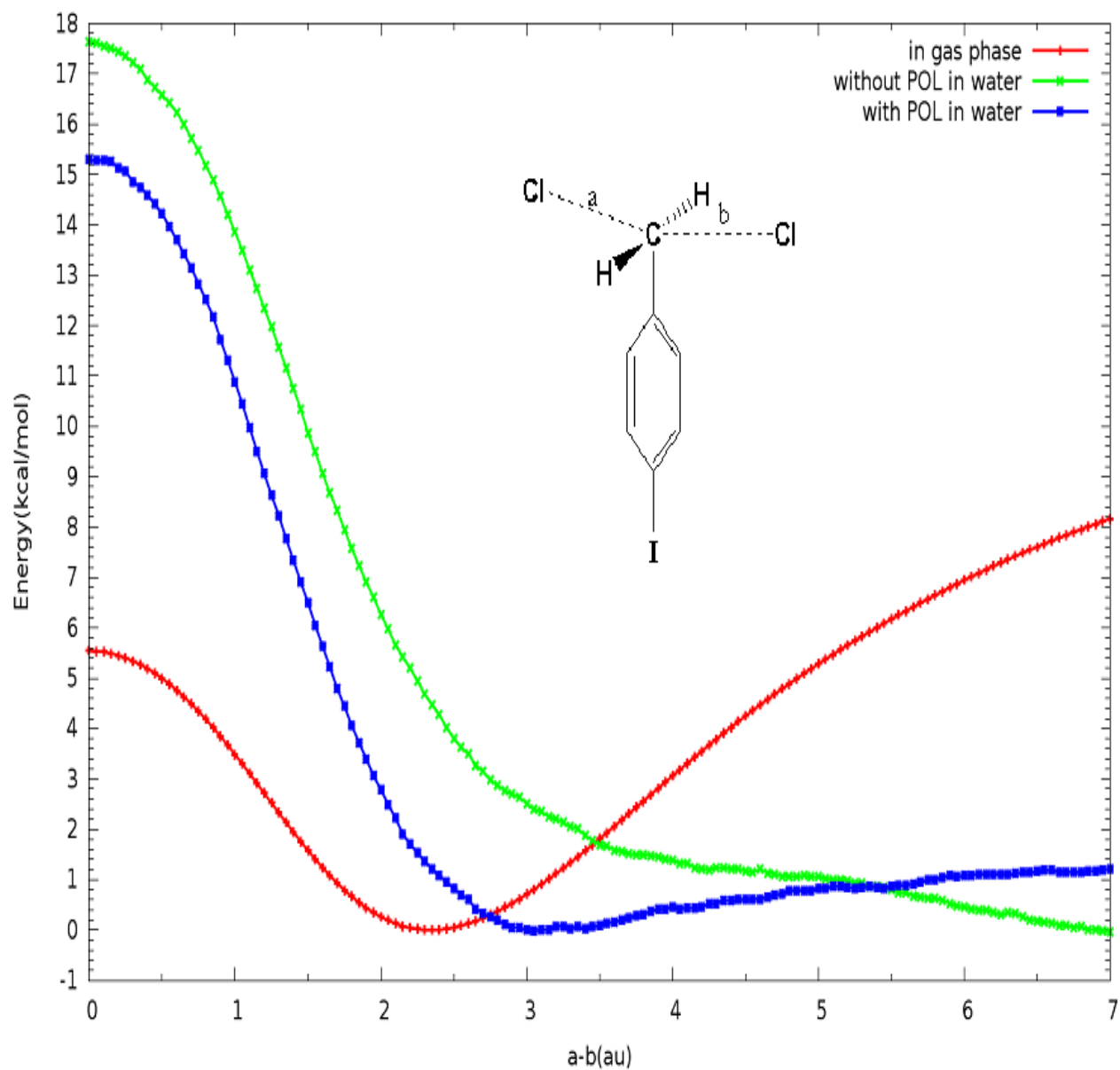


Figure 28. B3LYP energies (kcal/mole) *versus* the reaction coordinate (a_0) of the S_N2 reaction between the para-I benzyl chloride and the chloride ion in water and in the gas phase. The blue line corresponds to the reaction in water, which has polarizability in solute, while the green line corresponds to the reaction in water, which does not have polarizability in solute. The red line represents the reaction in the gas phase.

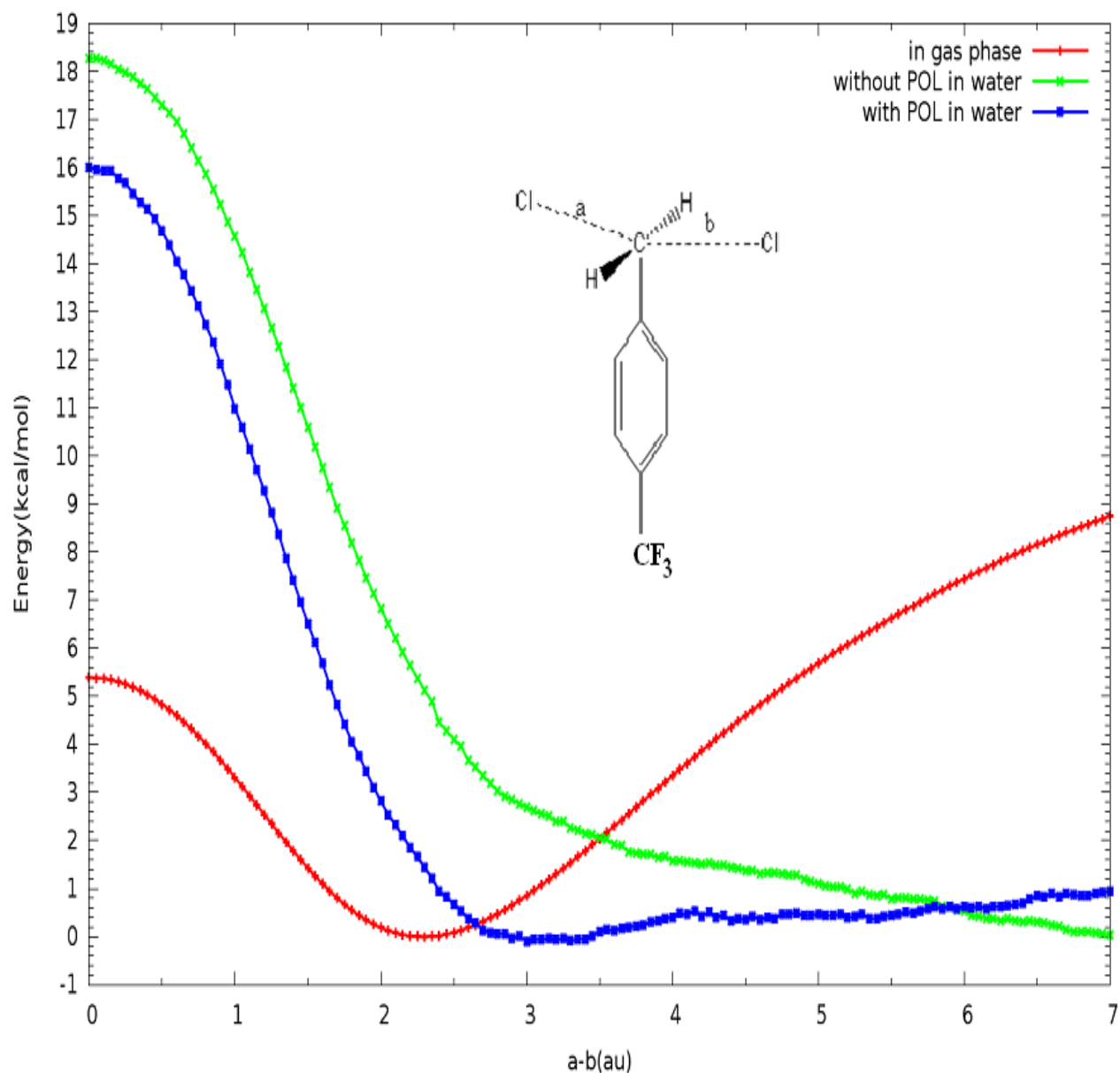


Figure 29. B3LYP energies (kcal/mole) *versus* the reaction coordinate (a_0) of the S_N2 reaction between the para- CF_3 benzyl chloride and the chloride ion in water and in the gas phase. The blue line corresponds to the reaction in water, which has polarizability in solute, while the green line corresponds to the reaction in water, which does not have polarizability in solute. The red line represents the reaction in the gas phase.

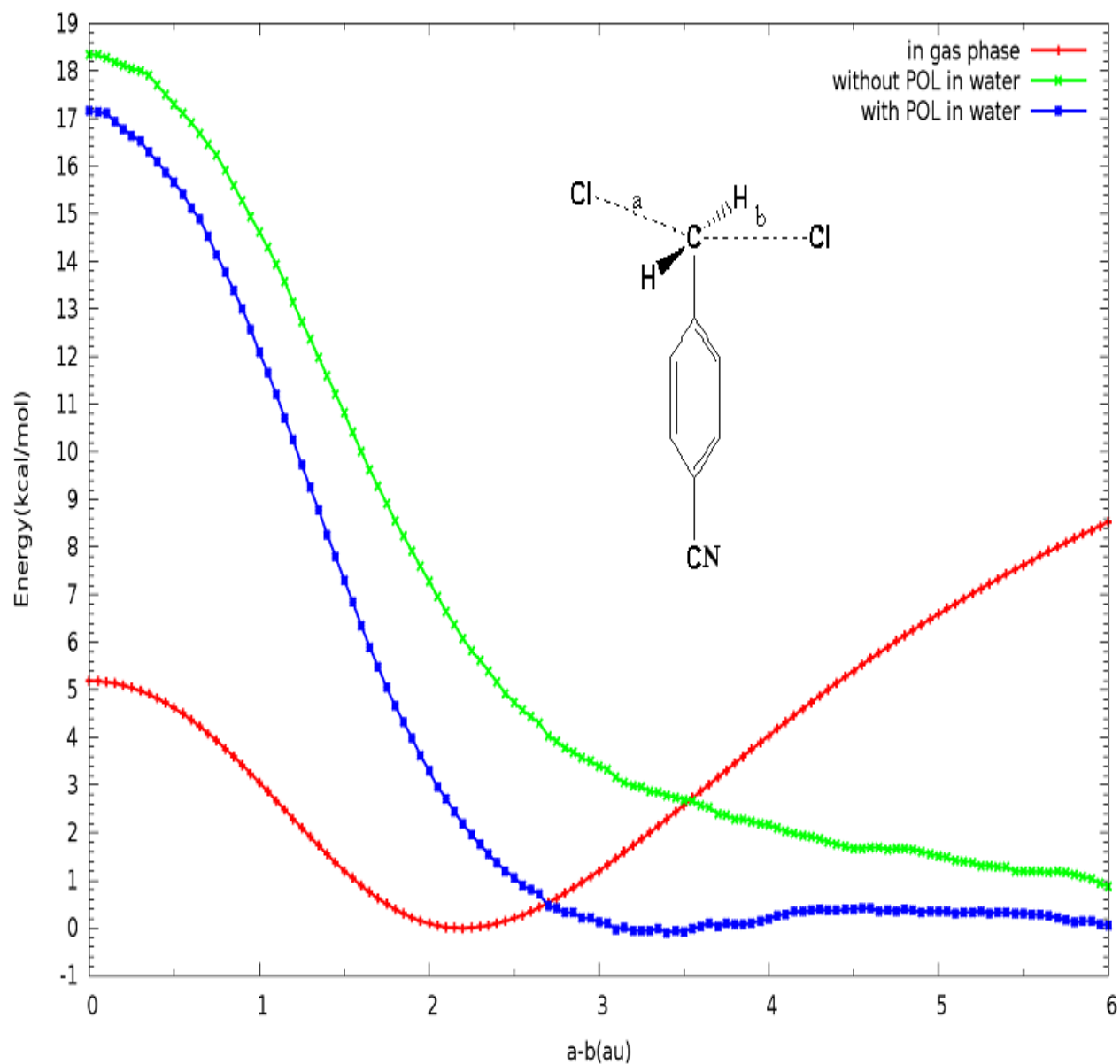


Figure 30. B3LYP energies (kcal/mole) *versus* the reaction coordinate (a_0) of the S_N2 reaction between the para-CN benzyl chloride and the chloride ion in water and in the gas phase. The blue line corresponds to the reaction in water, which has polarizability in solute, while the green line corresponds to the reaction in water, which does not have polarizability in solute. The red line represents the reaction in the gas phase.

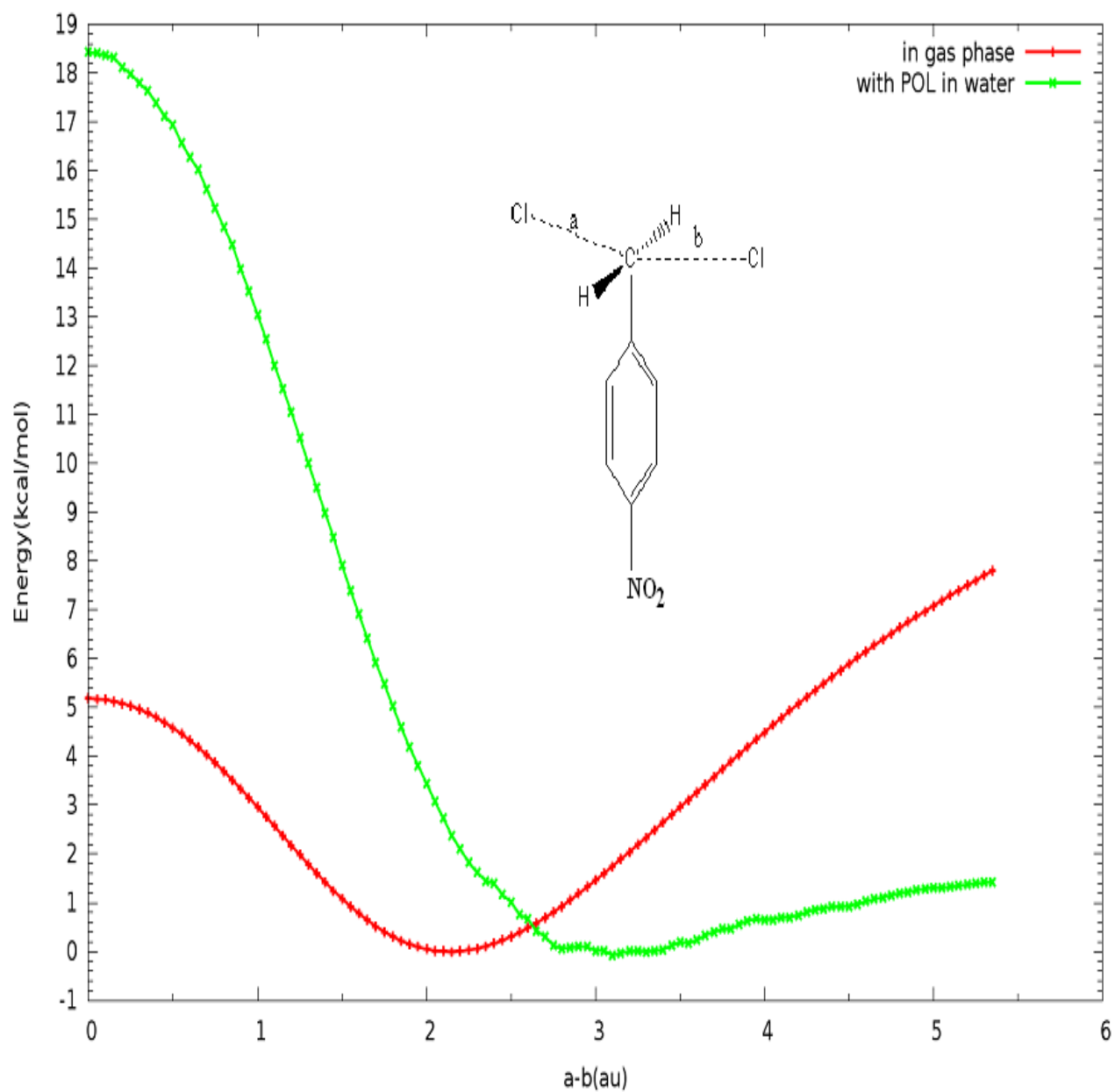


Figure 31. B3LYP energies (kcal/mole) *versus* the reaction coordinate (a_0) of the S_N2 reaction between the para- NO_2 benzyl chloride and the chloride ion in water and in the gas phase. The green line corresponds to the reaction in water, which has polarizability in solute. The red line represents the reaction in the gas phase.

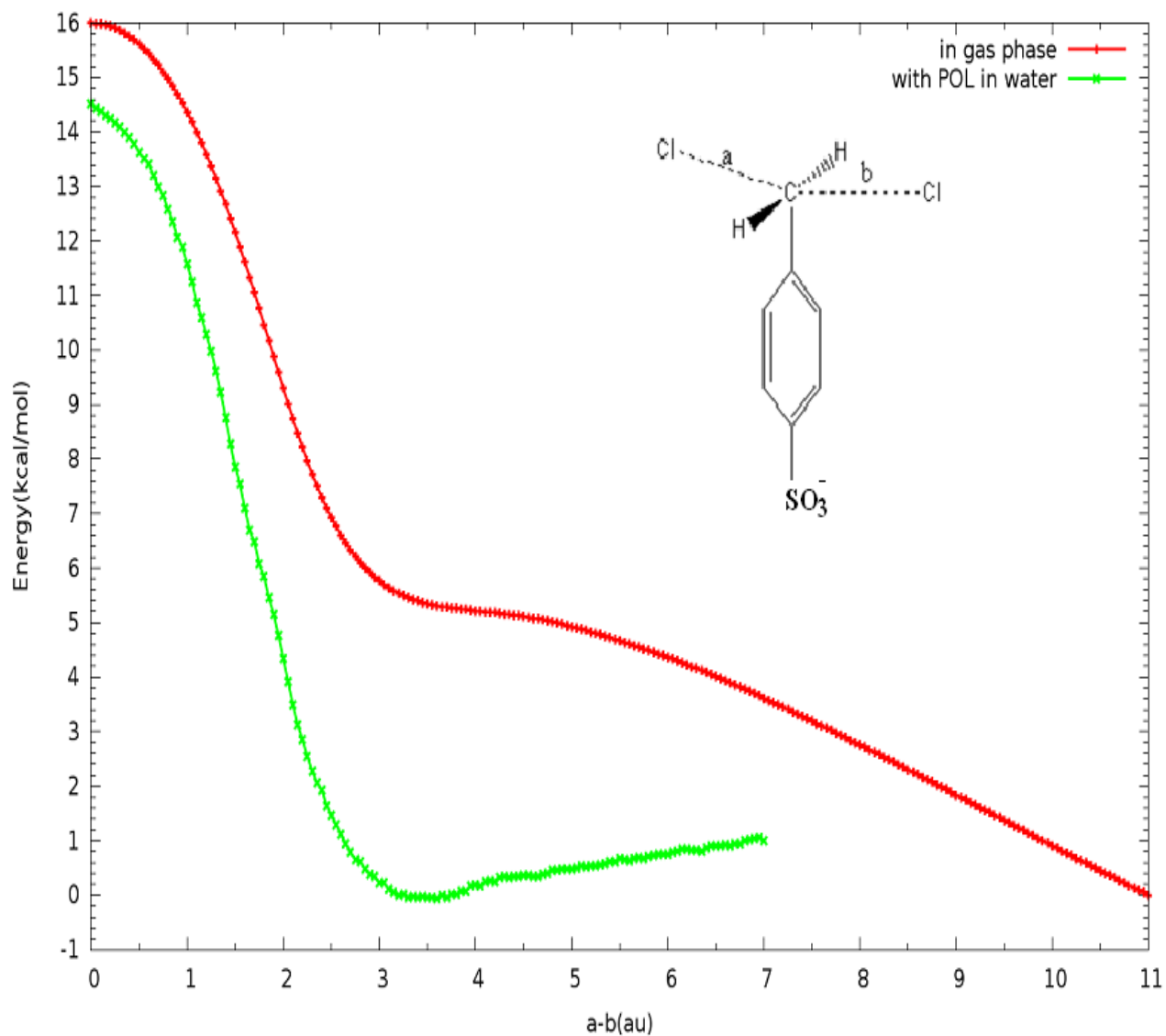


Figure 32. B3LYP energies (kcal/mole) *versus* the reaction coordinate (a_0) of the S_N2 reaction between the para- SO_3^- benzyl chloride and the chloride ion in water and in the gas phase. The green line corresponds to the reaction in water, which has polarizability in solute. The red line represents the reaction in the gas phase. The Hammett constant of para- SO_3^- is 0.09.

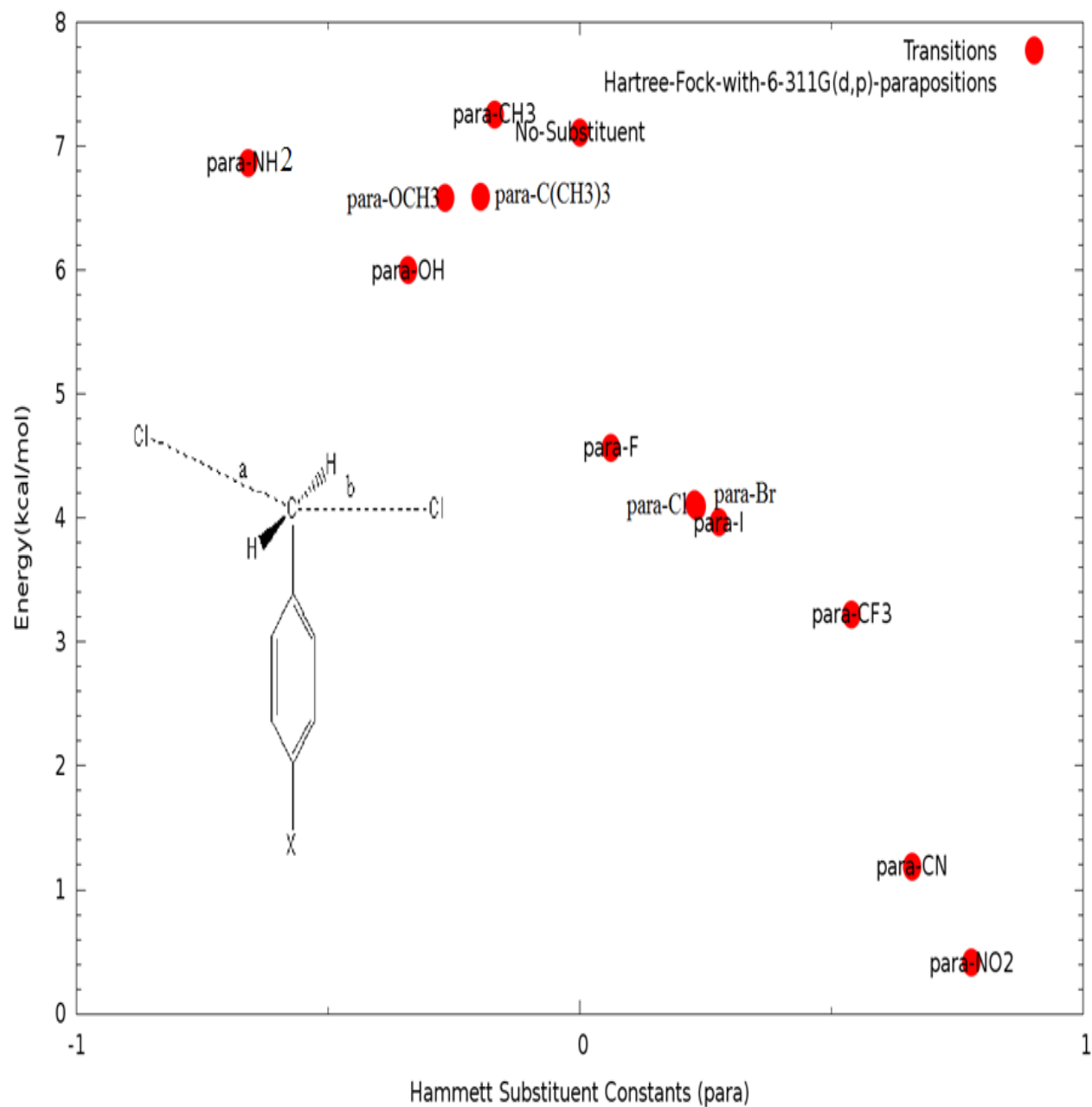


Figure 33. Transition state energies (relative to infinite separation, in kcal/mole) *versus* Hammett constants of the S_N2 reaction between para-substituted benzyl chlorides with different para substitution and the chloride ion in the gas phase, at the RHF/6-311G(d,p) level

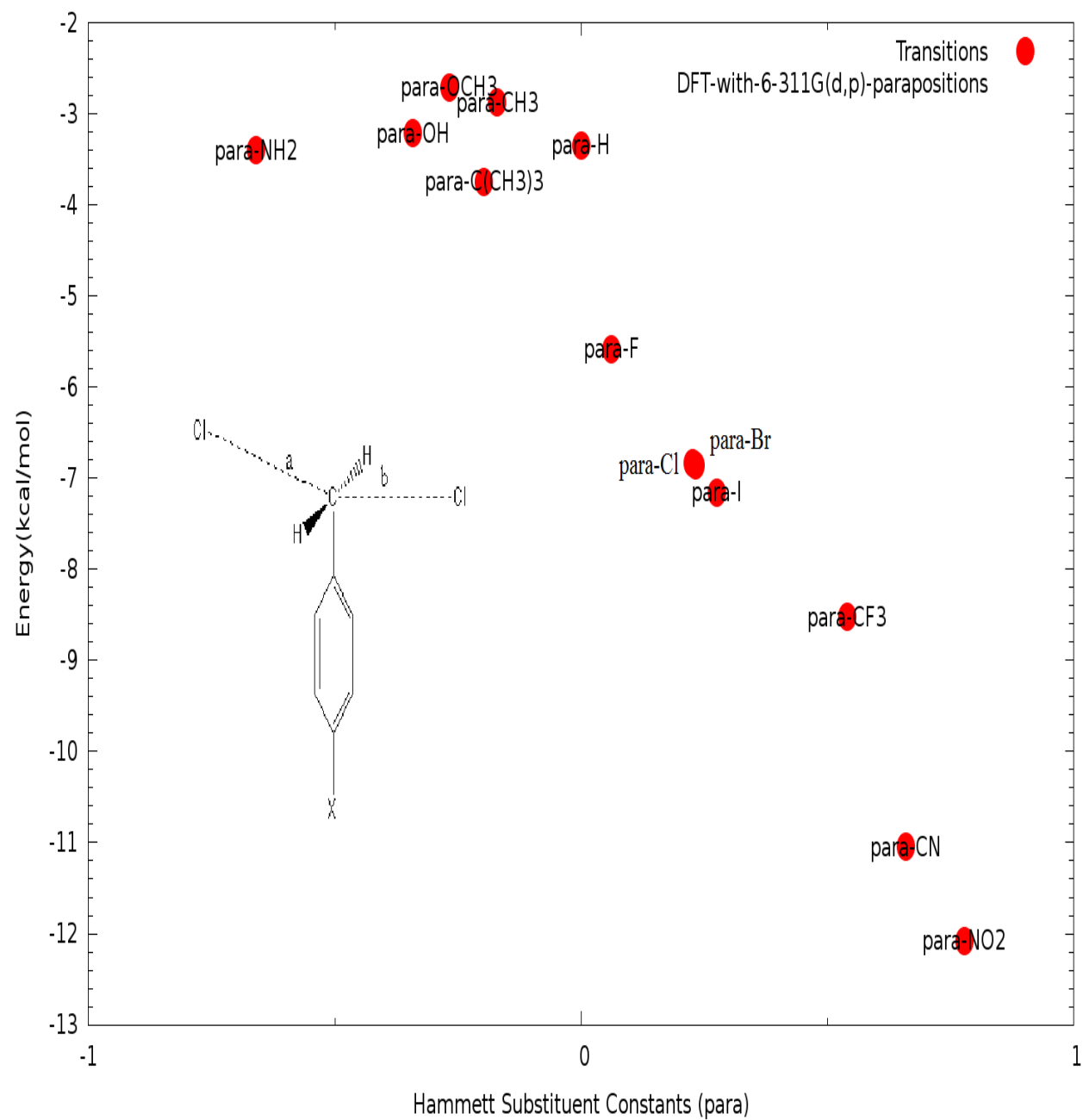


Figure 34. Transition state energies (relative to infinite separation, in kcal/mole) *versus* Hammett constants of the S_N2 reaction between para-substituted benzyl chlorides with different para substitutions and the chloride ion in the gas phase, at the B3LYP/6-311G(d,p) level

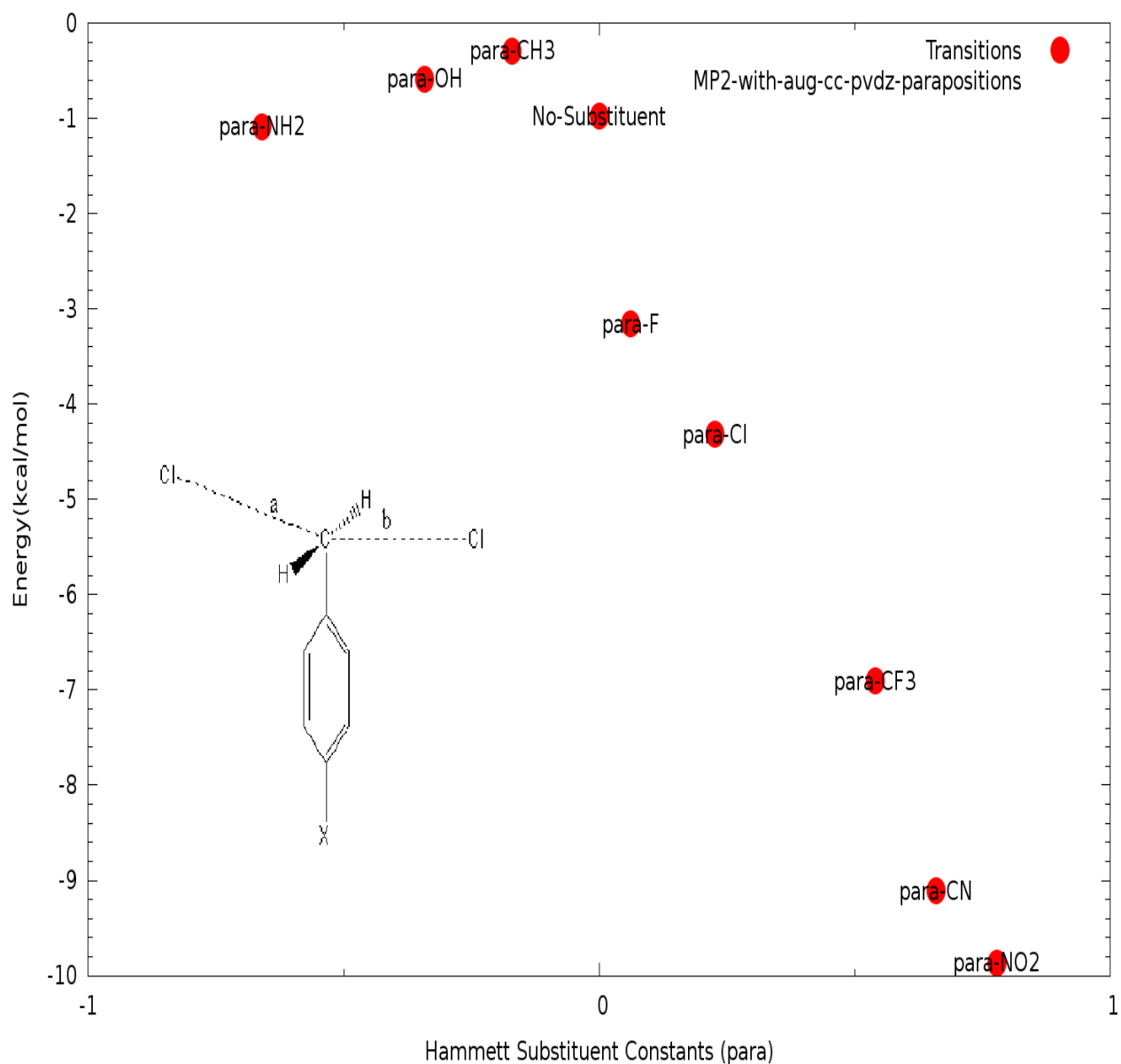


Figure 35. Transition state energies (relative to infinite separation, in kcal/mole) *versus* Hammett constants of the S_N2 reaction between para-substituted benzyl chlorides with different para substitutions and the chloride ion in the gas phase, at the MP2/6-311G(d,p) level

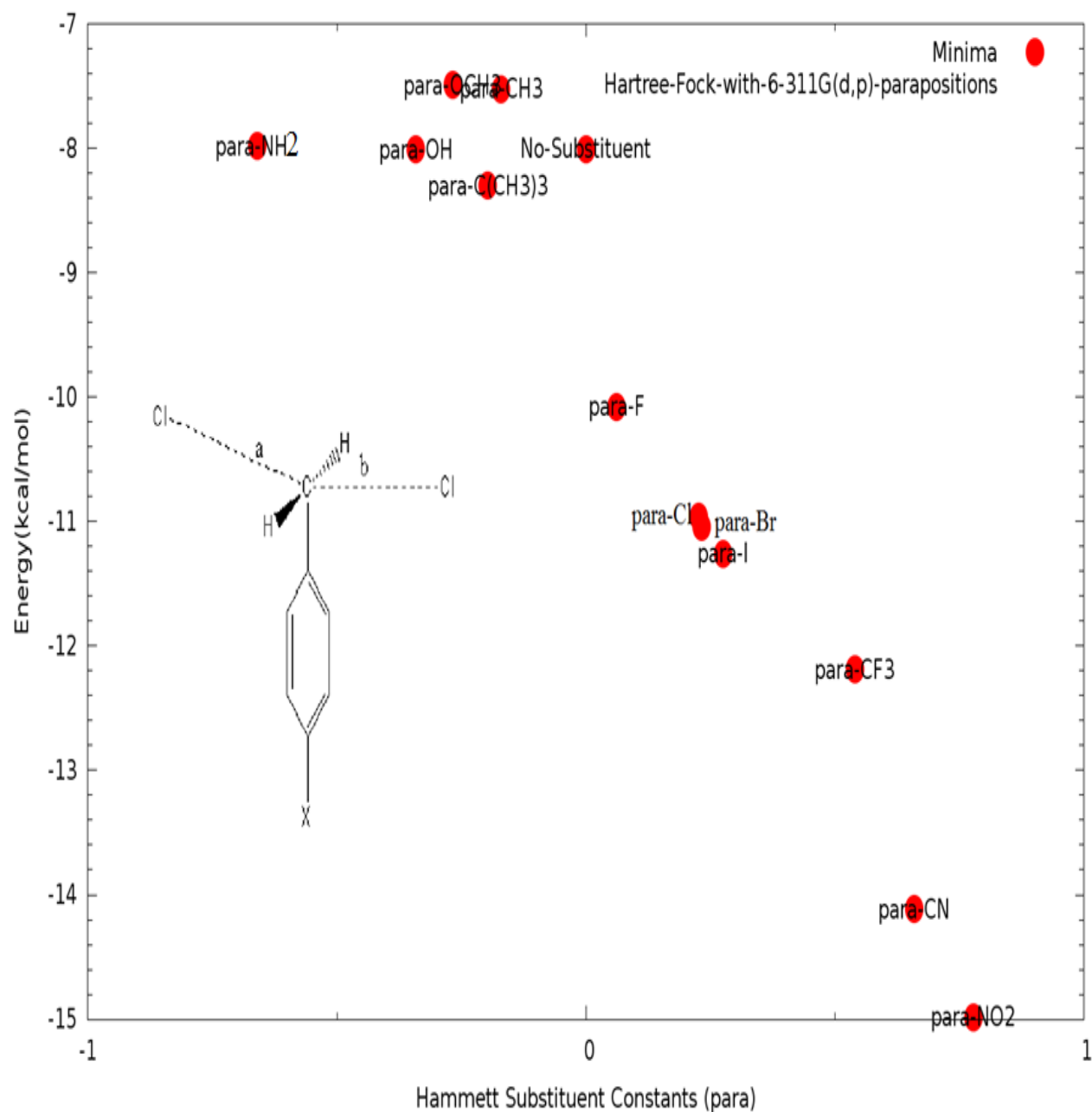


Figure 36. Energies of the reaction complex (relative to infinite separation, in kcal/mole) *versus* Hammett constants for the S_N2 reaction between para-substituted benzyl chlorides with different para-substitutions and the chloride ion in the gas phase at the RHF/6-311G(d,p) level.

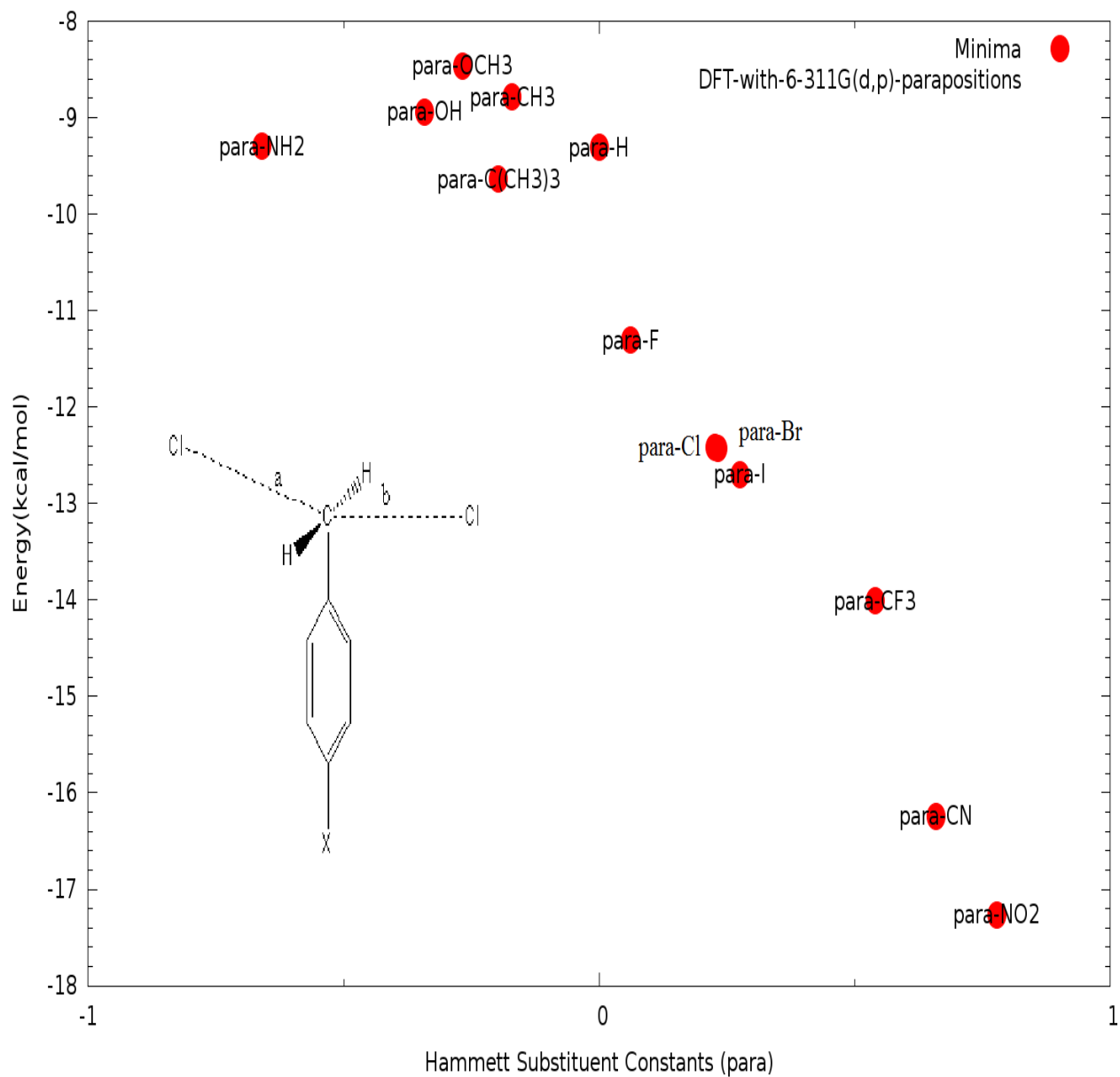


Figure 37. Energies of the reaction complex (relative to infinite separation, in kcal/mole) *versus* Hammett constants for the S_N2 reaction between para-substituted benzyl chlorides with different para-substitutions and the chloride ion in the gas phase at the B3LYP/6-311G(d,p) level.

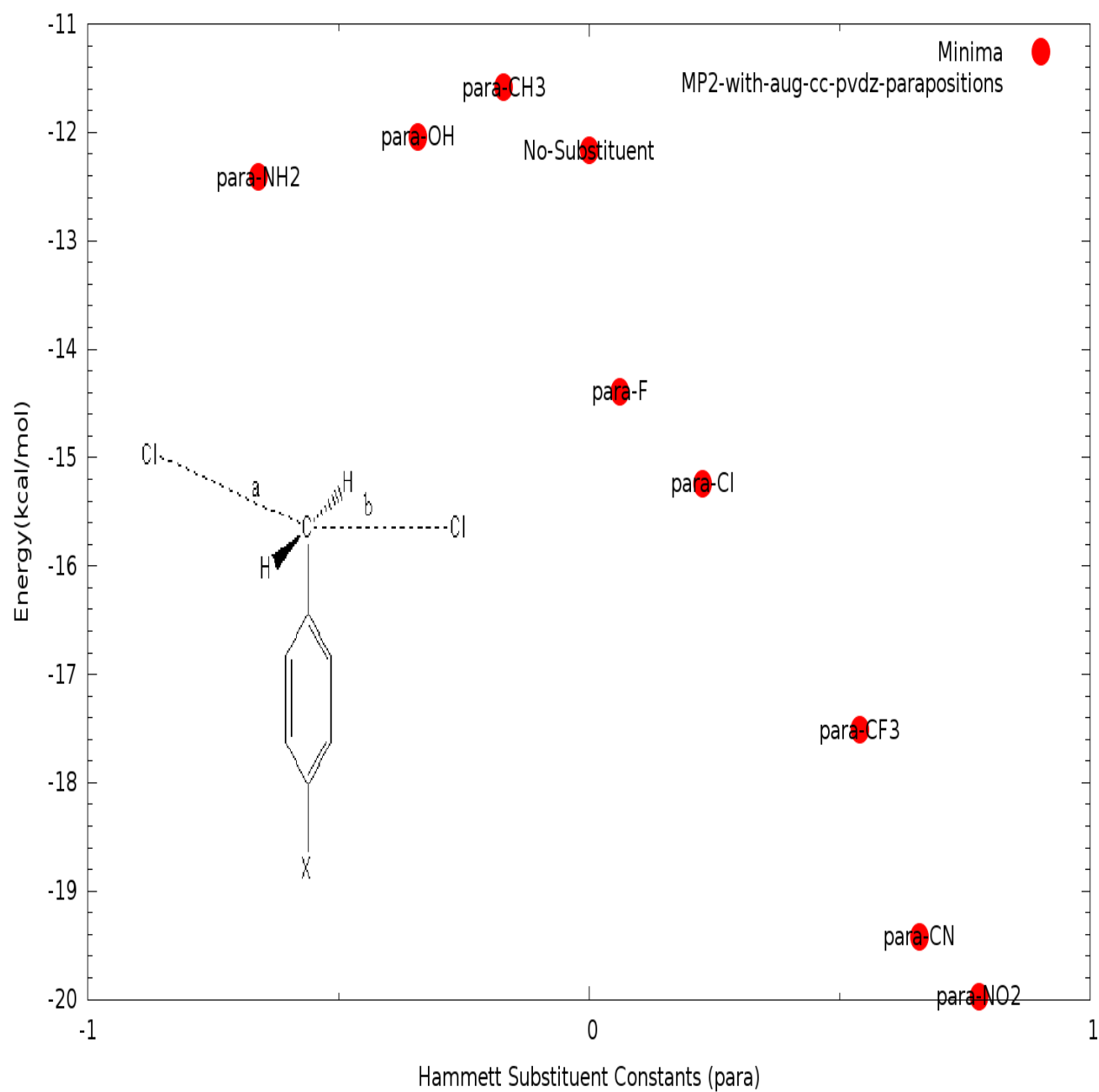


Figure 38. Energies of the reaction complex (relative to infinite separation, in kcal/mole) *versus* Hammett constants for the S_N2 reaction between para-substituted benzyl chlorides with different para-substitutions and the chloride ion in the gas phase at the MP2/6-311G(d,p)level.